5 Lymphoscintigraphy for the Differential Diagnosis of Peripheral Edema and Intracavitary Lymph Effusion

Martina Sollini, Roberto Boni, Andrea Marciano, Roberta Zanca, Francesco Bartoli, and Paola A. Erba

Contents

5.1 **Introduction** 79
5.2 **Differential Diagnosis** 81
5.3 **Diagnostic Characterization** 82
5.4 **Management of Lymphedema** 85
5.5 **Lymphoscintigraphy in the Management of Lymphedema** 87
5.6 **X-Ray Computed Tomography and Magnetic Resonance Imaging** 92
5.7 **Virtual Reality for Preoperative Planning** 99
Clinical Cases 102
References 140

Learning Objectives

- Learn how lymphedema is defined in clinical practice, and classified and staged according to the International Society of Lymphology (ISL) guidelines and the Clinical, Etiologic, Anatomic, and Pathophysiologic approach in Lymphology (CEAP-L).
- Learn the conditions to be ruled out in the differential diagnosis of lymphedema.
- Learn the main therapeutic options for patients with lymphedema.
- Learn how to use properly different imaging modalities (such as bioimpedance spectroscopy, dual-energy X-ray absorptiometry, ultrasonography, venous Doppler ultrasound, conventional lymphoscintigraphy, PET/CT lymphoscintigraphy, magnetic resonance lymphography) for the diagnosis and management of patients with lymphedema.
- Learn how to integrate the information deriving from each imaging procedure for prognostic assessment and for treatment planning and evaluation.

M. Sollini
Department of Biomedical Sciences, Humanitas University, Milan, Italy

R. Boni
Nuclear Medicine Service, "Papa Giovanni XXIII" Hospital, Bergamo, Italy

A. Marciano · R. Zanca · F. Bartoli · P. A. Erba (✉)
Regional Center of Nuclear Medicine, Department of Translational Research and Advanced Technologies in Medicine and Surgery, University of Pisa, Pisa, Italy
e-mail: paola.erba@unipi.it

5.1 Introduction

Patients with lower extremity lymphedema present initially unilateral painless swelling that starts on the dorsal aspect of the foot, but eventually progresses to involve also the proximal portion of the limb. The edema is initially a pitting edema, but over time the subcutaneous tissue becomes fibrotic, resulting in non-pitting brawny edema. The edema

G. Mariani et al. (eds.), *Atlas of Lymphoscintigraphy and Sentinel Node Mapping*,
https://doi.org/10.1007/978-3-030-45296-4_5

can then spread circumferentially if treatment is not initiated, involving the skin which becomes hyperkeratotic, hyperpigmented, and papillomatous or verrucous, with increased skin turgor. The Kaposi-Stemmer sign, in which the examiner is unable to pinch a fold of skin at the base of the second toe on the dorsal aspect of the foot, indicates clinical lymphedema [1–3]. Ultimately, the skin is at risk for ulcerating and is the site of subsequent infection. Swelling associated with lymphedema results in a sensation of heaviness, discomfort, and impaired mobility of the limb. Angiosarcoma may develop in chronic lymphedematous limbs (Stewart-Treves syndrome), but is most commonly seen in the upper extremity following mastectomy with axillary lymph node dissection [4]. This condition is often referred to as lymphangiosarcoma, which is actually a misnomer, since the tumor is not derived from lymphatic vessels, but is rather derived from vascular endothelial cells within a condition of chronic lymphedema.

The International Society of Lymphology (ISL) has established a staging system for defining the severity of this disease. It is thus possible to identify the progression of the condition and the potential for successful treatment and improvement. This staging system, which applies only to the limbs (arms and legs), is based on the degree of swelling and on the condition of the skin and tissues. In the latest revision of the document for the evaluation and management of peripheral lymphedema [5] a four-stage scale for classification of a lymphedematous limb has been defined for conditions with increasing severities, as follows:

5.1.1 Stage O Lymphedema: Latent or Preclinical Stage

At this stage the patient is at risk of developing lymphedema; however, no swelling or other visible evidence of impaired lymph drainage is present. Stage 0 can be present for months, or years, before more severe signs appear. If specialized treatment is started at this stage, it may be possible to prevent the development of further stages of lymphedema.

5.1.2 Stage I Lymphedema

This condition indicates an early accumulation of interstitial fluid that is relatively high in protein content. There is visible swelling with protein-rich lymph. The swelling can be temporarily reduced by elevation of the limb; however, it soon reappears when the limb is returned to a normal position. The swollen tissues are soft, and pitting edema is present. Treatment should initiate as early as these clinical signs are detected, since waiting for the swelling to increase, or for an infection to develop, only makes the condition more difficult to treat. Prompt treatment of this stage can often control the condition and may prevent it from becoming more severe.

5.1.3 Stage II Lymphedema

This stage denotes a further increase in swelling accompanied by concomitant tissue changes. Elevation of the limb will not reduce the swelling, and tissues become increasingly firm, due to fibrosis. Pressure against the limb produces only a slight pitting, or no pitting at all. The tissue changes at this stage increase the risks of even greater swelling, fibrosis, infections, and skin problems. Stage II lymphedema can usually be improved with intense treatment.

5.1.4 Stage III Lymphedema

Also known as *lymphostatic elephantiasis*, in this condition the tissue becomes extremely swollen and thickened, due to blockage of lymph flow and buildup of fluid in tissues. The tissues become increasingly fibrotic. Pressure does not produce any pitting. Normal elasticity is lost, and the skin hangs in folds and may change color. *Papillomas* and *hyperkeratosis* can develop. Changes in skin texture are disfiguring and can limit mobility. Infections become more common because of increased risks of ulcerations of the skin. These infections include fungal infections and open wounds that form within the skin folds. With intense therapy, stage III lymphedema can be improved and potentially be prevented from becoming even worse; however, it is rarely reversed to an earlier stage.

Within each stage, a functional severity assessment utilizes simple volume differences commonly determined using circumferential measurement (preferentially by flexible nonstretch tape) assessed as follows:

- Minimal (>5–<20% increase in limb volume), alternatively subdivided into
  - >5–10% as minimal
  - >10–<20% as mild
- Moderate (20–40% increase)
- Severe (>40% increase)

The above ISL stages only refer to the physical condition of the extremities. A more detailed and inclusive classification must be formulated according to improved understanding of the pathogenic mechanisms of lymphedema (e.g., nature and degree of lymphangiodysplasia, lymph flow perturbations, and nodal dysfunction as defined by anatomic features and physiologic imaging and testing), and underly-

ing genetic disturbances, which are increasingly being elucidated. Recent publications combining both physical (phenotypic) findings with functional lymphatic imaging as well as those classifications which propose inclusion of disability grading, assessment of inflammation, and even immunohistochemical changes determined by biopsy of nodes/vessels may be forecasting the future evolution of staging. In addition, incorporation of genotypic information, expanded from what is available even in current screening, would further advance staging and classification of patients with peripheral (and other) lymphedema.

Factors such as extension, occurrence of erysipelas attacks, inflammation, and other descriptors or complications within their own individual severity determinations might also be included.

A new classification of limb lymphedema was proposed in 2009, inspired by the **C**linical, **E**tiologic, **A**natomic, and **P**athophysiologic (CEAP) classification for chronic venous insufficiency of the lower limbs. It adopts the acronym CEAP by adding the letter **L** (Lymphatic) to underline the aspect "lymphedema." This clinical classification is subdivided into five classes depending on the presence of clinical signs such as:

- The presence of lymphedema: 5-point scale:
  - No edema
  - Edema that disappears with night rest
  - Edema that persists after night rest
  - Fibrotic edema
  - Elephantiasis with skin lesions
- Extension of lymphedema:
  - Lower limbs:
    Foot, leg, thigh, genital, trunk
  - Upper limbs:
    Hand, forearm, arm, shoulder
- Presence of lymphangitis and/or leg ulcers
- Loss of functionality of the limb (grade of disability)

The etiological aspect considers two types of alterations of the lymphatic system: congenital and acquired. Pathophysiological conditions are subdivided into five groups: agenesia or hypoplasia, hyperplasia, reflux, overload, and obstruction. The CEAP-L classification was created to categorize patients with definite and objective marks (Table 5.1), to generate clinical reports with a common and clear vocabulary, to stage the disease, to evaluate treatment, and to obtain epidemiological and statistical data [6]. Indeed, these authors found the application of the classification easy and highly reproducible in their experience.

Table 5.1 Clinical severity score [6]

1 point for each area of the limb involved
1 point for each limb involved
2 points for other areas involved (genitals, shoulders)
1–4 points according to the stage of edema
1 point symptomatic edema
1–3 points according to the stage of disability

Key Learning Points

- In patients with lower extremity lymphedema, clinical presentation progressively evolves from unilateral painless swelling on the dorsal aspect of the foot with pitting edema to circumferential involvement of the proximal portion of the limb; then to fibrosis of the subcutaneous tissue, non-pitting brawny edema, and skin changes that include hyperkeratosis and hyperpigmentation; and finally to papillomatous or verrucous skin, with increased skin turgor and increased risk for ulcers and subsequent infection.
- The Kaposi-Stemmer sign, in which the examiner is unable to pinch a fold of skin at the base of the second toe on the dorsal aspect of the foot, indicates clinical lymphedema.
- Angiosarcoma (Stewart-Treves syndrome) may develop in chronic lymphedematous limbs, as commonly seen in the upper extremity following mastectomy with axillary lymph node dissection.
- The ISL staging system applies only to the limbs and is based on the degree of swelling and on the condition of the skin and tissues. The current version is based on a three-stage scale for classification (from stage 0 to stage III); within each stage, a functional severity assessment (from minimal to severe) is used to assess the volume of the affected limb.
- The CEAP-L classification is subdivided into classes depending on the presence of clinical signs, such as presence and extension of lymphedema, presence of lymphangitis and/or leg ulcers, and loss of functionality of the limbs.
- The CEAP-L classification enables to categorize patients, generate clinical reports, stage the disease, evaluate treatment, and obtain epidemiological and statistical data.

5.2 Differential Diagnosis

Lymphedema should be considered whenever an edematous extremity without pain or inflammation is observed. Chronic venous insufficiency can be difficult to differentiate from early lymphedema because both exhibit pitting edema, and the skin changes typical of late-stage lymphedema are not

present yet. Nevertheless, chronic venous insufficiency is often bilateral, rather than unilateral as is generally the case for lymphedema. Lymphoscintigraphy is often necessary to distinguish the two conditions, although such discrimination cannot always be made, since chronic venous insufficiency can actually lead to secondary lymphedema. Similarly, deep vein thrombosis can cause a postphlebitic syndrome, which can result in lipodermatosclerosis and chronic swelling of the limb [2, 3]. In nonfilarial regions of tropical Africa, Central America, and the Indian subcontinent, there is a condition that clinically presents in a similar fashion as filariasis, called podoconiosis, or nonfilarial elephantiasis. Moreover, in case of unilateral extremity lymphedema, especially in adults, solid tumors (primary and/or metastatic), lymphomas, and soft-tissue sarcomas, which may obstruct or invade more proximal lymphatics, must be considered.

Exclusion of general medical causes of lower extremity swelling should be a priority. These causes include, but are not limited to, renal failure, protein-losing nephropathy, hypoalbuminemia, congestive heart failure, pulmonary hypertension, drug-induced edema, obesity, and pregnancy [7]. Other conditions to consider in the differential diagnosis include lipedema (also known as lipomatosis of the leg), "armchair legs" (descriptive term that results from sitting in a chair all day and night with one's legs in a dependent position), and postoperative swelling.

Key Learning Points

- Chronic venous insufficiency is similar in presentation to early-stage lymphedema, but it is often bilateral rather than unilateral.
- Deep vein thrombosis can cause a postphlebitic syndrome, which can result in lipodermatosclerosis and chronic swelling of the limb.
- In nonfilarial regions of tropical Africa, Central America, and the Indian subcontinent, there is a condition that clinically presents in a similar fashion as filariasis, called podoconiosis.
- In case of unilateral limb lymphedema, especially in adults, solid tumors (primary and/or metastatic), lymphomas, and soft-tissue sarcomas must be considered.
- Lower extremity swelling could originate from general medical causes such as renal failure, protein-losing nephropathy, hypoalbuminemia, protein-losing enteropathy, congestive heart failure, pulmonary hypertension, drug-induced edema, obesity, and pregnancy.
- The diagnostic differential includes also lipedema and "armchair leg" edema.

5.3 Diagnostic Characterization

In 1976, Stemmer described the inability to pinch the skin of the proximal phalanx of the second or third toe in patients with lymphedema [8]. If the examiner is unable to grab the dorsal skin between his/her thumb and index finger, then the "Stemmer sign" is positive suggesting lymphedema [9]. However, the thickened skin and excess subcutaneous fibroadipose tissue with edema (as a consequence of inflammation, adipose deposition, and fibrosis) [10–12] might prevent the pinching of the dorsal skin of the extremity in patients with lymphedema. In contrast, other causes of swelling or limb overgrowth such as venous stasis, heart disease, liver failure, renal insufficiency, rheumatologic disease, lipedema, hemihypertrophy, posttraumatic swelling, and vascular anomalies do not result in enough inflammatory fibroadipose formation to prevent the pinching of the dorsal skin of the hand or foot. Furthermore, abnormalities in the body mass index (BMI) have been found to be associated with both false-negative and false-positive Stemmer signs. In particular, patients with lymphedema and a normal or reduced BMI could exhibit minimal swelling and a falsely negative sign, whereas obese patients without lymphedema could have a false-positive sign. On the other hand, obesity per se negatively affects lymphatic function by causing inflammation, fibrosis, and destruction of lymphatics [13–15]. The Stemmer sign has a sensitivity of 92% to predict lymphedema in patients who have the disease and a specificity of 57% to exclude lymphedema in patients who do not have the condition. A negative Stemmer sign does not rule out lymphedema, typically in patients with a normal BMI and stage I disease [16].

Objective measurement of limb swelling can be problematic. On the other hand, assessing size differences of the extremities and quantitative discrepancies between the unaffected and the affected limbs is critical, particularly in the early phases of lymphedema. Estimating differences in limb volume has been used as an indirect measure of changes in lymph fluid volume over time or with treatment, and is typically done through circumferential measurements, or through immersion techniques based on the measurement of volume displacement [17]. However, these methods are time consuming and somewhat operator dependent. Moreover, since these techniques measure only the overall volume of the limbs, possible differences in volume caused by left-right dominance, asymmetrical muscle atrophy, fibrous tissue deposition, or weight gain may incorrectly be attributed to fluid accumulation [18].

Bioimpedance spectroscopy (BIS) is a noninvasive procedure wherein an electrical current is passed through a body segment, and impedance to flow of the current is measured. This technique, which attempts to directly measure lymph

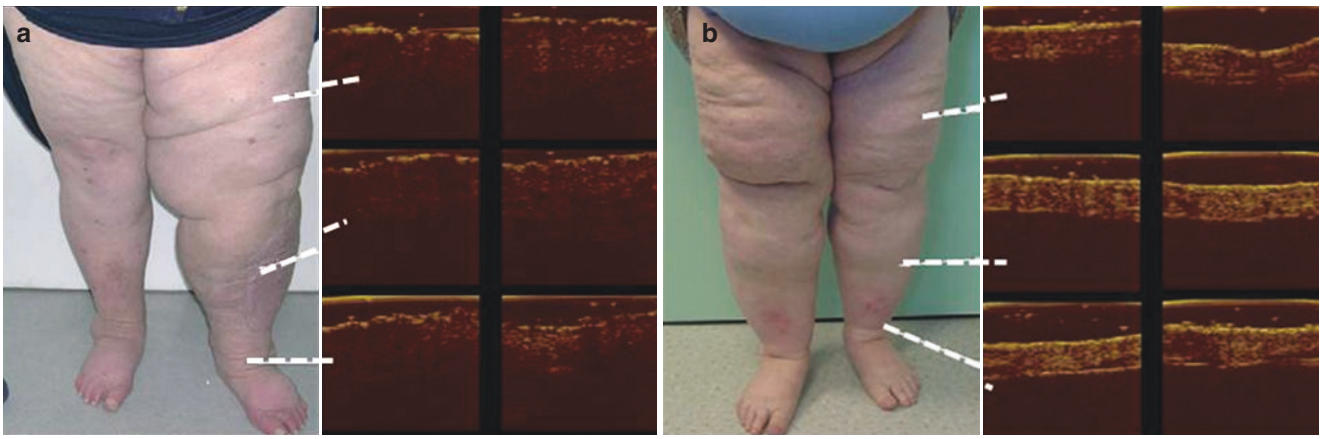

Fig. 5.1 Clinical appearance (left panel) and ultrasound pattern (right panel) in patients with lymphedema (**a**) or with lipedema (**b**). Increased volume of both lower limbs with predominant enlargement of the left is evident in the patient with lymphedema; the corresponding ultrasound examination indicates decreased echogenicity and increased thickness of the dermis. In the patient with lipedema increased lower limb volume is similarly evident, but with more pronounced symmetry; the corresponding ultrasound examination identifies normal echogenicity and thickness of the dermis, therefore confirming the diagnosis of lipedema versus lymphedema (*adapted from Naouri M* et al. [27])

fluid volume [19], is based on the principle that tissues such as fat and bone act as insulators, while electrolytic fluids conduct electricity; these features would make it possible to assess properties unique to lymphatic fluid, through measurement of the flow of current. BIS measures lymphedema based on the fact that low-frequency currents selectively pass through extracellular fluid compartments, whereas high-frequency currents pass through both the intra- and the extracellular fluids (the latter being selectively expanded in lymphedema) [20]. BIS analyzes both lymph fluid impedance and total fluid impedance [21], and impedance to current flow has been found to inversely correlate with fluid accumulation; therefore, reduced impedance values in an extremity indicate the presence of lymphedema.

Dual-energy X-ray absorptiometry (DEXA, or biphotonic absorptiometry) may help classify and define a lymphedematous limb but its greatest potential use may be to assess the chemical composition of limb swelling (especially increased fat deposition, which by its added weight can lead to muscle hypertrophy) [5].

A variety of other techniques have been described to measure limb edema, but most of them have not been validated or are either too complex or expensive for routine use [22, 23]. A practical difficulty in the clinical setting, even with validated techniques, is that extravascular fluid volume undergoes cyclic changes over days or weeks, and limb volume also has a pronounced circadian variation.

High-resolution cutaneous *ultrasonography* can be used to identify lymphedema, based on the presence of increased dermal thickness and decreased echogenicity as compared with lipedema and venous insufficiency [24]. In fact, in lymphedema loss of echogenicity of the skin and global and homogeneous dermal hypoechogenicity are observed, in contrast to the elective superficial dermis localization of edema described in patients with venous insufficiency [25, 26]. These findings are caused by the accumulation of protein-rich exudative interstitial fluid in the skin and subcutaneous tissue; this fluid remains trapped at the production site because of its high protein content, whereas transudate edema caused by venous insufficiency is more mobile and accumulates in the superficial dermis only. However, in order to analyze dermal changes for identifying and quantifying dermal edema, the ultrasound device should operate at 20 MHz [27]. Figure 5.1 shows the clinical and ultrasound appearance for patients with lymphedema and with lipedema, respectively.

Whenever the clinical diagnosis of lymphedema is controversial, it can be either confirmed or ruled out with lymphoscintigraphy, which is considered the method of choice to evaluate the lymphatic pathways and their drainage pattern [28]. Direct lymphangiography using an iodine oil contrast agent capable of visualizing the lymphatics [29] (Fig. 5.2) is no longer routinely performed, because it can lead to life-threatening complications and is difficult to perform [31].

A venous Doppler ultrasound examination is often required to assess for deep venous thrombosis or venous disease, which can be associated with lymphedema. In fact, 20–30% of the patients with advanced chronic venous disease have associated lymphatic dysfunction, presumably due to secondary damage from overload, or from recurrent cellulitis [32].

If filariasis is suspected, one can perform a blood smear (collected at night) looking for the presence of microfilariae. Antigen testing by immunochromatographic card test (Binax) or enzyme-linked immunosorbent assay (TropBio) is more sensitive than microfilaria detection, irrespective of the time of the day blood is drawn [33].

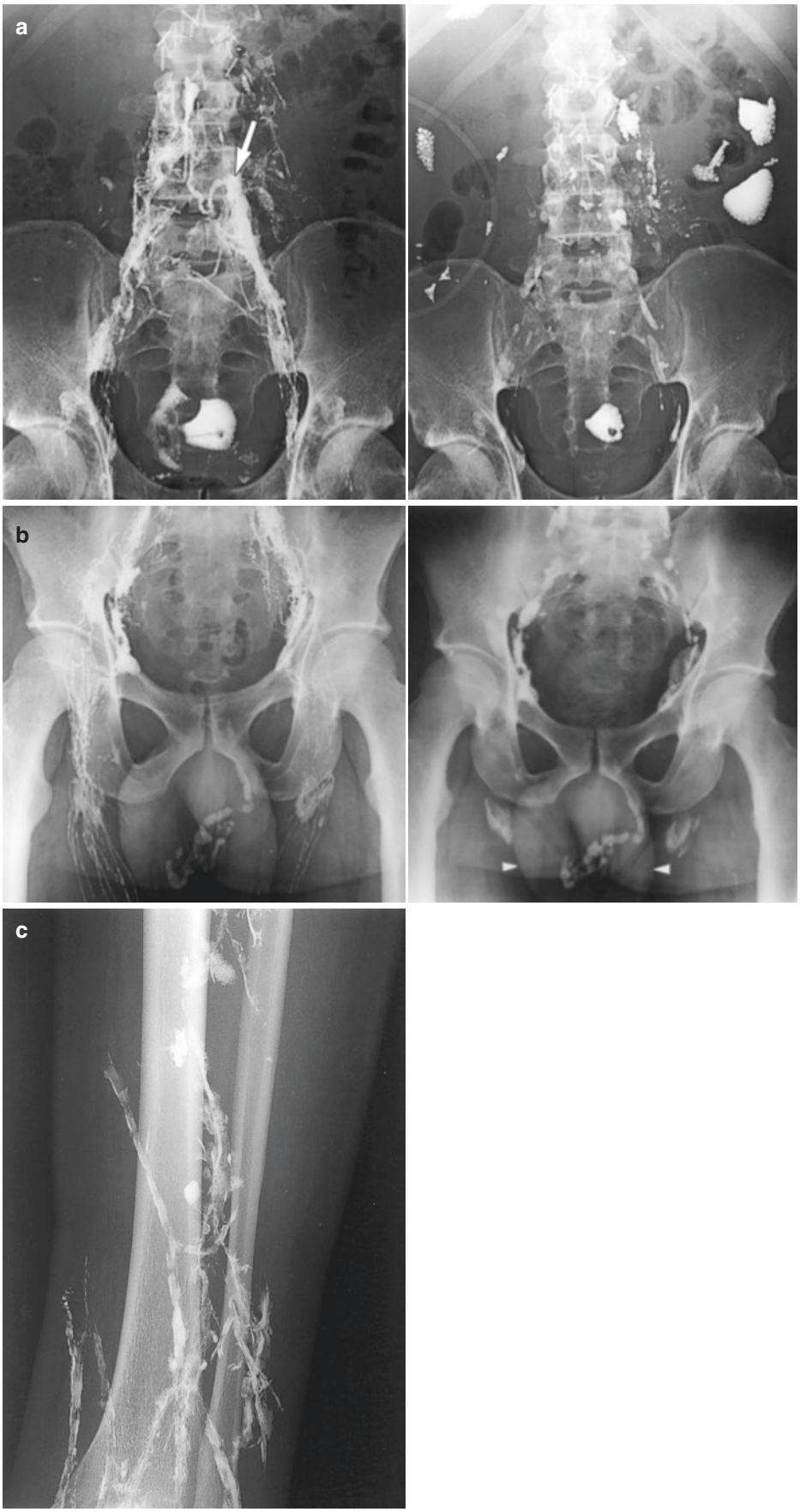

Fig. 5.2 (**a**) Iodine oil lymphogram in a patient with chylous ascites, affected by AIDS-related peritoneal tuberculosis. Images obtained during the filling phase (right panel) show peritoneal extravasation of the contrast material. The site of leakage is seen immediately to the left of L4 (arrow). Images obtained during the storage phase (left panel) show extensive leakage in the form of oily droplets within the peritoneal cavity. (**b**) External genitalia lymphedema of parasitic origin: images obtained during the filling phase (left panel) show filling of the scrotum by left-sided lymphatic reflux; images obtained during the lymph node phase at 24 h (right panel) show accumulation of contrast material in the scrotum (arrowheads). The lymph nodes are normal. (**c**) Edema of the left leg caused by aplasia of the lymphatic vessels. The lymphogram obtained immediately after administration of the contrast agent shows no lymphatic vessels, associated with perivascular extravasation. Lymphatic drainage of the contrast material occurs mainly along the venous vessel sheaths (*adapted from Guermazi A* et al [30])

In addition to a thorough clinical history and physical examination, other diagnostic tests to rule out alternative causes of lower extremity edema include a complete metabolic profile, serum albumin, and urinalysis to screen for renal failure, hypoalbuminemia, and/or protein-losing enteropathy.

Key Learning Points

- The Stemmer sign has 92% sensitivity to predict lymphedema in patients who have the disease and 57% specificity to exclude lymphedema in patients without lymphedema.
- The body mass index (BMI) is associated with both false-negative and false-positive Stemmer signs, as a high BMI can lead to a false-positive while a low BMI can lead to a false-negative Stemmer sign.
- Circumferential measurements, or immersion techniques based on displacement, can be used to measure the limb volume.
- Reduced impedance values in an extremity are correlated with lymphedema.
- DEXA may be used to assess the chemical composition of limb swelling, especially increased fat deposition and muscle hypertrophy.
- Ultrasonography can rule out lipedema and venous insufficiency. In lymphedema a loss of echogenicity of the skin and a global and homogeneous dermal hypoechogenicity are observed, in contrast to the elective superficial dermis localization of edema described in venous insufficiency.
- A venous Doppler ultrasound examination is often needed to assess for deep venous thrombosis or venous disease, which can be associated with lymphedema.
- A blood smear or an antigen test can be performed to rule out filariasis.
- A complete metabolic profile, serum albumin, and urinalysis to screen for renal failure, hypoalbuminemia, and/or protein-losing enteropathy may be necessary for a complete differential diagnosis of lymphedema.

5.4 Management of Lymphedema

As a chronic and potentially disabling condition, lymphedema is associated with significant morbidity in terms of functional, cosmetic, and emotional consequences. Treatment efforts aim at minimizing the associated swelling, at restoring cosmesis and functionality of the limb, and at preventing potential complications associated with lymphedema, in particular infections such as cellulitis and lymphangitis. Treatments are lengthy and expensive, and involve a multidisciplinary approach that can include rehabilitative therapy (elevation, exercise, compression devices, manual lymph drainage), skin care, and surgery [34, 35]. Therapy of peripheral lymphedema can be classified into conservative or nonoperative procedures and operative procedures.

Nonoperative treatment consists of physical therapy and adjuvants such as combined physical therapy and intermittent pneumatic pressure (or "pneumomassage"). Pneumomassage, thermal therapy, simple elevation (particularly by bed rest) of a lymphedematous limb, low-level laser therapy, and aquatic therapy/water-based exercise programs are the most common nonoperative procedures.

Drug therapies have so far been disappointing in the management of lymphedema. Although diuretic drugs are often prescribed, this therapy is actually not beneficial in lymphedema and should be employed only in patients with specific comorbidities or complications. Coumarin, a benzopyrone, has been reported to have some favorable effect on lymphedema, probably due to its mechanism of action that reduces vascular permeability, and thus capillary filtration. In addition, coumarin is thought to activate macrophage activity, which increases protein degradation, thus resulting in a reduction in fibrotic tissue. However, the clinical trials reported so far are generally of poor quality and long-term results of treatment of lymphedema with these agents are not available. Furthermore, some reports of hepatotoxicity have raised serious concern on their use [36]. Antibiotics should be administered for superimposed acute lymph stasis-related inflammations (cellulitis/lymphangitis or erysipelas) [5]. In case of lymphatic filariasis to eliminate microfilariae from the bloodstream, diethylcarbamazine, albendazole, or ivermectin is recommended [5]. Efficacy of boosting immunity by intra-arterial injection of autologous lymphocytes is unclear and requires independent, reproducible validation. Recent proposals for the use of anti-inflammatory drugs have not yet demonstrated efficacy and may face drawbacks if administered in the long term [5].

No special diet or restricted fluid intake has proved to be of therapeutic value for most uncomplicated peripheral lymphedemas. In breast cancer-related lymphedema and in obese patients, weight reduction has been shown to help. In chylous reflux syndromes a diet as low as possible or even free of long-chain triglycerides (absorbed via intestinal lacteals) and high in short- and medium-chain triglycerides is of benefit especially in children. Specific vitamin supplements may be needed in very low or no-fat diets. Some groups suggest diets with substances that may lower inflammation, but current clinical evidence is not sufficiently validated [5].

In complicated patients with lymphatic system overgrowth such as lymphangiodysplasia, specialized centers utilize pharmacotherapeutic options such as octreotide, OK-432, rapamycin, or other antiproliferative agents, in particular in newborns and children [5].

Surgical procedures aim to alleviate peripheral lymphedema by enhancing lymph return. When performed in

advanced stages, surgery usually requires long-term combined physical therapy and/or other "pneumomassage" after the procedure to maintain edema reduction and ensure vascular/shunt patency.

Worldwide, surgical resection (in several forms) is the most widely used operative technique to reduce the bulk of lymphedema, in particularly in cases affecting the genitalia. Microsurgical procedures include (1) derivative methods such as lympho-venous anastomoses and (2) multiple lymphatic-venous anastomoses in a single surgical site with both the superficial and deep lymphatics. By these procedures a positive pressure gradient (lymphatic-venous) is created, thus evading the phenomenon of gravitational reflux without interrupting the distal peripheral superficial lymphatic pathways. Reconstructive methods are sophisticated techniques involving the use of a lymphatic collector (LLA) or an interposition vein segment (LVLA) to restore lymphatic continuity in lymphedema conditions due to a locally interrupted lymphatic system. Autologous lymph vessel transplantation mimics the normal physiology and has shown long-term patencies of more than 10 years. This procedure has generally been reserved to patients with unilateral peripheral lymphedema of the leg (due to the need for one healthy leg to harvest the graft), but it has also been utilized for bilateral upper extremity lymphedema where two healthy legs are available for harvesting lymphatic vessels [5].

Transplantation of superficial lymph nodes from an uninvolved area together with its vascular supply (vascularized lymph node transplantation) to the site of lymphadenectomy for cancer has been proposed both as a preventive and therapeutic approach to limb lymphedema. Liposuction (or suction-assisted lipectomy) using a variety of methods has been shown to completely reduce non-pitting, primarily non-fibrotic, extremity lymphedema due to excess fat deposition that has not responded to nonoperative therapy in both primary and secondary lymphedemas [5]. Surgical resection by "debulking" of excess skin and subcutaneous tissue of the lymphedematous limb can be associated with complications such as superficial lymphatic removal, significant scarring, risk of infection, and difficult wound healing. Debulking has been used mainly in the treatment of the most severe forms of fibrosclerotic lymphedema (elephantiasis) and in cases of advanced genital lymphedema. Caution should be exercised in removing enlarged lymph nodes or soft-tissue masses (e.g., lymphangiomas) in the affected extremity, as lymphedema may worsen thereafter [5].

The implantation of engineering/lymphatic tubes to transport lymph or engineered tubes/devices to promote new substitute lymphatic growth have not yet documented long-term value in large-scale studies, and these techniques are currently under controlled clinical investigation [5].

Omental transposition, enteromesenteric bridge operations, and implantation of threads to promote perilymphatic spaces (substitute lymphatics) have not shown long-term value and at the moment should not be considered as valid surgical options [5].

Key Learning Points

- Lymphedema is associated with significant morbidity including functional, cosmetic, and emotional consequences.
- Therapy is based on a multidisciplinary approach including rehabilitative therapy, skin care, and surgery.
- Nonoperative treatments consist of physical therapy and adjuvants.
- Medical treatments (diuretics, coumarin), diet, or restricted fluid intake is of limited value in patients with peripheral lymphedema.
- Surgical procedures aim to alleviate peripheral lymphedema by enhancing lymph return.
- Surgery usually requires long-term combined physical therapy and/or other "pneumomassage" treatments after the procedure.
- Surgical resection (in several forms) is the most widely used operative technique to reduce the bulk of lymphedema.
- Microsurgical procedures include (1) derivative methods such as lymphatic-venous anastomoses and (2) multiple lymphatic-venous anastomoses in a single surgical site with both the superficial and deep lymphatics.
- Sophisticated reconstructive techniques involve the use of a lymphatic collector or an interposition vein segment to restore lymphatic continuity.
- Liposuction has been shown to completely reduce non-pitting, primarily non-fibrotic, in patients with extremity lymphedema.
- Debulking has been used mainly in the treatment of the most severe forms of fibrosclerotic lymphedema (elephantiasis) and in cases of advanced genital lymphedema.
- The implantation of engineering/lymphatic tubes to transport lymph or engineered tubes/devices is currently under clinical investigation.
- Omental transposition, enteromesenteric bridge operations, and implantation of threads to promote perilymphatic spaces have not shown long-term value and at the moment should not be considered as valid surgical options.

5.5 Lymphoscintigraphy in the Management of Lymphedema

Qualitative and quantitative lymphoscintigraphy has been widely used for the differential diagnosis of lymphedema, for predicting the risk to develop lymphedema as well as for assessing the efficacy of physical and/or surgical treatments.

5.5.1 Lymphoscintigraphy for the Differential Diagnosis of Lymphedema

Lymphoscintigraphy has proved extremely useful for depicting the specific lymphatic abnormality and it has largely replaced conventional oil contrast lymphography for visualizing the lymphatic network. Although different protocols can be used (different radiotracers and administered activities, different injection volumes, intracutaneous versus subcutaneous or subfascial injections, one or more injections, different protocols of passive and active physical activity, varying imaging times, static and/or dynamic techniques—as discussed in detail in Chap. 4), the images, which can be easily repeated, offer remarkable insight into lymphatic structural abnormalities and (dys)function. Lymphoscintigraphy provides a functional assessment of lymphatic pumping, stasis, and obstruction that guides treatment and determines prognosis for expected outcome of treatment [37–40]. Lymphoscintigraphy is also employed to define the clinical characteristics, investigations, management, and outcomes of lymphedema in pediatric patients [41]. Purely qualitative analysis has been reported to be very accurate for confirming or excluding the diagnosis of lymphedema, with sensitivity as high as 92–96% and specificity as high as 100% [42]. Nevertheless, etiology of lymphedema is not invariably identified solely on the basis of lymphoscintigraphic images. In fact, despite the fact that patients with primary lymphedema tend to show a lack of lymphatic vessels and absent or delayed transport whereas those with secondary lymphedema tend to show obstruction with visualization of discrete lymphatic trunks and slow transport [43], primary lymphedema cannot be reliably differentiated from secondary lymphedema on the basis of lymphoscintigraphic findings alone [44].

For the lower limbs, a high positive association of popliteal lymph node uptake with the severity of lymphatic obstruction defined as appearance of dermal back flow was found in patients with both primary and secondary lymphedema [45, 46]. The duration of lymphedema was also longer in patients with dermal backflow and popliteal lymph nodes visualized during lymphoscintigraphy; both popliteal lymph node uptake and dermal backflow were important signs indicating longer disease duration and higher severity of lymphatic dysfunction [46]. In addition, a strong association between skin rerouting and popliteal lymph node visualization has been found; in particular, skin changes were detected in 38% of the patients with positive popliteal node uptake [45].

A recent study showed that transit time and dermal backflow at lymphoscintigraphy (found in about 97% of extremities by 45 min postinjection) did not predict clinical severity when adjusted for other clinical variables [47]. A subgroup analysis of a large study showed that false-negative lymphoscintigraphy occurs most likely in primary lymphedema with long duration of disease and infection history similar to patients with true-positive lymphoscintigraphy. However, repeated lymphoscintigraphies over time during follow-up showed appearance of lymphatic dysfunction consistent with lymphedema. Therefore, the results of this study suggest that patients with a high clinical suspicion of lymphedema and a normal lymphoscintigram are better treated conservatively, and that lymphoscintigraphy should be repeated in these cases [48].

Key Learning Points

- Qualitative and quantitative lymphoscintigraphy has been widely used for the differential diagnosis of lymphedema, for predicting the risk to develop lymphedema as well as for assessing the efficacy treatments, as it provides a functional assessment of lymphatic pumping, stasis, and obstruction in adults as well as in pediatric patients.
- Qualitative analysis of lymphoscintigraphy has 92–96% sensitivity and specificity close to 100% for the diagnosis of lymphedema.
- Primary lymphedema cannot be reliably differentiated from secondary lymphedema on the basis of lymphoscintigraphic examination alone.
- For the lower limbs, a high positive association of popliteal lymph node uptake with the dermal back flow was found in patients with both primary and secondary lymphedema.
- The duration of lymphedema is longer in patients with dermal back flow and popliteal lymph nodes visualized during lymphoscintigraphy.
- Patient with a high clinical suspicion of lymphedema and a normal lymphoscintigram are better treated conservatively; lymphoscintigraphy should be repeated in these cases to show the underlying lymphatic dysfunction.

5.5.1.1 Lymphoscintigraphy in Lipedema

In a recent study [49] in a prospective cohort study of women meeting the clinical criteria of lipedema, lymphoscintigraphy showed abnormal patterns in 47% of the patients, with no significant differences between the severity of lymphoscintigraphic abnormalities and clinical stage of lipedema. In addition, lymphoscintigraphic findings showed that patients with lipedema also presented impaired lymphatic transport assessed as transport index (TI) abnormalities. In addition, more severe lipedema may be associated with greater lymphatic transport abnormalities, with the mean TI being significantly greater for extremities with severe (stage 3/4) lipedema than those with mild or moderate (stage 1/2) lipedema (15.1 versus 9.7, $P = 0.049$). Mean difference in TI scores between each lower extremity for individual patients was 6.43 (±7.96 standard deviation) [50].

Key Learning Points

- Approximately 47% of patients with clinical lipedema have lymphoscintigraphic abnormalities indicating impaired lymphatic drainage.
- More severe lipedema may be associated with greater abnormalities in lymphatic transport.

5.5.1.2 Lymphoscintigraphy for Predicting the Risk to Develop Lymphedema

Lymphoscintigraphy can be used to predict the risk to develop lymphedema. In fact, in patients undergoing surgery for breast cancer, abnormalities of lymphatic drainage in postsurgical lymphoscintigraphy increases the risk of developing arm lymphedema [51–53]. It has also been shown that upper extremity lymphatic drainage after axillary lymph node dissection is not impaired in terms of lymphatic transport and/or venous function impairment after the axillary lymph node dissection procedure in comparison to the preoperative status. Qualitative analysis of lymphoscintigrams revealed most commonly disappearance of previously functioning lymph nodes and appearance of dermal backflow in subjects who developed lymphedema thereafter. Conversely, appearance of functioning lymph nodes in different locations after axillary lymph node dissection may indicate protection from development of upper extremity lymphedema [54]. In the postoperative period after breast surgery, a significant worsening of the degree of lymph node uptake and the velocity of lymph node visualization in the absence of dermal backflow and collateral circulation was observed, independently of postoperative complications or clinical characteristics [55]. On the contrary, the maximum lymphatic-pump pressure in the women who later developed breast cancer-related lymphedema was 1.7-fold higher than in those who did not develop lymphedema. Moreover, the rate of lymph tracer transport into the forearm was 2.2-fold greater in the women who later developed lymphedema [56]. Quantitative lymphoscintigraphy performed between 4 and 8 weeks after surgery to evaluate the lymphatic system in the early postoperative period, to be correlated with clinical results at the 1-year follow-up, revealed that the ratio of radiocolloid uptake rate of the affected to normal axilla and the ratio of radioactivity of the affected to normal axilla were significantly lower in the lymphedema group than in the non-lymphedema group. After adjusting the model for all significant variables (body mass index, N-stage, T-stage, type of surgery, and type of lymph node surgery), the ratio of radioactivity of the affected to normal axilla was associated with lymphedema (odds ratio = 0.14; 95% confidence interval, 0.04–0.46; $P = 0.001$) [57]. Similarly, functional lymphatic changes detected by lymphoscintigraphy after external beam radiation therapy can predict the development of arm lymphedema. Recently, lymphoscintigraphy including SPECT/CT of the axillary region has been employed to evaluate the impact of including, as target volumes in the radiation treatment plan, lymph nodes involved in arm drainage that could affect lymphedema [53]. This study demonstrated that radiation doses to these lymph nodes vary between zero and the full prescribed dose, therefore possibly affecting the development of lymphedema.

In patients with gynecological cancer-related lymphedema the prognostic assessment of qualitative lymphoscintigraphy before complex decompressive therapy showed that severity of dermal back flow, clinical stage, and therapy compliance are independent predictors of therapeutic response [58].

In patients undergoing surgery for melanoma of the trunk, primary prevention with microsurgical lympho-venous anastomosis prevented lymphedema after inguinal lymphadenectomy. In addition, lymphatic-venous multiple anastomoses proved to be successful for treating clinical lymphedema, particularly at the early stages [59]. Similar results have also been reported for patients with breast cancer [60, 61]. In addition, when lymphoscintigraphies performed in patients who underwent lymph node dissection (limited to the intra-abdominal lymph nodes) with or without radiotherapy for histologically confirmed ovarian, uterine, or prostate cancer were compared to lymphoscintigraphies obtained in patients with primary lower limb lymphedema, the appearance of lower limb lymphedema does not appear to be related to cancer treatment(s), but rather lower limb lymphedema may represent the development of a primary lymphatic disease that was latent prior to surgery [62].

The lack of visualization of inguinal lymph nodes predicted late postoperative leg edema also in patients with tibial fractures treated surgically [63].

Key Learning Points

- In patients undergoing surgery for breast cancer, lymphoscintigraphy shows disappearance of previously functional lymph nodes and appearance of dermal backflow in subjects who developed lymphedema, while appearance of functional lymph nodes in different locations after surgery indicates protection from the development of upper extremity lymphedema.
- Quantitative lymphoscintigraphy shows that the ratio of radioactivity of the affected to normal axilla is significantly lower in the lymphedema patients.
- Severity of dermal back flow, clinical stage, and therapy compliance are independent predictors of therapeutic response in patients with gynecological cancer-related lymphedema before complex decongestive therapy.
- In patients submitted to intra-abdominal lymph node dissection for histologically confirmed cancer, the appearance of lower limb lymphedema seems to be correlated with the development of a primary lymphatic disease that was latent prior to the therapeutic interventions.

5.5.1.3 Lymphoscintigraphy for Assessing the Efficacy of Physical and/or Surgical Treatments

Lymphoscintigraphy has been used in the assessment of interventional approaches in patients with lymphedema, including manual lymphatic massage [64–69], pneumatic compression [70–72], hyperthermia [73], pharmacologic therapies [74, 75], and surgery (both microsurgery [76–79] and vascularized lymph node transplantation [80]).

In women undergoing therapy for postmastectomy lymphedema, the degree of lymphatic function impairment prior to the treatment as assessed by lymphoscintigraphy correlates inversely with the outcome of manual lymphatic therapy [37]. Similarly, in patients with clinical stage I unilateral extremity lymphedema, lymphoscintigraphy can predict long-term response to multi-approach physical therapy. In this regard, the visualization of a main lymphatic vessel without collateral lymphatic vessels was the best predictor for a favorable response [81], as also was persisting lymph node visualization 4 h after radiocolloid administration [82].

In a recent study, the extent of dermal backflow (small extent/large extent), the level of lymphatic flow (trunk flow pattern/upper arm-restricted pattern/forearm-restricted pattern groups), and the visualization of lymph nodes (visualized/non-visualized) at lymphoscintigraphy were correlated with the change in the circumferential difference between the two sides of the body, the upper arm and forearm, with the clinical outcome being variable in patients undergoing nonsurgical treatment. Upper arm edema was more significantly reduced after sympathetic ganglion block rather than after complex decongestive therapy in the small extent group, the forearm-restricted pattern group, and the non-visualized group. In the other groups, sympathetic ganglion block and complex decongestive therapy showed comparable therapeutic effects without statistical differences [83]. Lymphatic regeneration following both free-tissue [84] and lymphatic vessel transplantation [85] has also been assessed with lymphoscintigraphy. Additionally, lymphoscintigraphic classification of patients with secondary lymphedema correlates closely with the clinical stage scale and with findings at intraoperative examination during lymphatico-venous anastomosis [86]. In unilateral lymphedema, lymphoscintigraphic abnormalities of the contralateral limb may also be demonstrated in about 32% of patients [87]. The changes in clinical symptoms and the postoperative lymphoscintigraphic changes did not always correspond. However, there was a trend for the percentage of lymphoscintigraphic deterioration to be greater in the group with clinical deterioration [88].

An improvement of the transport index, well correlated with arm's volume reduction, was observed during long-term follow-up of patients with lymphedema treated with autologous lymph vessel transplantation, confirming that this procedure indeed improves lymph drainage [89, 90]. Similarly, postoperative lymphoscintigraphy showed improved lymphatic drainage in all cases of lymphedema submitted to a combined double-gastroepiploic vascularized lymph node transfer and a modified radical reduction with preservation of perforator vessels [80, 91].

The indications for lymphoscintigraphy can schematically be summarized as follows:

- Differential diagnosis of edema to distinguish venous from lymphatic etiology
- Assessment of pathways of lymphatic drainage
- Quantitation of lymph flow
- Identification of patients at high risk of developing lymphedema following axillary lymph node dissection
- Evaluation of the efficacy therapeutic interventions for lymphedema

Lymphoscintigraphy with ^{99m}Tc-sulfur colloid has recently been compared to the diagnostic performance of a new technique, PET/CT after interstitial injection of ^{68}Ga-labeled NOTA Blue Evans (^{68}Ga-NEB) [92]. This study showed that ^{68}Ga-NEB activity could be clearly observed in the lymphatic route on the PET/CT images from all the patients, showing consistent results in 8/13 cases; diagnostic images of ^{68}Ga-NEB PET/CT were obtained much faster than the conventional lymphoscintigraphic images. In the

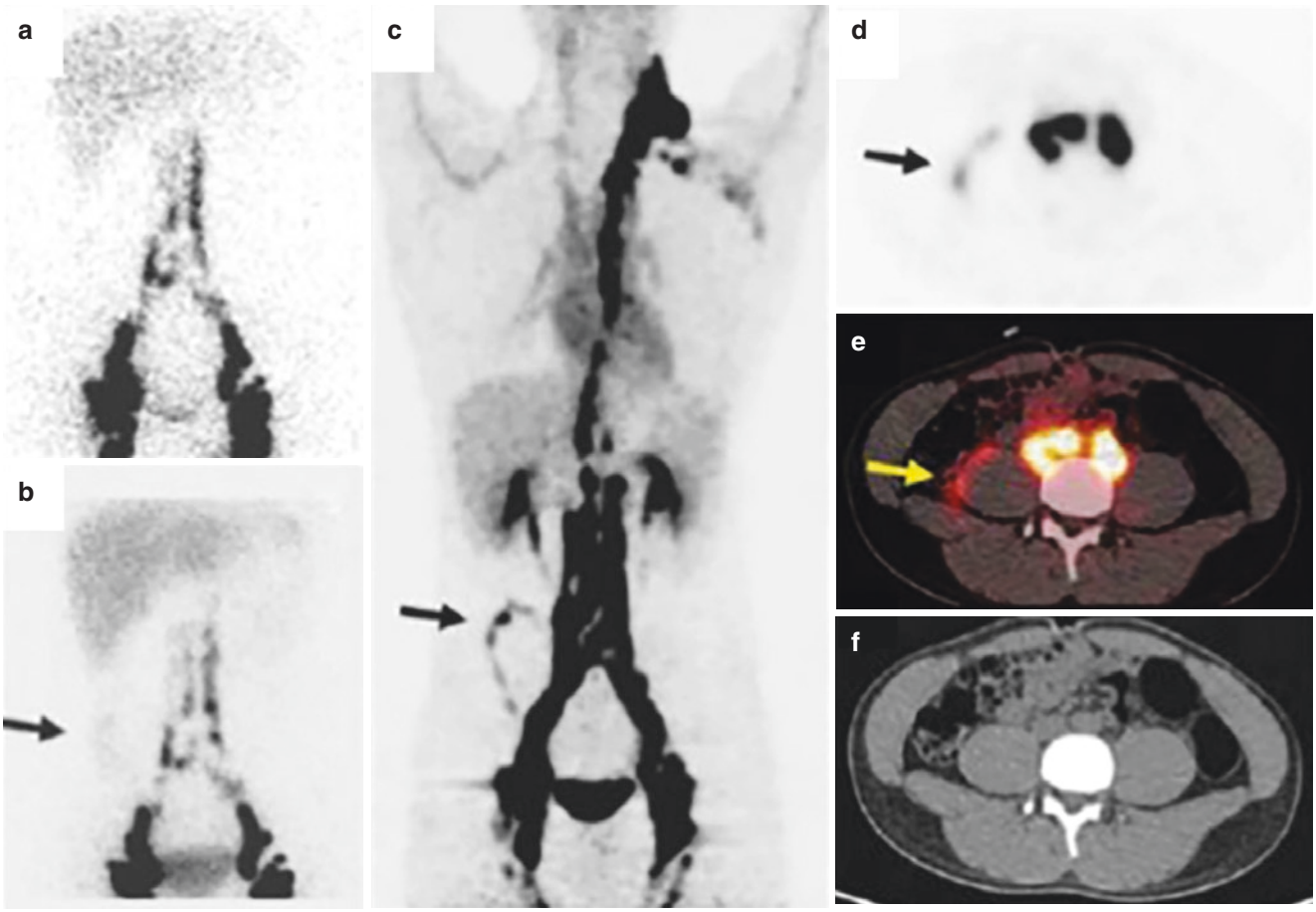

Fig. 5.3 A 17-year-old man (patient 4) with abdominal discomfort for more than 6 months. Chylous ascites was suspected, and nuclear medicine was consulted. ^{99m}Tc-sulfur colloid anterior image of the abdomen acquired 60 min after injection (**a**) was unremarkable. The image acquired 6 h after injection (**b**), however, revealed diffuse, mild radioactivity on the right side of the lower abdomen (arrow). In the ^{68}Ga-NEB MIP image (**c**) acquired 5 min after tracer injection, clear linear activity (arrow) could be seen in the right abdomen. In transaxial PET (**d**), fusion (**e**), and CT (**f**) images, this activity (arrows) was located in the immediate anterolateral border of the right psoas muscle, indicating the site of the chyle leak. Intense activity in the inguinal, iliac, and paraspinal lymph nodes and thoracic duct was also better appreciated in ^{68}Ga-NEB PET/CT images (*adapted from Zhang W* et al. [92])

remaining five cases, ^{68}Ga-NEB PET/CT provided additional information in five patients (38.5% of the whole group under study). In particular, one patient had chyloperitoneum, two had chylothorax, and one had postsurgical limp swelling; ^{99m}Tc-sulfur colloid lymphoscintigraphy was unable to localize the site of chyle leak, whereas ^{68}Ga-NEB PET/CT successfully identified the leak (Figs. 5.3, 5.4, and 5.5). In addition, in a young woman who had cystic lesions and pleural effusion, the site of chest abnormality was visualized on ^{68}Ga-NEB PET/CT but not on ^{99m}Tc-sulfur colloid lymphoscintigraphy (Fig. 5.6). Therefore, this study suggests the feasibility of using of ^{68}Ga-NEB PET/CT as an alternative to conventional lymphoscintigraphy in the evaluation of lymphatic disorders.

Key Learning Points

- Lymphoscintigraphy has been used to assess interventional approaches in patients with lymphedema, including manual lymphatic massage, pneumatic compression, hyperthermia, pharmacologic therapies, and surgery, both microsurgery and vascularized lymph node transplantation.
- In women undergoing therapy for postmastectomy lymphedema, the degree of lymphatic function impairment prior to the treatment as assessed by lymphoscintigraphy correlates inversely with the outcome of manual lymphatic therapy.

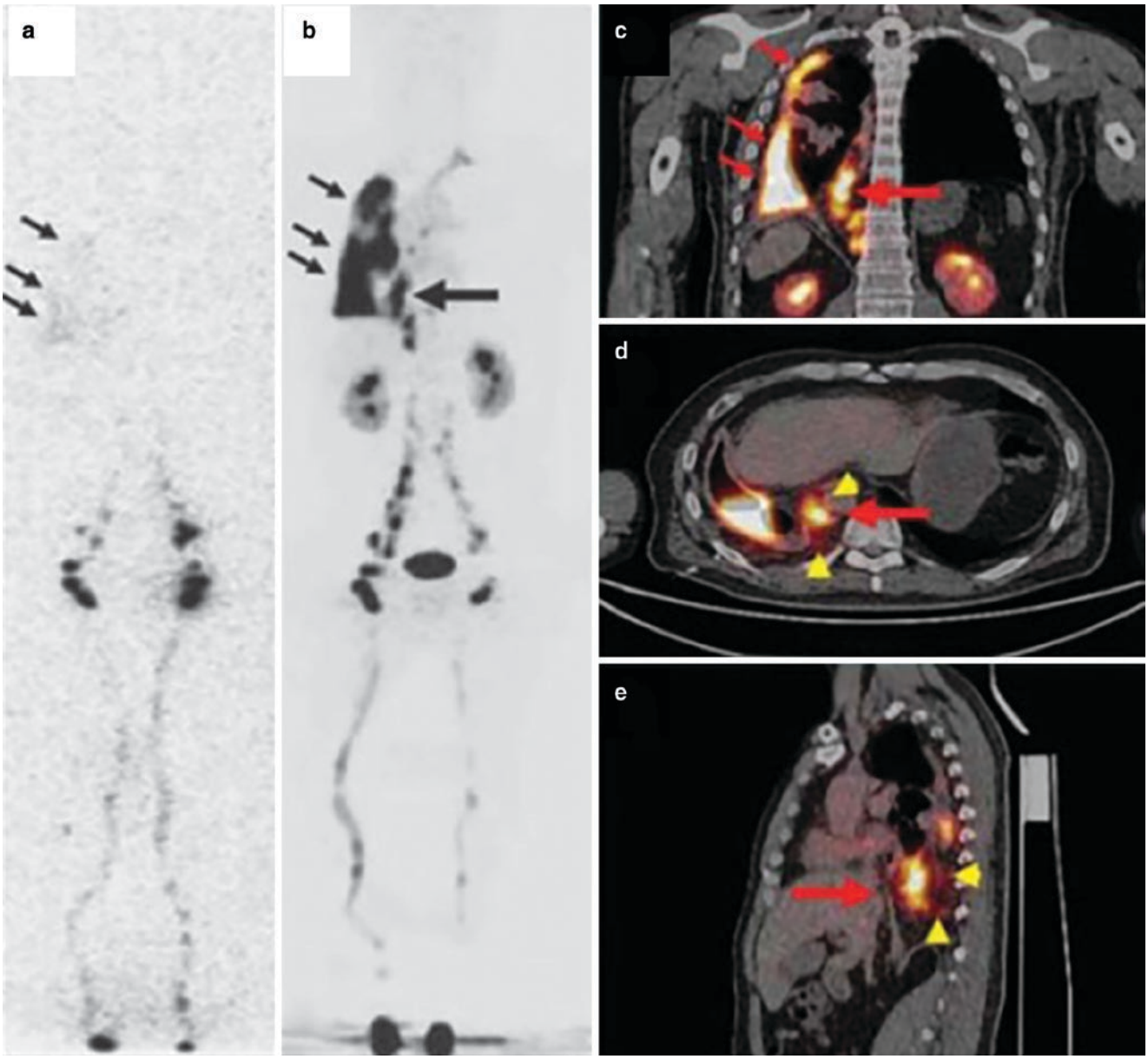

Fig. 5.4 A 43-year-old man with right-side persistent pleural effusion (patient 3). The patient had a remote history of motor vehicle accident. Laboratory examination of the fluid after thoracocentesis demonstrated chylothorax. ^{99m}Tc-sulfur colloid scintigraphy (**a**) revealed diffuse, mild activity in the right chest, consistent with the clinical findings of right chylothorax. However, the potential site of the chyle leak could not be identified. In comparison, ^{68}Ga-NEB PET/CT (**b**: MIP; **c**: coronal fusion; **d**: axial fusion; **e**: sagittal fusion) not only showed activity in the right-chest pleural effusion (small arrows), but also clearly revealed an additional vertically linear intense activity (large arrow) centered in the dilated thoracic duct and cisterna chyli with mild activity surrounding (arrowheads), consistent with the site of the leak (*adapted from Zhang W* et al. [92])

- In patients with clinical stage I unilateral extremity lymphedema the visualization of a main lymphatic vessel without collateral lymphatic vessels at lymphoscintigraphy is the best predictor of long-term response to multi-approach physical therapy.

- ^{68}Ga-NEB PET/CT provides more information than lymphoscintigraphy with ^{99m}Tc-sulfur colloid, is faster than conventional lymphoscintigraphy, and is able to localize the site of the leak especially inside the thorax and abdomen.

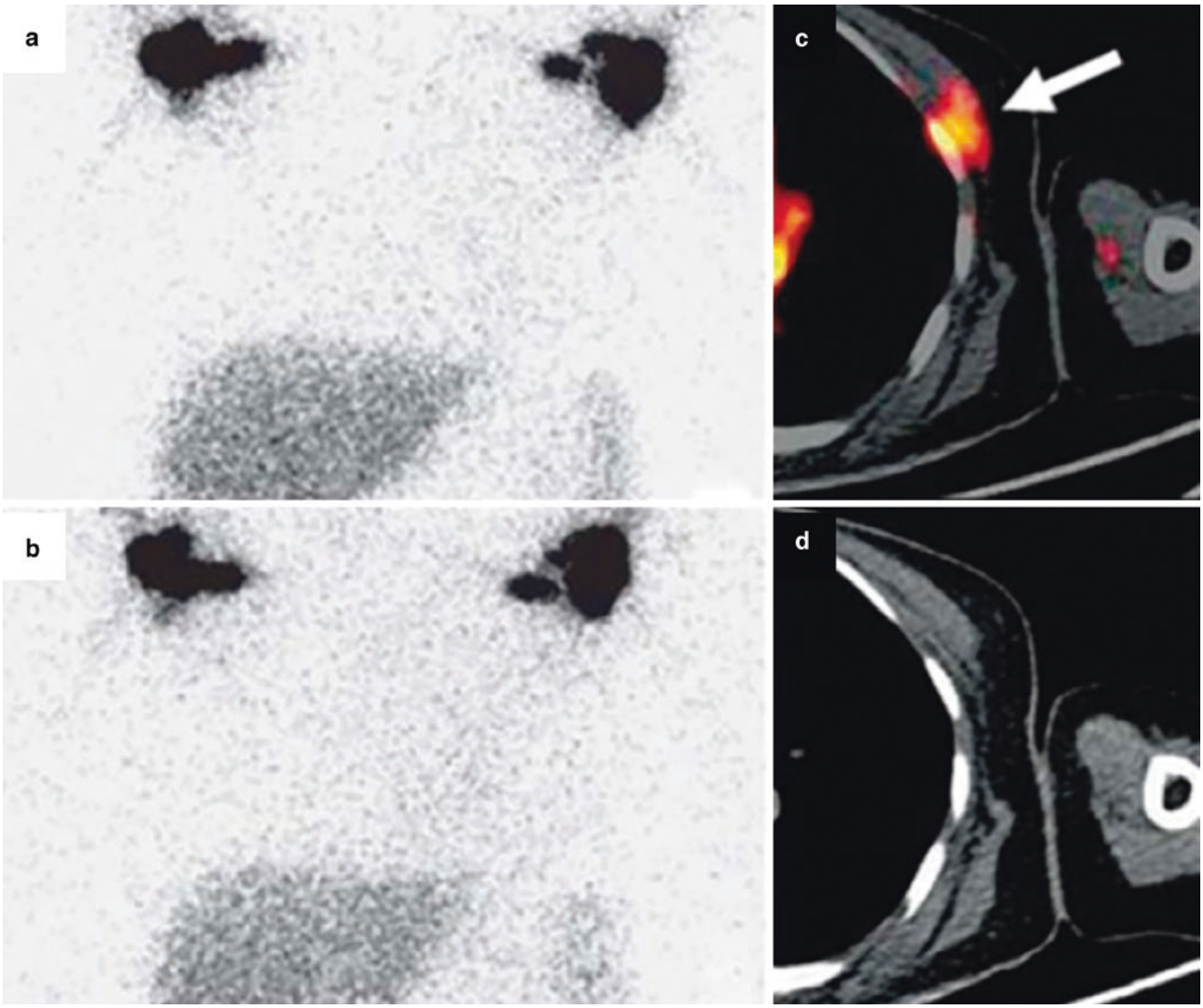

Fig. 5.5 Anterior ^{99m}Tc-sulfur colloid (SC) images were acquired at 2 h (**a**) and 6 h (**b**) after subcutaneous tracer injection between the thumb and index finger of the hands in a 44-year-old woman (patient 1) who had left-chest swelling and was status post-left mastectomy for breast cancer. The images revealed axillary lymph nodes bilaterally and minimally more tracer activity in the left chest without evidence of the site of the leak. In comparison, the transaxial images (**c**: fusion; **d**: CT) of the ^{68}Ga-NEB PET/CT acquired at 30 min after injection demonstrated a focal activity (arrow) underneath the left pectoralis major muscle, at the level of the left anterior fourth rib, indicating the site of the chyle leak (*adapted from Zhang W* et al. [92])

5.6 X-Ray Computed Tomography and Magnetic Resonance Imaging

X-ray computed tomography (CT) scanning or magnetic resonance imaging (MRI) of the lower extremities can detect in patients with lymphedema a "honeycomb" pattern of the subcutaneous tissue that is not characteristic of other types of edema. CT and MRI have been used to describe the morphologic changes due to the subcutaneous lipomatous hypertrophy [93–96].

CT-lymphography (CT-LG) was performed in patients with upper limb lymphedema [97]. Three-dimensional observation of deeper tissues at CT-LG has been used to help elucidating the mechanism of dermal backflow. According to the data obtained by Yamada et al. [98], lymphatic vessels that branch from collecting lymphatic vessels toward the dermis have an inner diameter wide enough to be confirmed with CT (Fig. 5.7). This was likely the observation of lymph flowing back to new or existing abnormal lymphatic vessels as it moves toward the dermis. From there, lymph flows back through capillary lymphatic vessels, leading to its storage in interstitial spaces (Fig. 5.8). It is unclear why such a phenomenon occurs there, but due to upstream blockage or increased internal pressure of lymphatic vessels, lymph appears to flow back from deeper areas to shallower areas, as if to escape [98].

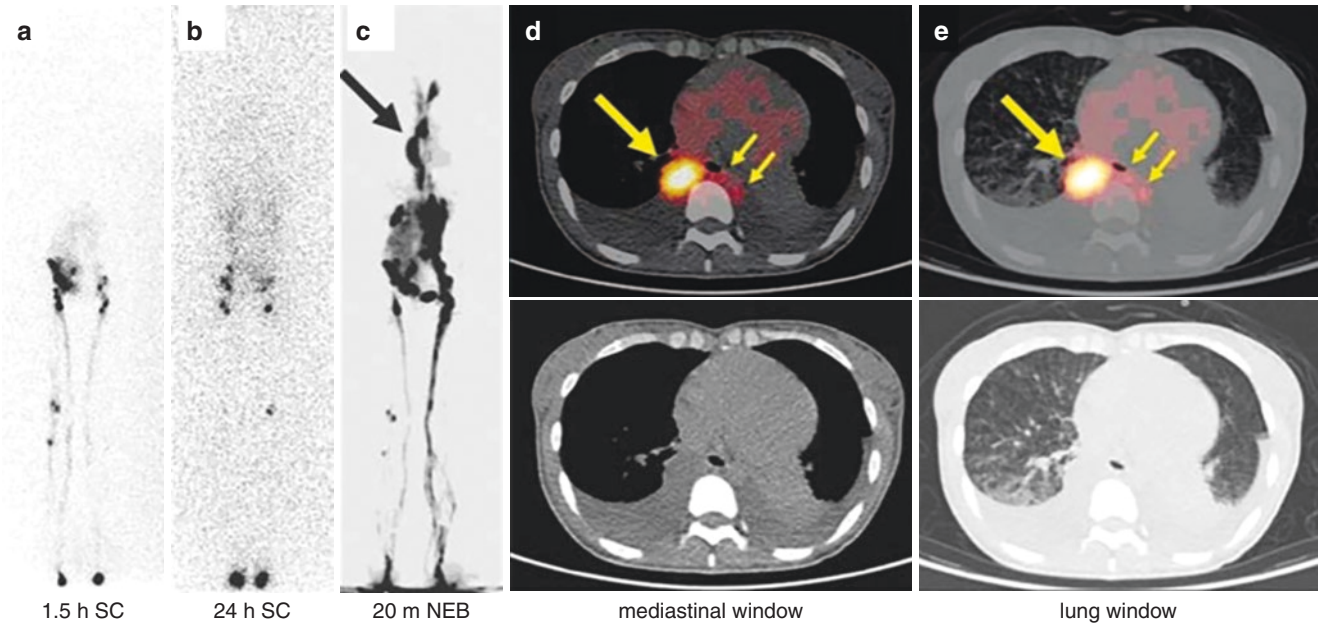

Fig. 5.6 A 25-year-old woman presented with shortness of breath for 3 months (patient 11). A diagnostic CT (images not shown) revealed many cystic structures in the chest, abdomen, and pelvis. In addition, bilateral pleural effusion was noted, which was subsequently shown as chylothorax. For this reason, lymphoscintigraphy was performed. The ^{99m}Tc-sulfur colloid (SC) images at 1.5 h (**a**) and 24 h (**b**) after injection in the feet both showed that the tracer reached abdomen/pelvis without much chest activity. However, in ^{68}Ga-NEB MIP PET image (**c**) acquired 20 min after tracer injection, there was clear, intense vertical activity (large arrow) in the thorax. In transaxial images (**d**: mediastinal window; **e**: lung window), the vertical activity was in an enlarged thoracic duct (large arrows). The chyle leak (small arrows) from the thoracic duct to the left chest was also noted. There were also many small cysts in both lungs (**e**) (*adapted from Zhang W* et al. [92])

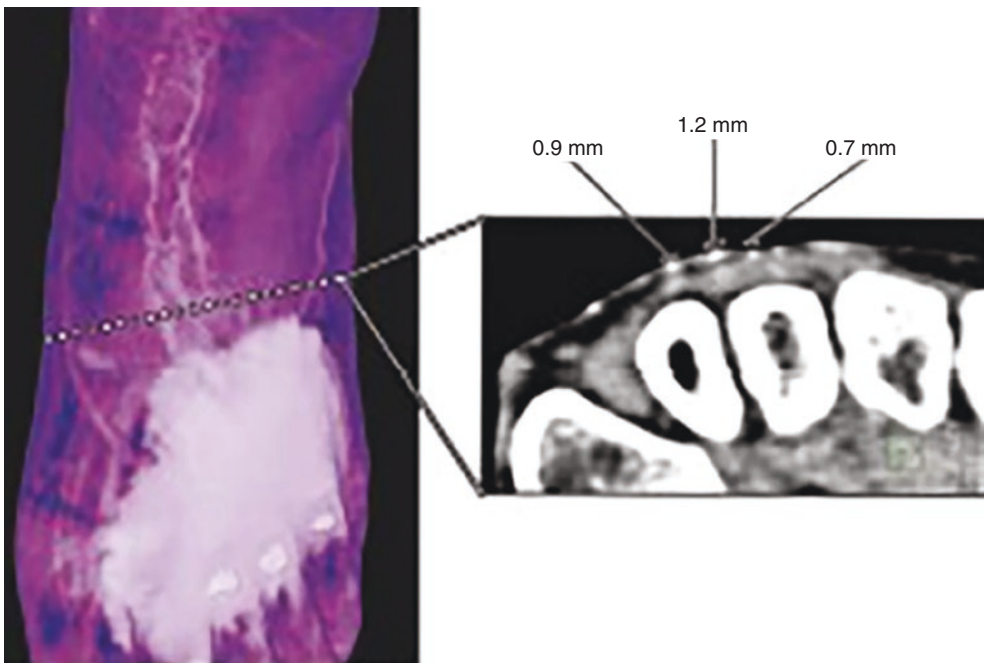

Fig. 5.7 Three-dimensional imaging of lymphatic system. In the images (left: 3D reconstructed image, right: 1-mm-slice image), lymphatic vessels were clearly identified with higher contrast than surrounding tissues, and the diameters were measured (*adapted from Yamada K* et al. [98])

High-resolution magnetic resonance lymphangiography (MRL) following interstitial, intracutaneous injection of an extracellular, paramagnetic contrast agent has recently been proposed for identifying abnormal lymphatic pathways [99–101]. This technique, that has proved to be technically feasible in patients with primary or secondary lymphedema [63, 102, 103], visualizes the lymphatic vessels in a limb with lymph flow disturbances, but not the lymphatic vessels of a healthy limb. This is most probably due to the faster lymph flow speed in the healthy limb. Therefore, lymph circulation disorders should be suspected when contrast-enhanced lymphatic vessels are visualized with this test. Migration of the

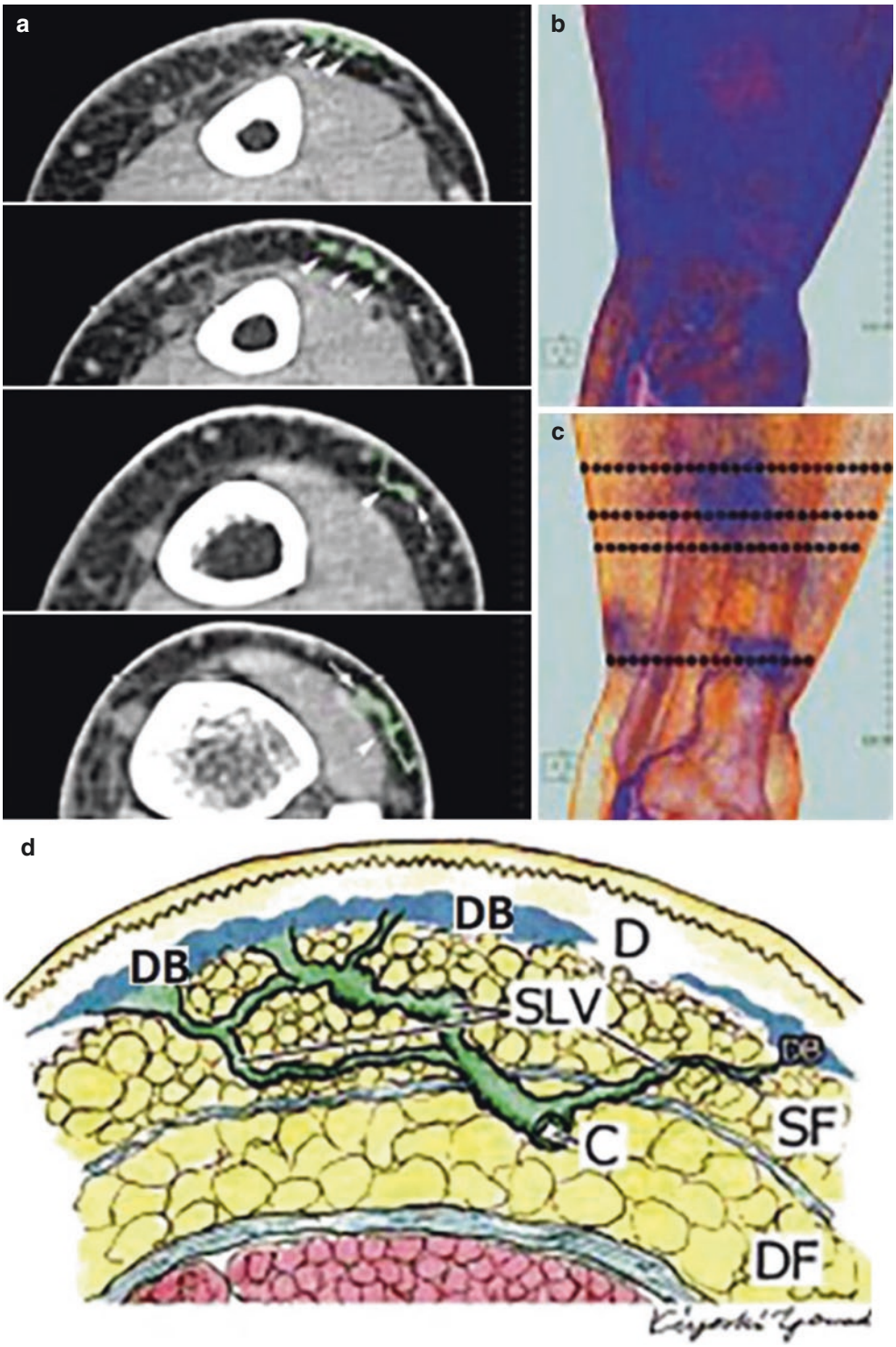

Fig. 5.8 Detailed analysis of dermal backflow (DB) sites with CT-LG. Slice images (**a**, 1–4 from top to bottom) show some collecting lymphatic vessels (arrow) branching upward and medially toward the dermis (arrowhead), transitioning to the DB. In the representative high-contrast 3D image (**b**), lymphatic vessels were hidden under DB and could not be observed, but in the representative lower-contrast 3D image (**c**, where horizontal lines indicate the level of transaxial sections shown in ((**a**), lymphatic vessels that were previously hidden under the DB could now be recognized. Panel (**d**) is a schematic representation of DB: *C* Collector, *SLV*, small lymphatic vessel; *D*, dermis; *SF*, superficial fat layer; *DF*, deep fat layer; *DB* (blue area in the dermis), dermal backflow. (*Adapted from Yamada K* et al. [98])

contrast agent by the draining lymphatic system to regional lymph nodes also allows real-time observation of the transport function of the lymphatic system and of the lymph nodes within a reasonable length of time. Furthermore, the specificity of absorption and transport of the contrast agent by the lymphatic system permits to visualize detailed morphologic changes of the lymphatic vessels and of the regional lymph nodes. Finally, quantitative assessment of abnormal lymph flow kinetics may be achieved by tracing the flow within the lymphatic vessels and comparing dynamic nodal enhancement and time-signal intensity curves between edematous and contralateral limbs. Figures 5.9 and 5.10, and 5.11 depict different MRL patterns in patients with lymphedema. However, it should be noted that MRL is still in an

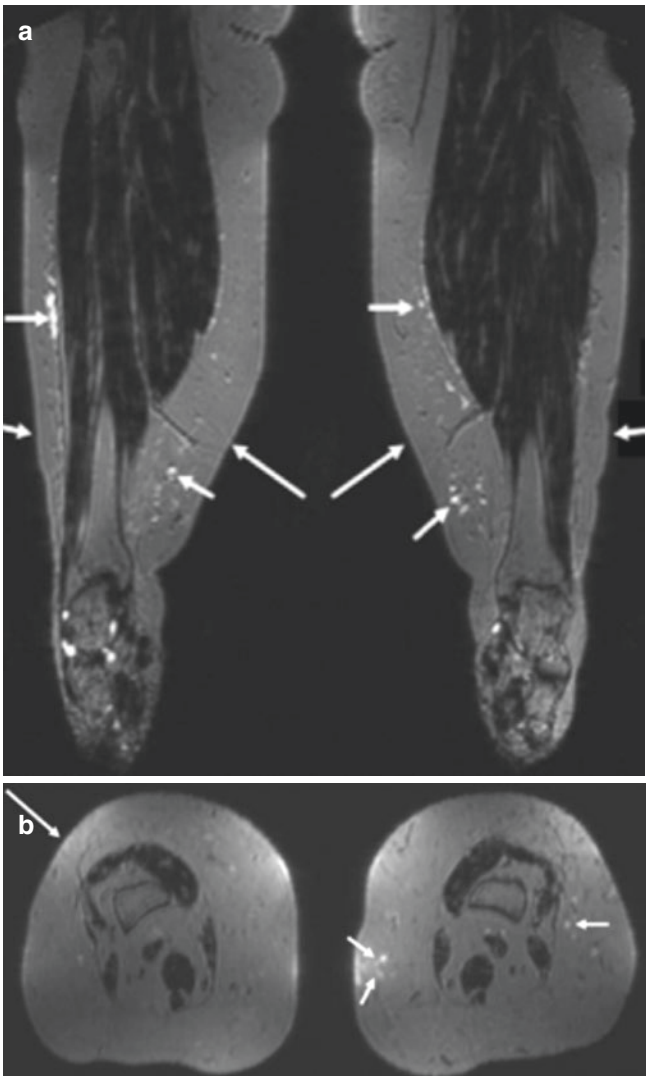

Fig. 5.9 Coronal (**a**) and axial heavily (**b**) T2-weighted 3D-TSE source images obtained in a patient with bilateral lipo-lymphedema of the lower extremities. The images show an increased layer of subcutaneous fat at the lower legs (upper panel, long arrows), subcutaneous regions of lymphedema (upper panel, short arrows), and severely enlarged layer of subcutaneous fat up to a diameter of 7.5 cm at the upper portion of both legs (lower panel, long arrows). Additionally, small areas of epifascial lymphedema are seen (short arrows in **b**) (*adapted from Lohrmann C* et al. [101])

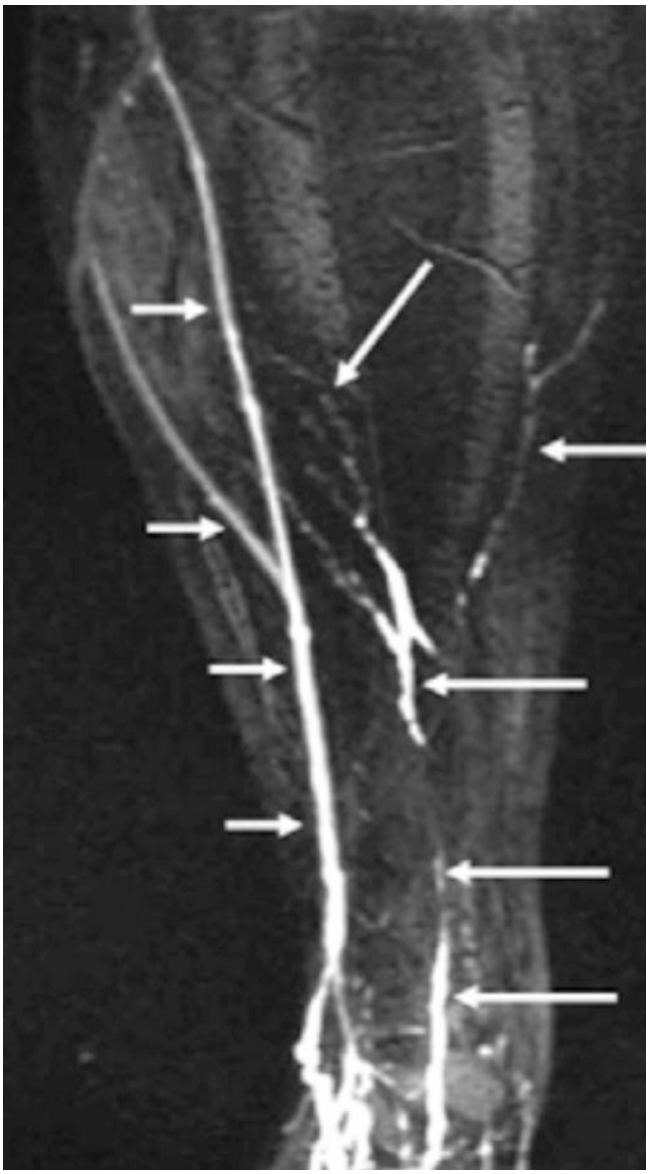

Fig. 5.10 Frontal 3D spoiled gradient-echo MRL MIP image obtained 45 min after gadoteridol injection in a patient with bilateral lipedema, showing clearly enlarged lymphatic vessels that have a typical bead-like appearance up to a diameter of 2 mm at the level of the right lower leg (large arrows), indicating a subclinical status of lipo-lymphedema. High uptake of contrast material is evident in the lymphatic vessels at the right lower leg as well as in a vein (small arrow) (*adapted from Lohrmann C* et al. [101])

experimental validation phase, since the extravascular intracutaneous injection of contrast agents is an off-label use of such compounds. Side effects such as moderate necrosis, hemorrhage, and edema have been described. Furthermore, incorrect interstitial injection of the contrast agent may lead to severe venous contamination.

The first correlations between lymphoscintigraphic pattern as evaluated with ^{99m}Tc-nanocolloid (injected subcutaneously at the interdigital web) and MRL findings (3 Tesla system, gadopentetate dimeglumine, and mepivacaine injected intracutaneously in the first three interdigital spaces of the forefoot) demonstrated clear concordance between the results of the two techniques, lymphoscintigraphy visualizing better the inguinal lymph nodes, and MR depicting the lymph vessels and morphology of lymph vessel abnormalities [30]. Figures 5.12 and 5.13 represent two examples of comparison between the two techniques in the same patient.

Further studies in upper extremity lymphedema [104] where MRL was performed before and after injection of a contrast agent by using a coronal T1-weighted 3D gradient-

echo sequence with spectral fat saturation demonstrated higher spatial resolution and better depiction of lymph vessels with MRL than with lymphoscintigraphy. When MRL and lymphoscintigraphy are reported using a semiquantitative classification according to five patterns of lymphatic abnormalities (delay of drainage, drainage pattern, enhancement of lymph nodes, depiction of lymph vessels, anatomic levels), MRL lymphangiography showed sensitivities of 100% for all four categories, while lymphoscintigraphy yielded a sensitivity of 83.3% for delineation of lymph vessels and 100% for the other three categories. Specificity of MR lymphangiography was 85.7% for delay of drainage and 100% for other three categories, while lymphoscintigraphy showed specificity of 66.7% for pattern of lymphatic drainage and 100% for other three categories. Delay and pattern of drainage were the same in 83.3% and non-visualization of axillary LNs was indistinguishably noted in all patients on both techniques. Anatomic level of enhanced lymph vessel was identical in 66.7% of the patients (Figs. 5.14 and 5.15). MR lymphangiography showed better performance for depiction of abnormal lymph vessels. MR lymphangiography and lymphoscintigraphy yielded similar results in all or most patients for evaluation of axillary lymph node enhancement and lymphatic drainage in upper extremity.

In another study [105], contrast-enhanced MRL was applied to the evaluation of the lower limb, providing superior anatomical and functional information, with high spatial resolution, in comparison to various techniques used in the diagnosis of lower limb lymphedema (i.e., lymphoscintigraphy, direct lymphography, unenhanced MR), and allowing more accurate diagnosis and classification of patients suffering from lymphoedema.

Another application of contrast-enhanced MRL is in the diagnosis of occult chylous leak after thoracic duct emboli-

Fig. 5.11 Three-dimensional contrast MR lymphangiographies displaying various patterns of lymphatic drainage. (**a**) Increased skin lymphatic and dermal backflow in the medial and lateral region of lower leg (arrow), and dilated collectors in the upper part of leg (arrowhead). (**b**) Radially arranged dilated vessels in the lower leg of a patient with primary lymphedema. (**c**) Enhanced lymphatic vessels (arrowheads) distributed as a slender network over the lower extremity. (**d**) Bunches of extremely dilated and significantly enhanced lymphatic vessels (arrowheads) located in the medial and lateral portion of the thigh. (**e**) Single enhanced and dilated lymphatic vessel in a patient with primary lymphedema (arrowheads) with irregular outline in the leg. (**f**) Intensely enhanced dilated lymph vessel (arrowheads) with clear outline in the thigh (*adapted from Liu NF* et al. [102])

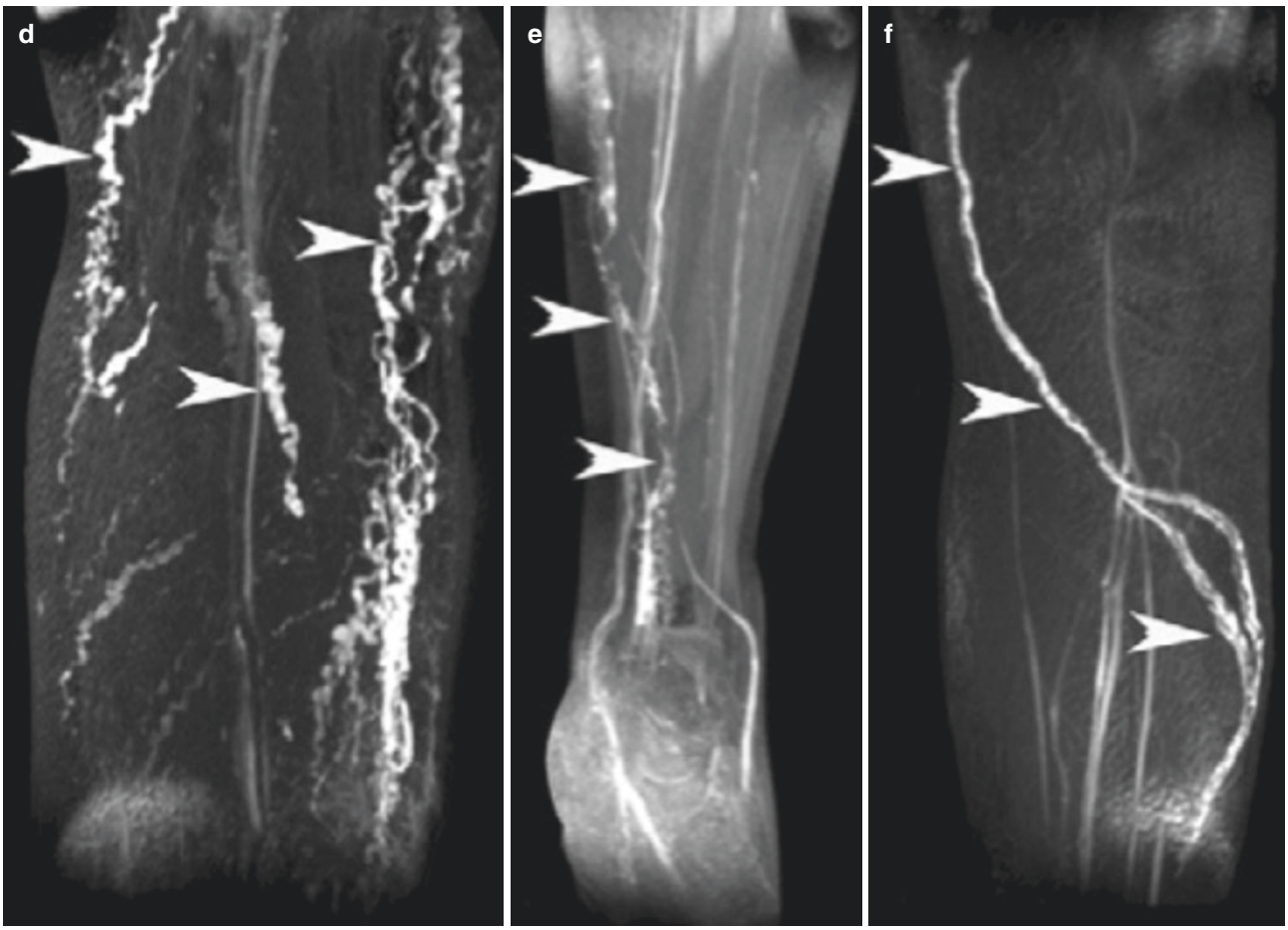

Fig. 5.11 (continued)

zation. In a case report [106] the direct contrast-enhanced MRL allowed the diagnosis of an occult chylous fluid leak from the right retroperitoneum into the right pleural space, after failure of both conventional lymphangiography and prophylactic TDE.

MRL has also been performed in combination with ^{68}Ga-NEB PET or as part of a PET/MR examination for visualizing morphologic and functional characteristics of lymphatic vessels, evaluating lymphedema, and guiding surgical intervention. Preoperative ^{68}Ga-NEB PET combined with MRL has been shown providing advantageous 3D images, higher temporal resolution, shorter time lapse before image acquisition after tracer injection, and more accurate pathological lymphatic vessel distribution with respect to traditional techniques (i.e., lymphoscintigraphy). This strategy has demonstrated significant advantages in the evaluation of lymphedema severity, staging, and pathological location of lymph vessels to make individualized treatment plans [107]. Combined ^{68}Ga-NEB TOF-corrected PET/MR was used in patients with different clinical severity of unilateral lower limb lymphedema [108], with semiquantitative imaging assessment (ratio of the standardized uptake value (SUV) of superficial lymphatic vessel (SLV) versus SUV of deep lymphatic vessel (DVL) (SUVslv/dlv)). In this study, a significant difference in the SUVslv between the affected limbs and normal limbs in all subjects was found (not found in the SUVdlv) and the SUVslv/dlv of the affected limbs showed statistical differences within the groups with minimal, moderate, and severe lymphedema with a negative correlation, thus promising in evaluating bilateral lower limb lymphedema.

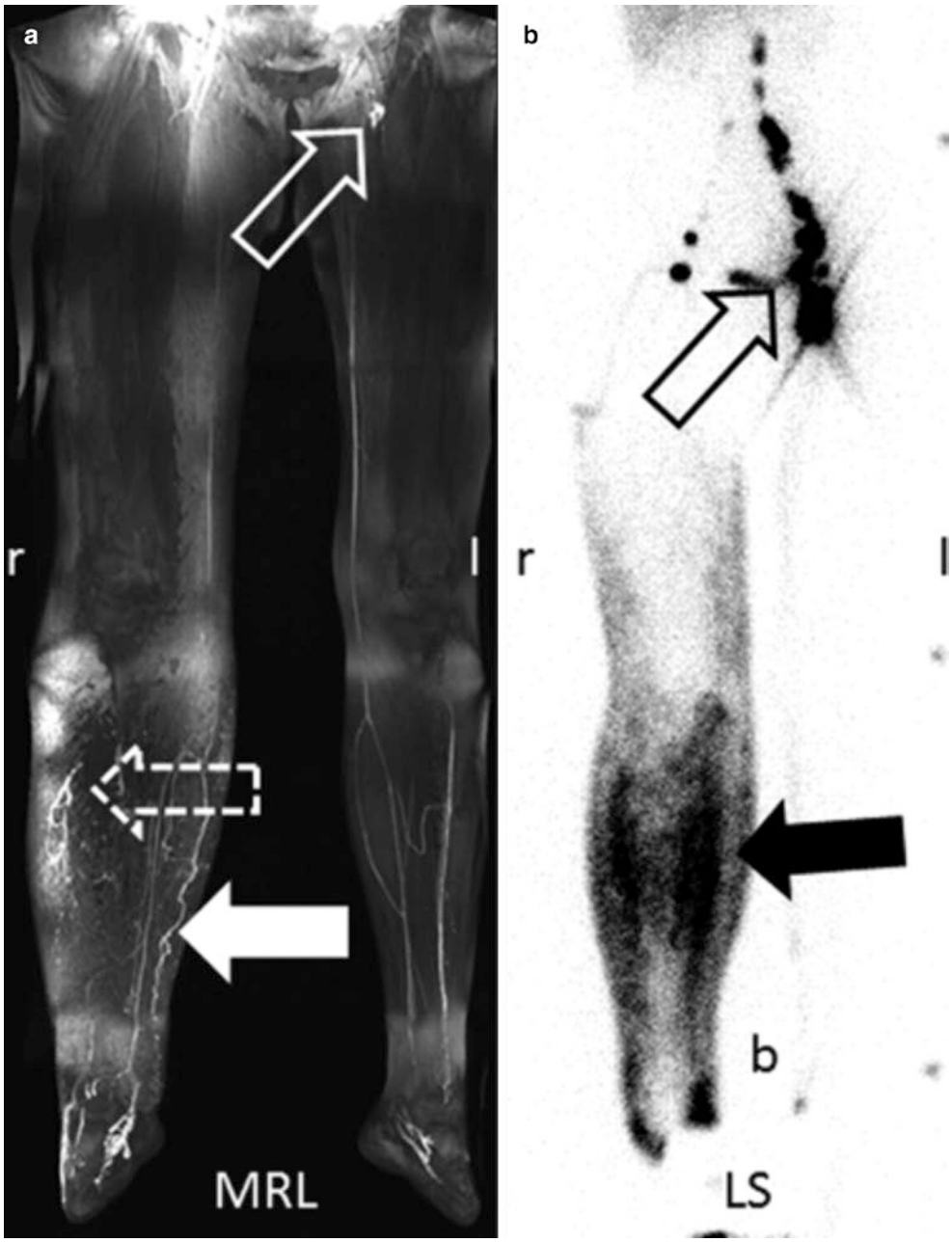

Fig. 5.12 Patient with stage II lymphedema of the right leg. (**a**) MRL image obtained with a 3.0 Tesla system after intracutaneous injection in the first three interdigital spaces of the forefoot of gadopentetate dimeglumine and mepivacaine. (**b**) Late-phase (2 h) lymphoscintigraphic images. In the right leg, diffuse lymphatic drainage (dashed arrow) and lymphangiectasia (solid white arrow) were detectable. MRL shows an early enhancing lymph node in the left groin (open arrow) and no contralateral iliac lymph node enhancement, thus suggesting delayed drainage in this leg. Lymphoscintigraphy clearly depicts diffuse drainage pattern (solid black arrow) and diminished right-sided inguinal lymph nodes. The radiocolloid was almost completely drained from the left leg at the time of acquisition, so that lymph vessels on this side were no longer visible (*adapted from Notohamiprodjo M* et al. [63])

Key Learning Points

- Three-dimensional observation of deeper tissues at CT-LG has been used to help elucidating the mechanism of dermal backflow.
- MRL following interstitial, intracutaneous injection of an extracellular, paramagnetic contrast agent has proved to be technically feasible in patients with primary or secondary lymphedema, although it is still an experimental procedure.
- MRL allows real-time observation of the transport function of the lymphatic system and of the lymph nodes, depiction of detailed morphologic changes of the lymphatic vessels and of the regional lymph nodes, and quantitative assessment of abnormal lymph flow kinetics.
- MRL and lymphoscintigraphy have been compared in some studies.
- MRL has also been performed as part of ^{68}Ga-NEB PET/MR.

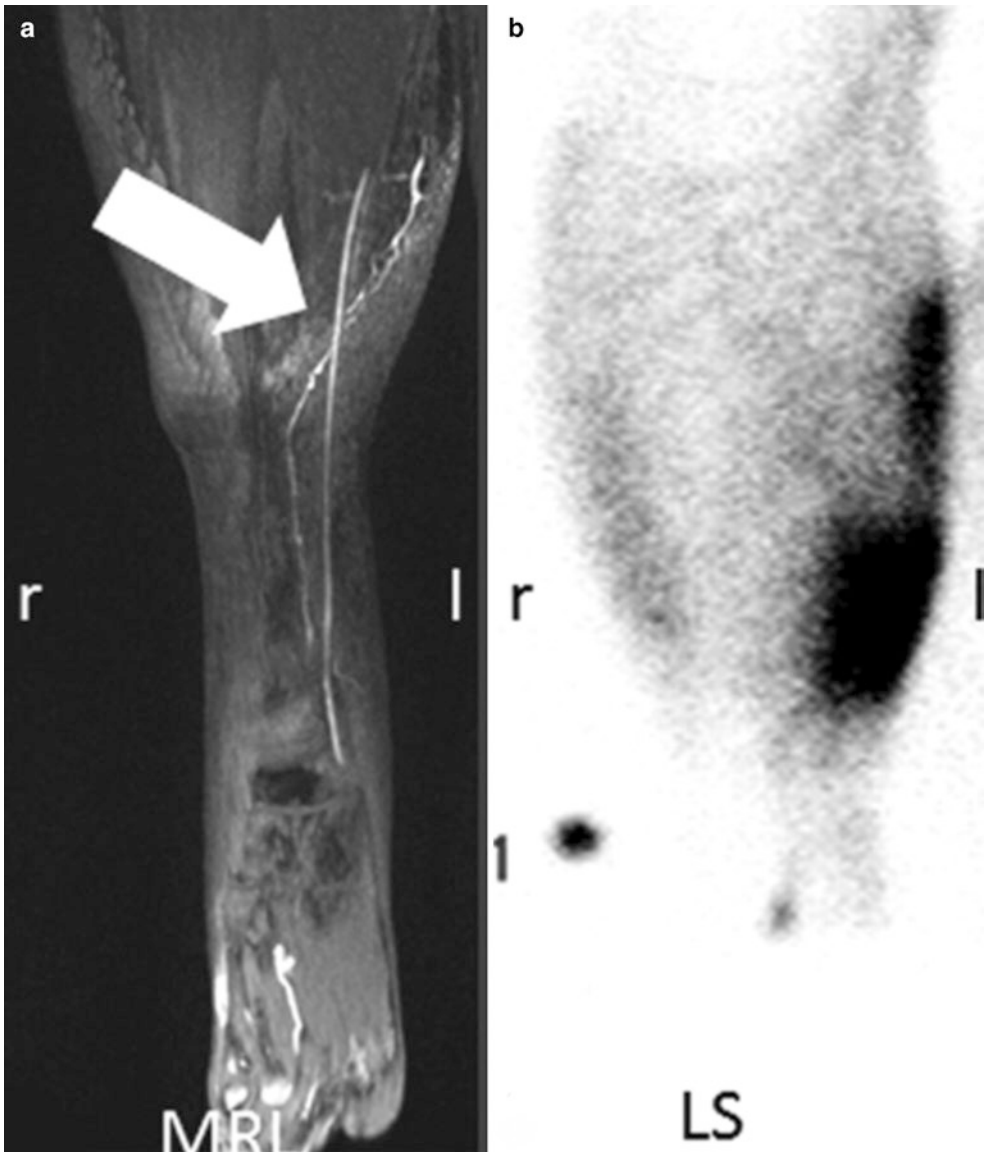

Fig. 5.13 Patient with stage II lymphedema of the left leg. (**a**) MRL image obtained with a 3.0 T MR system after injection of gadopentetate dimeglumine and mepivacaine in the first three interdigital spaces of the forefoot. (**b**) Late-phase (2 h) lymphoscintigraphic images. Lymphoscintigraphy shows that the pretibial lymph vessel is masked by the localized dermal backflow, whereas the lymph vessel is clearly visible in the MRL image. The marker position is indicated by "1" (*adapted from Notohamiprodjo M* et al. [63])

5.7 Virtual Reality for Preoperative Planning

Conventional images of lymphoscintigraphy and SPECT/CT processed by dedicated software to visualize this 3D patient-specific model, creating detailed 3D image of the anatomical structures, were used to plan lympho-venous anastomosis through virtual reality in a patient with a lymphatic malformation. The strategy of this intervention was to identify the lymphatics leaking into the malformation and to interrupt the inflow towards the lesion by redirecting the lymph toward the venous system. Localization of the lymphatic malformation was achieved without iatrogenic damage to the adjacent structures, an important goal, as previous resection was only temporarily successful, and scarring is a well-known complication of multistage surgery [109].

Key Learning Point
A personalized planning for lympho-venous anastomosis was performed in virtual reality elaborating the SPECT/CT images, resulting in a better localization of the leak and avoiding iatrogenic damage to the adjacent structures.

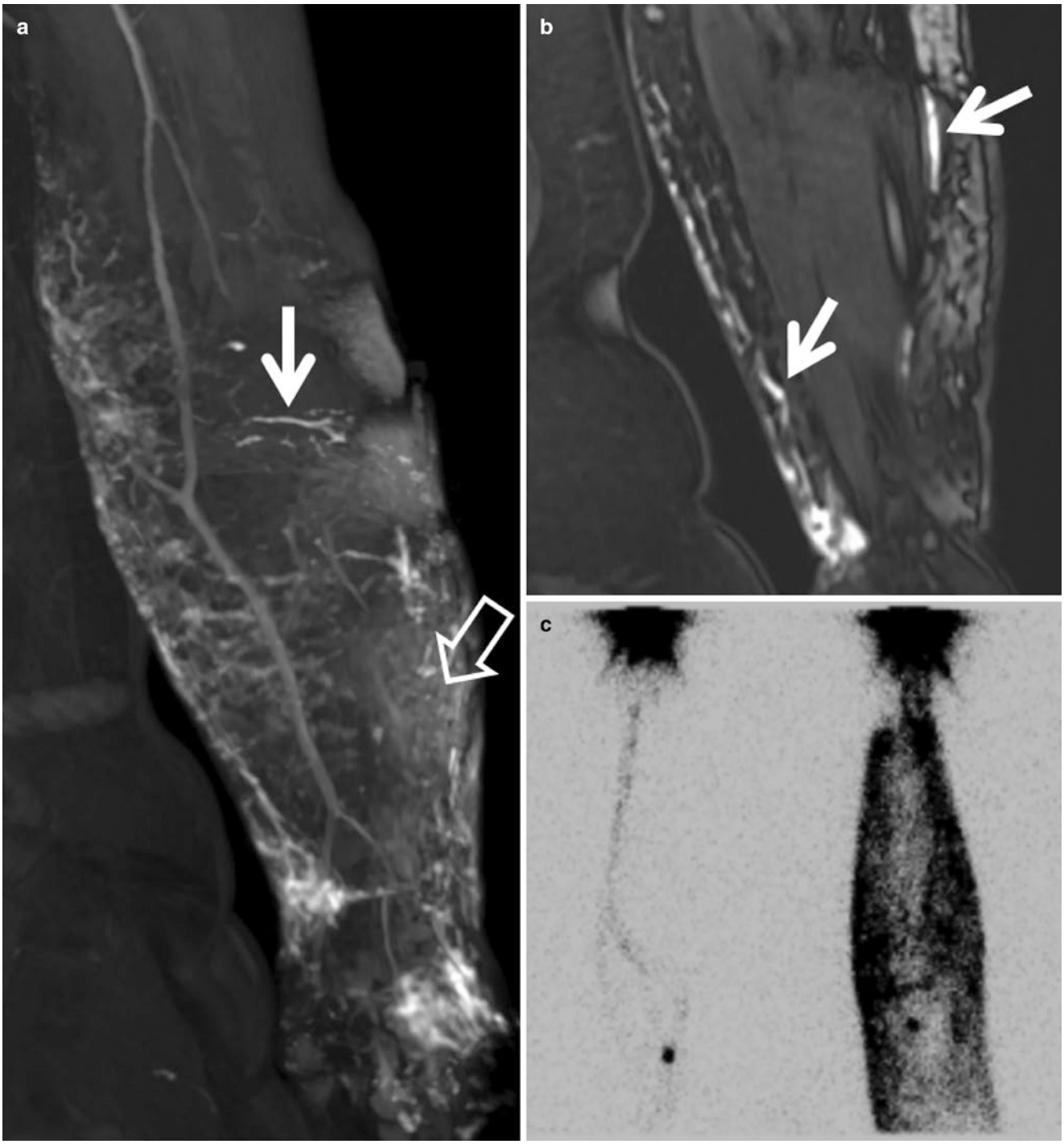

Fig. 5.14 Interstitial and vascular pattern of lymphatic drainage in a 48-year-old woman with stage II lymphedema of the left arm. (**a**, **b**) Beaded, dilated appearance of lymph vessels (lymphangiectasia) (solid arrow) and diffuse, interstitial enhancement (open arrow) around lymph vessels are visualized on maximum intensity projection images of MR lymphangiography 15 min after gadobutrol injection (**a**). The anatomical depth of lymph vessels (solid arrow) is demonstrated in coronal images (**b**). Lymphoscintigraphy image acquired 2 h after radiotracer injection shows diffuse lymphatic drainage at the left forearm (**c**) (*adapted from Bae JS* et al. [104])

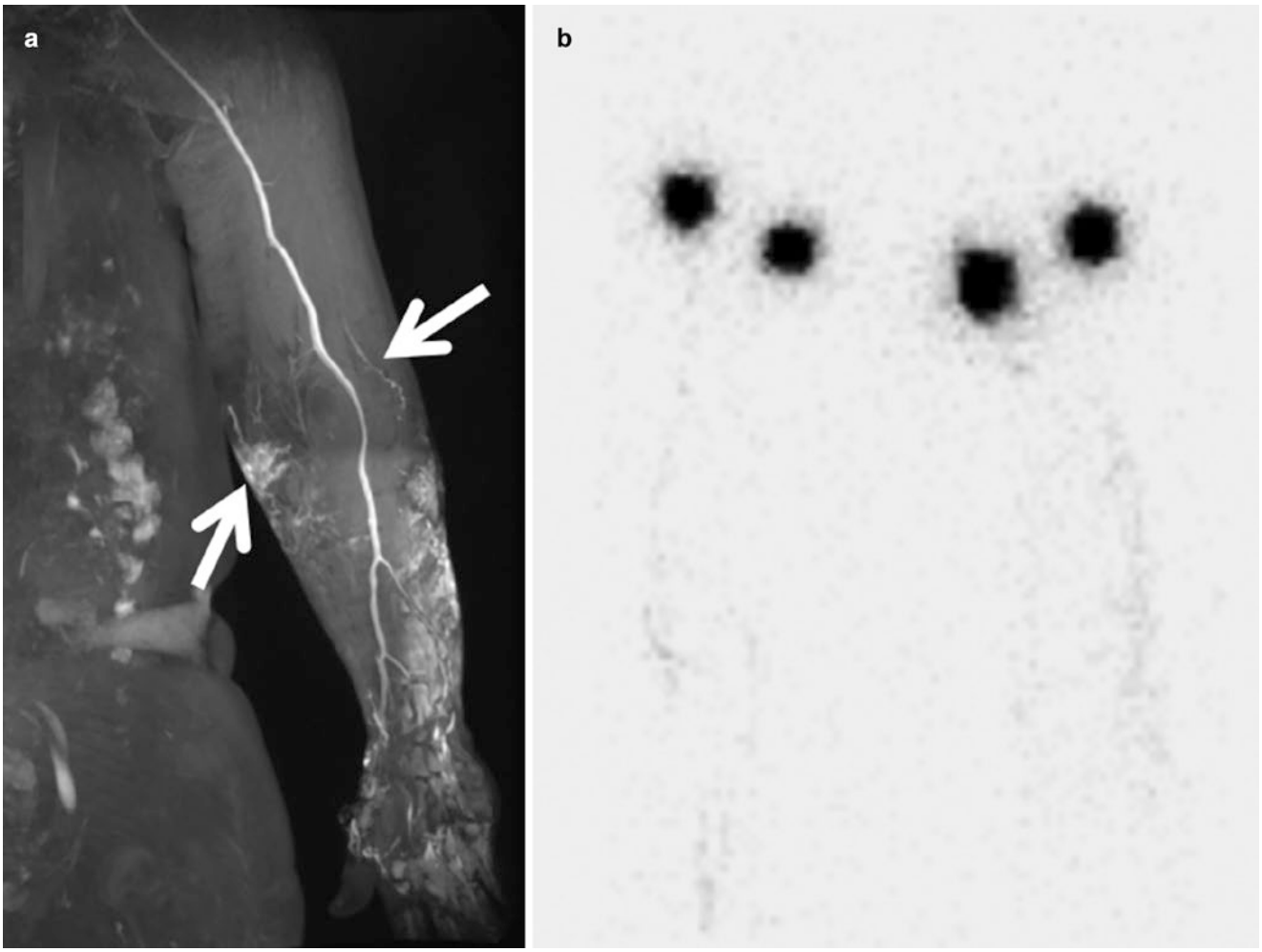

Fig. 5.15 Comparison of depiction of lymph vessels by MR lymphangiography and lymphoscintigraphy in a 55-year-old woman with stage II lymphedema. (**a**) MR lymphangiography clearly demonstrates beaded appearance of lymph vessels (white arrows) at the left elbow at both ulnar and radial sides. (**b**) Lymphoscintigraphy revealed only faint dotted line at the corresponding area (*adapted from Bae JS* et al. [104])

Clinical Cases

Case 5.1: Upper Limb Monocompartmental Lymphoscintigraphy in Stage III Primary Lymphedema of the Upper Left Arm Without Lymphadenomegaly

Luciano Feggi, Chiara Peterle, Corrado Cittanti, Valentina de Cristofaro, Stefano Panareo, Ilaria Rambaldi, Virginia Rossetti, and Ivan Santi

Background Clinical Case

A 45-year-old woman presented with spontaneous onset of mild non-pitting swelling in the upper left arm, in the absence of vascular lesions (stage III primary lymphedema with no lymphadenomegaly).

Anatomic location of edema: Left upper limb.

Lymphoscintigraphy

Lymphoscintigraphy was performed following administration of two aliquots of 2 mL containing 111 MBq ^{99m}Tc-albumin nanocolloid. Radiopharmaceutical injections were performed superficially in both hands (injection in first, second, third, and fourth interdigital spaces in each hand). A dual-detector SPECT gamma camera (E-cam Siemens Medical Solutions, Hoffman Estates, IL) equipped with low-energy high-resolution (LEHR) collimators was used to obtain planar images.

Planar images were acquired 5 min (early images) and 4 h (late images) after injection in anterior view (256 × 256 matrix, zoom factor 1.00, acquisition time 200 s for each view).

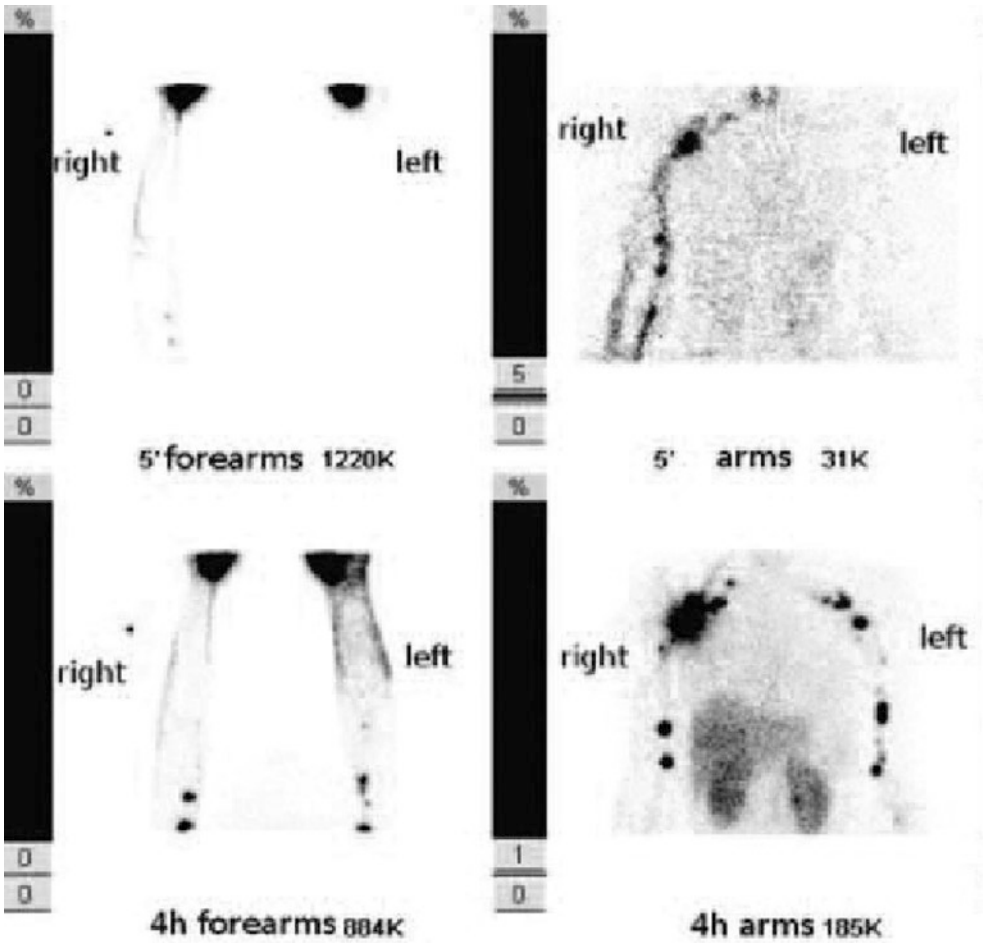

Fig. 5.16 Delayed drainage at the left upper limb in the early acquisitions and "dermal flow" in the 4-h acquisitions. A similar pattern is observed for lymph node uptake in the spot acquisitions over the thorax-upper abdomen: no lymph node uptake in the left axilla in the early acquisitions, however with some uptake in the delayed acquisitions (the left-side lymph nodes remaining always less evident than the contralateral lymph nodes). Based on the results of lymphoscintigraphy, the patient underwent combined therapy for lymphedema (pneumatic compression, wrapping of forearm, and massages)

Case 5.2: Upper Limb Monocompartmental Lymphoscintigraphy in Non-pitting Edema of the Upper Left Limb in Patient with Rheumatoid Arthritis

Luciano Feggi, Chiara Peterle, Corrado Cittanti, Valentina de Cristofaro, Stefano Panareo, Ilaria Rambaldi, Virginia Rossetti, and Ivan Santi

Background Clinical Case

A 40-year-old woman with a history of rheumatoid arthritis and mild non-pitting edema in left upper limb (left hand and forearm) for 6 months.

Anatomic location of edema: Left upper limb.

Lymphoscintigraphy

Lymphoscintigraphy was performed following administration of two aliquots of 2 mL containing 74 MBq ^{99m}Tc-albumin nanocolloid. Radiopharmaceutical injections were performed superficially and bilaterally (injection in first, second, third, and fourth interdigital spaces in each hand). A dual-detector SPECT gamma camera (E-cam Siemens Medical Solutions, Hoffman Estates, IL) was used to obtain planar images. Time of acquisition after injection: 5 min after injections (early images): (a) hands and forearms (laid upon collimator); (b) arms and thorax; 4 h after injection (late images): (a) hands and forearms (laid upon collimator); (b) arms and thorax (256 × 256 matrix, zoom factor 1.00, acquisition time 200 s for each view).

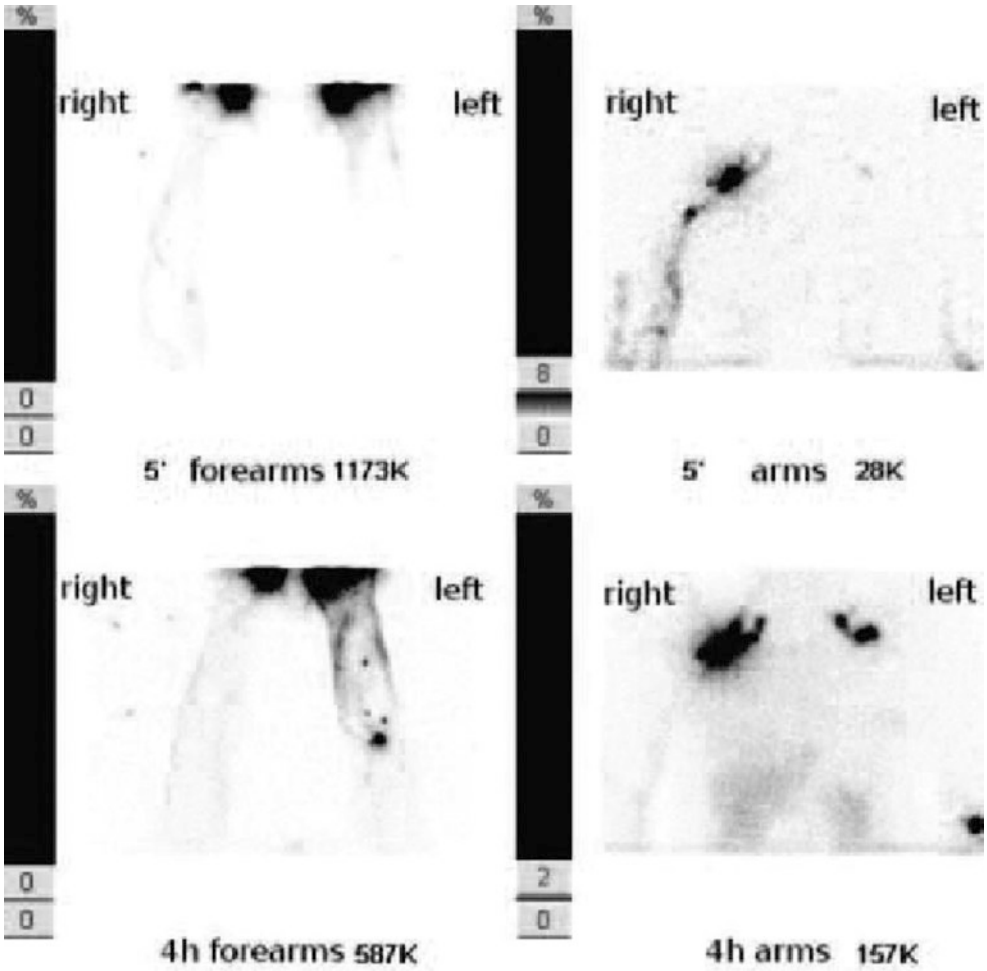

Fig. 5.17 Delayed drainage at left upper limb in the early acquisitions and "dermal flow" in the 4-h acquisitions. The pattern of lymphatic drainage is not totally normal also in the right arm, where no uptake in epitrochlear lymph nodes can be observed. No lymph node uptake in the left axilla at early imaging, with some uptake in the delayed acquisitions (but still much less intense than in the right axilla). Based on the results of lymphoscintigraphy, the patient underwent combined therapy for lymphedema (pneumatic compression, wrapping of forearm, and massages)

Case 5.3: Axillary Reverse-Mapping Lymphoscintigraphy in Breast Cancer Patient with Positive Sentinel Lymph Node (SLN) Before Lymphadenectomy

Luciano Feggi, Chiara Peterle, Corrado Cittanti, Valentina de Cristofaro, Stefano Panareo, Ilaria Rambaldi, Virginia Rossetti, Ivan Santi, and Paolo Carcoforo

Background Clinical Case

A 66-year-old woman underwent surgery for a left breast cancer finding positive SLN. Axillary dissection is necessary in patients with positive SLNs in breast cancer; in axillary basin lymph nodes may drain from either breast or arm; still, a lymph node which drains from both breast and arm is very rarely found, so the surgeon can spare a few nodes to preserve lymphatic arm drainage.

The ARM technique (axillary reverse mapping) allows to mark lymph nodes which drain from both hand and arm, so the surgeon can distinguish radioactive nodes (arm drainage) from "cold" ones (breast drainage) and remove only the breast-related ones.

Anatomic location of edema: No edema.

Lymphoscintigraphy

Lymphoscintigraphy was performed following administration of two aliquots of 0.4 mL containing 74 MBq ^{99m}Tc-albumin nanocolloid. Radiopharmaceutical injections were performed superficially and bilaterally (injection in first, second, third, and fourth interdigital spaces in each hand). A dual-detector SPECT gamma camera (E-cam Siemens Medical Solutions, Hoffman Estates, IL) equipped with low-energy high-resolution (LEHR) collimators was used to obtain planar images.

Time of acquisition after injection: (a) hands and forearms, 5 min after injection (laid upon collimator); (b) arms, 10 min after injection (anterior planar view); (c) axillary regions and thorax, 15 min after injection (anterior planar scan using cobalt wire as a landmark); (d) second acquisition only on axillary regions and thorax (anterior planar scan using cobalt wire as a landmark). Before late image of axillary regions and thorax, a radioguided occult lesion localization (ROLL) (after second nanocolloid intratumoral injection with ultrasound guidance) was performed to allow the surgeon to remove the breast primary tumor and left axillary nodes in one single time.

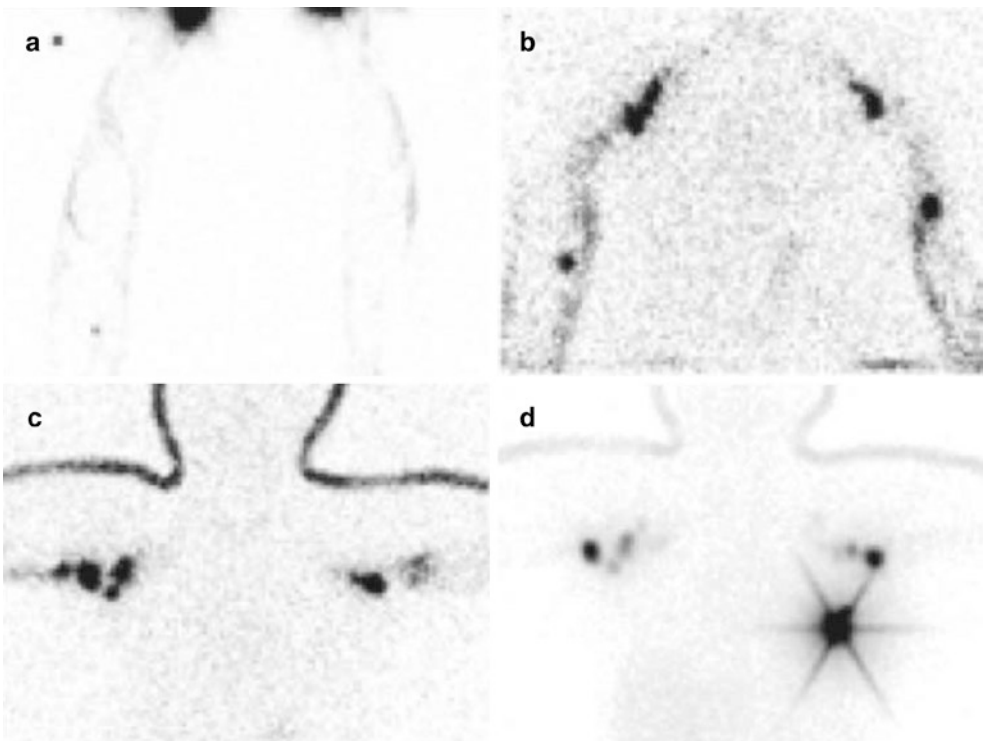

Fig. 5.18 Early acquisitions (**a**–**c**): normal lymphatic drainage in both upper limbs (mild delay in left upper limb early drainage; a month earlier, the patient underwent SLN removal in the left axillary basin). In *panel* (**d**) (late acquisition) the axillary reverse-mapping lymphoscintigraphy (ARM) is displayed, while the hottest focus in the left breast corresponds to intratumoral injection of ^{99m}Tc-albumin macroaggregates for ROLL. The lymph nodes that drain the upper limb, that accumulate the radiocolloid, will be spared during axillary dissection, thus decreasing the risk of secondary lymphedema possibly caused by axillary dissection

Case 5.4: Axillary Reverse-Mapping Lymphoscintigraphy in Breast Cancer Patient with Infiltrative Lobular Carcinoma and Positive SLN Before Lymphadenectomy

Luciano Feggi, Chiara Peterle, Corrado Cittanti, Valentina de Cristofaro, Stefano Panareo, Ilaria Rambaldi, Virginia Rossetti, Ivan Santi, and Paolo Carcoforo

Background Clinical Case

A 49-year-old woman with left breast cancer (infiltrative lobular carcinoma with positive SLN); we performed an ARM lymphoscintigraphy (axillary reverse-mapping lymphoscintigraphy), before the surgeon performed axillary dissection to spare lymph nodes that drain from hand and arm.

Anatomic location of edema: No edema.

Lymphoscintigraphy

Lymphoscintigraphy was performed following administration of two aliquots of 0.4 mL containing 74 MBq ^{99m}Tc-albumin nanocolloid. Radiopharmaceutical injections were performed superficially and bilaterally (injection in first, second, third, and fourth interdigital spaces in each hand). A dual-detector SPECT gamma camera (E-cam Siemens Medical Solutions, Hoffman Estates, IL) equipped with low-energy high-resolution (LEHR) collimators was used to obtain planar images.

Planar images were acquired in anterior view (256 × 256 matrix, zoom factor 1.00, acquisition time 200 s for each view).

Time of acquisition after injection: (a) hands and forearms, 5 min after injection (laid upon collimator); (b) arms, 10 min after injection (anterior planar scan); (c) axillary regions and thorax, 15 min after injection (anterior planar scan using cobalt wire as a landmark); (d) second acquisition only (late image) on axillary regions and thorax (anterior planar scan using cobalt wire as a landmark).

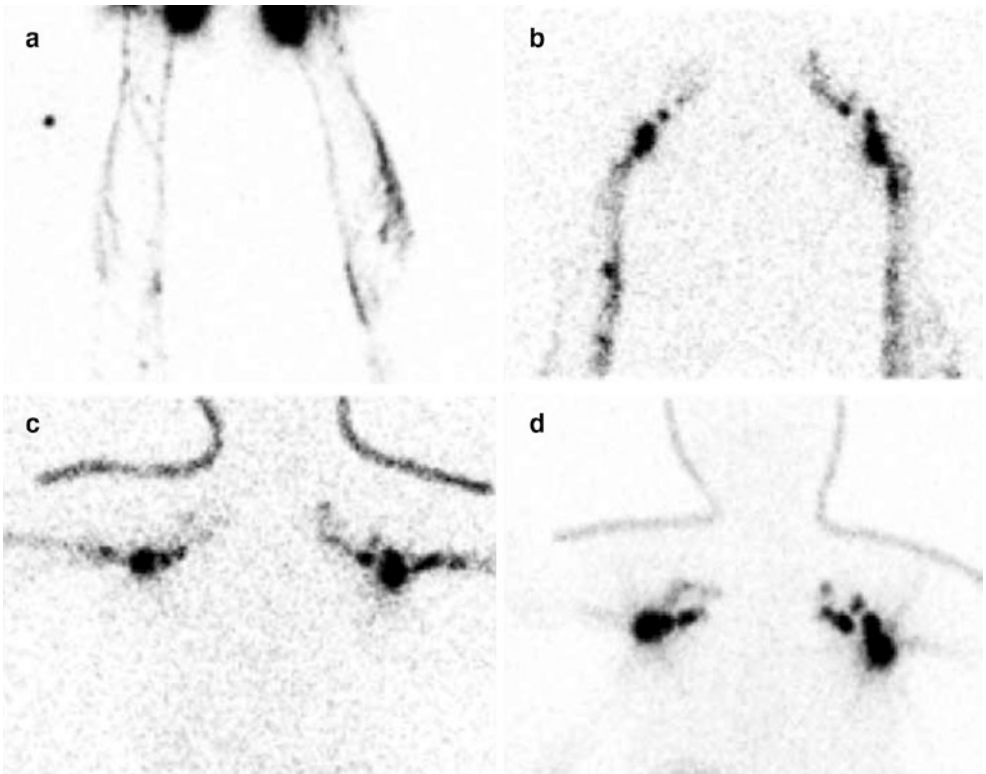

Fig. 5.19 Early images (**a**–**c**) show normal lymphatic drainage in both upper limbs (mild delay in left upper limb early drainage; 1 month earlier, the patient underwent SLN removal in the left axillary basin). *Panel* (**d**) is the late scan of axilla and thorax. The lymph nodes that drain the upper limb, that accumulate the radiocolloid, will be spared during axillary dissection, thus decreasing the severity of secondary lymphedema possibly caused by axillary dissection

Case 5.5: Lower Limb Monocompartmental Lymphoscintigraphy in Patient with Bilateral Swelling and Non-pitting Edema of the Lower Limbs

Luciano Feggi, Chiara Peterle, Corrado Cittanti, Valentina de Cristofaro, Stefano Panareo, Ilaria Rambaldi, Virginia Rossetti, and Ivan Santi

Background Clinical Case

A 62-year-old man with spontaneous onset of bilateral swelling and non-pitting edema in the lower limbs since 1 year.

Anatomic location of edema: Lower limbs.

Lymphoscintigraphy

Lymphoscintigraphy was performed following administration of two aliquots of 2 mL containing 111 MBq ^{99m}Tc-albumin nanocolloid. Radiopharmaceutical injections were performed superficially and bilaterally (injection in first, second, and fourth interdigital spaces and in the outer retromalleolar space in each foot). A dual-detector SPECT gamma camera (E-cam Siemens Medical Solutions, Hoffman Estates, IL) equipped with low-energy high-resolution (LEHR) collimators was used to obtain planar images. Planar images were acquired 10 min after radiopharmaceutical administration and walking exercise and 4 h, respectively, after injection (256 × 256 matrix, zoom factor 1.00, acquisition time 200 s for each view) in anterior planar scan from feet to abdominal region.

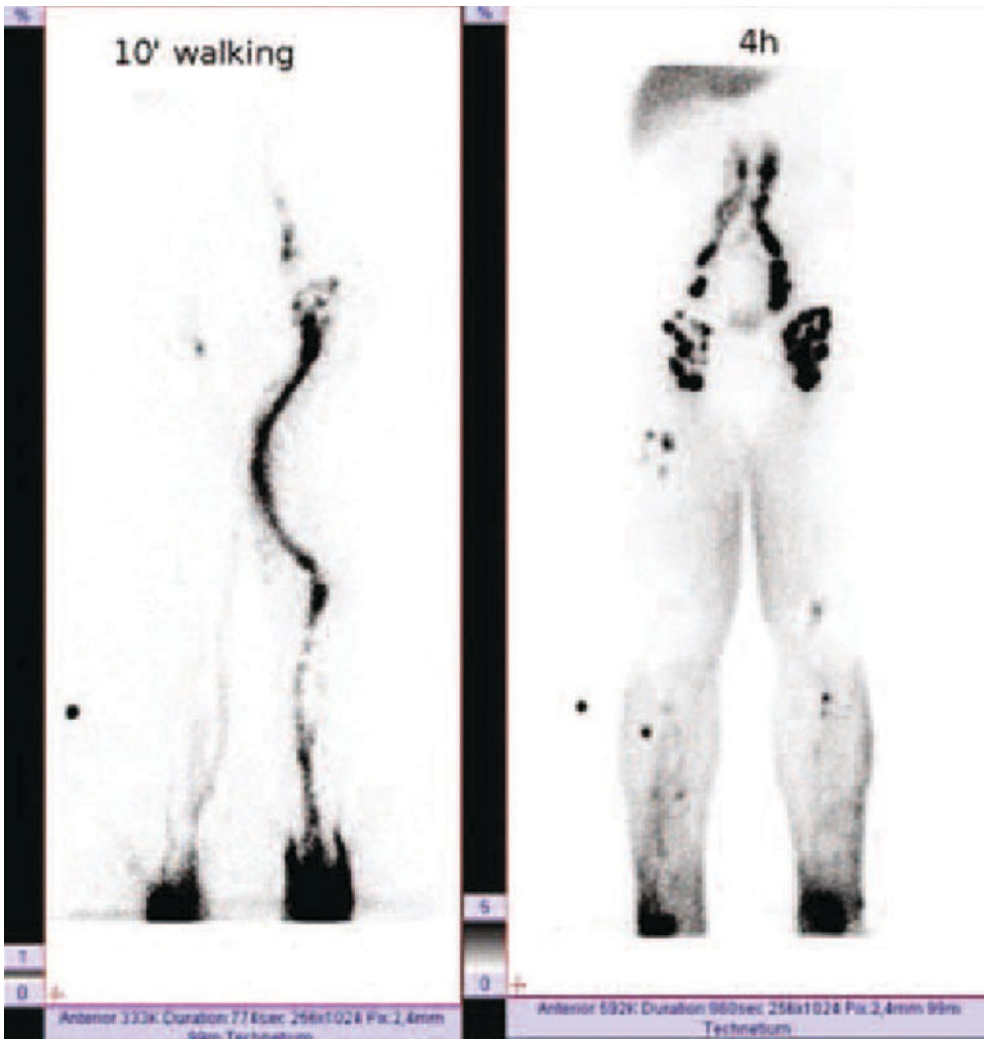

Fig. 5.20 Bilateral abnormal patterns of lymphatic drainage, as indicated by markedly delayed flow on the right side and mildly delayed flow on the left side in the early acquisition. The delayed acquisition shows the presence of bilateral "dermal backflow" with asymmetrical lymph node uptake (including an alternate pattern from the popliteal to the inguinal and to the lumbo-aortic lymph nodes). Based on the results of lymphoscintigraphy, the patient underwent combined therapy for lymphedema (pneumatic compression, wrapping of forearm, and massages)

Case 5.6: Lower Limb Bicompartmental Lymphoscintigraphy in Patient with Edema of the Left Lower Limb

Paola Anna Erba and Luisa Locantore

Background Clinical Case

A 47-year-old woman with edema of the left lower limb. Normal Doppler ultrasound. No family history of lymphedema.

Anatomic location of edema: Lower left limb.

Lymphoscintigraphy

For the deep lymphatic circulation (DLC): two aliquots of ^{99m}Tc-nanocolloid, 7 MBq each of injection in 0.1 mL in the first and second intermetatarsal space, identified by palpating the soles of both feet immediately proximal to the distal heads of the metatarsal bones on each side, inserting the needle by about 12–13 mm to reach the intermetatarsal muscles below the deep fascia plantaris. *For the superficial lymphatic circulation (SLC)*: three aliquots of about 10 MBq in 0.1 mL on the dorsum of each foot, inserting the needle subdermally in sites corresponding approximately to the prior palmar injections, about 1–2 cm proximally to the interdigital web. Spot and whole-body images were obtained from the distal feet up to the abdomen.

Spot images: 180 s/view, matrix 128 × 128, zoom 1.33

Whole-body images: matrix 128 × 1024, zoom 1, speed: 12 cm/min

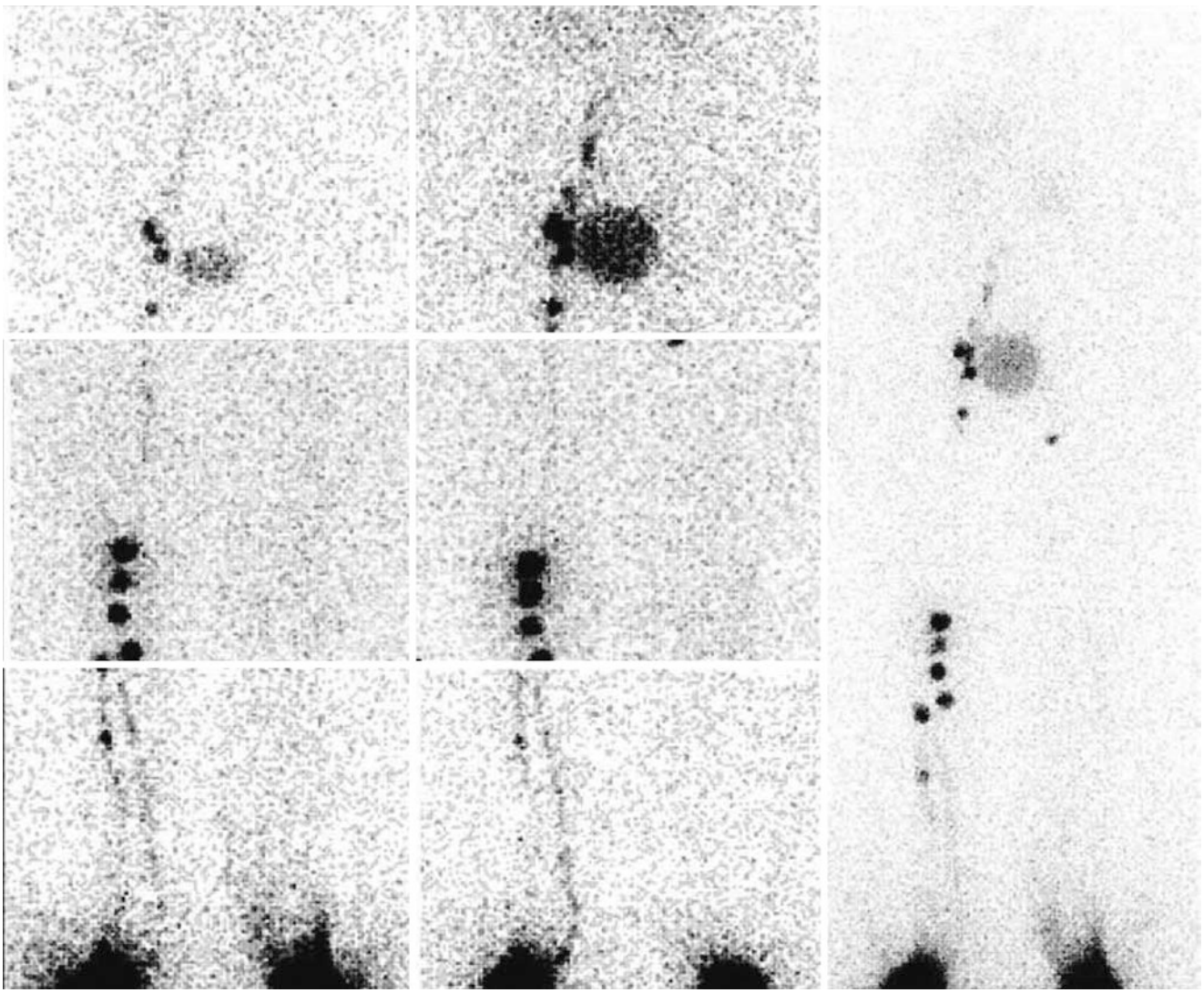

Figs. 5.21 and 5.22 Clear impairment of left lower lymph flow is evident in both the spot images (*Fig. 5.21*) and the whole-body image (*Fig. 5.22*), with minimal "dermal flow" at the distal medial portion of the left leg after radiocolloid injection for evaluating the DLC. No uptake can be seen in the left popliteal lymph nodes, while a single inguinal lymph node is detected after radiocolloid injection for the SLC. In addition, the DLC and SLC are simultaneously visualized at the right lower limb after radiocolloid injection for evaluating the DLC, indicating communication between the deep and the superficial lymphatic circulations. Multiple popliteal lymph nodes are detected on the right side, with normal pattern of the inguinal lymph nodes. Lumbo-aortic lymph nodes are faintly visualized, similarly as liver uptake

Case 5.7: Lower Limb Monocompartmental Lymphoscintigraphy in Patient with Bilateral Lower Limb Lymphedema

Giuseppe Rubini and Filippo Antonica

Background Clinical Case

A 32-year-old man with bilateral lower limb lymphedema. Clinicians suspected congenital dysplasia of the lower limb lymphatic vessels. Legs appeared edematous, size increased and the patient complained about fatigue and continuous pain even during sleep time. His daily actions were very limited.

Anatomic location of edema: Lower limbs.

Lymphoscintigraphy

Lymphoscintigraphy was performed following injections of two aliquots containing ^{99m}Tc-albumin nanocolloid, 37 MBq each of injection in 0.1 mL in the first and second intermetatarsal spaces. A dual-detector SPECT gamma camera (Millennium GE Healthcare, Milwaukee, WI) equipped with low-energy high-resolution (LEHR) collimators was used to obtain whole-body images after radiopharmaceutical injection. Whole-body planar images were acquired in anteroposterior projection, with a 256 × 1024 matrix and zoom factor 1.00 (speed: 12 cm/min) from the distal feet up to the abdomen.

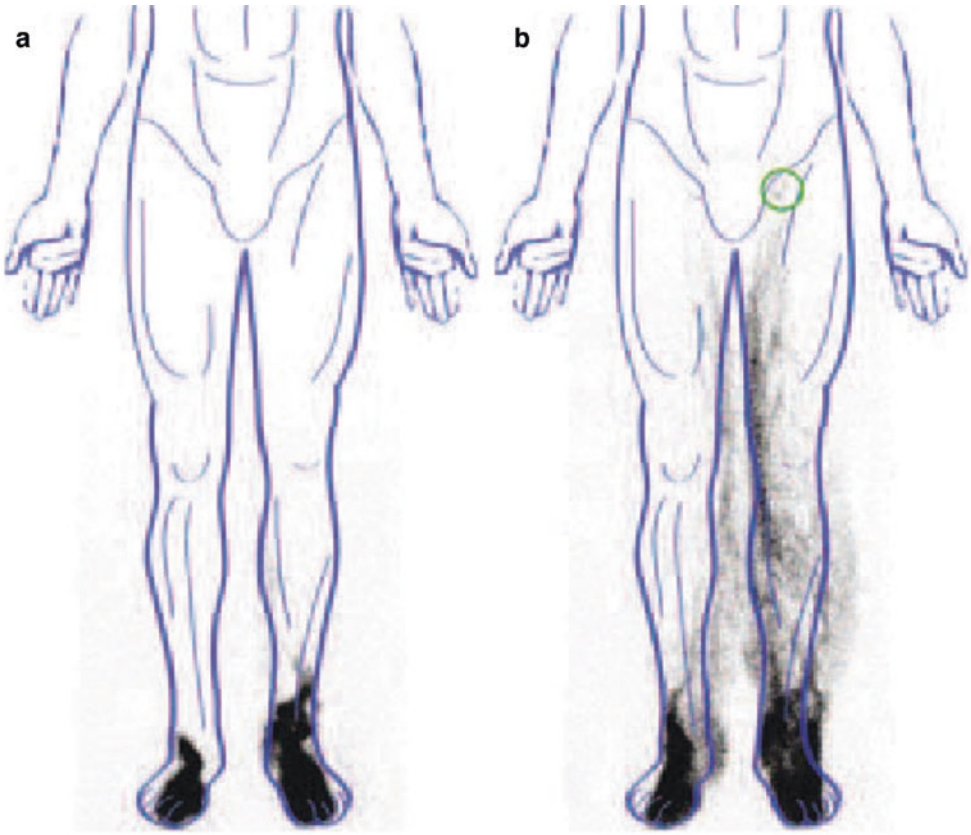

Fig. 5.23 Schematic representation of whole-body images in anterior view at 5–10, 30, 60, and 90 min (**a**–**d**, respectively) after radiocolloid injection and walking to stimulate lymphatic circulation. Radiocolloid drainage is delayed in both lower limbs, especially on the right side (no visualization of the groin lymph nodes in early scans). In later acquisitions, the right groin lymph nodes appear (*red circle*), delayed with respect to the right groin (*green circles*)

Fig. 5.23 (continued)

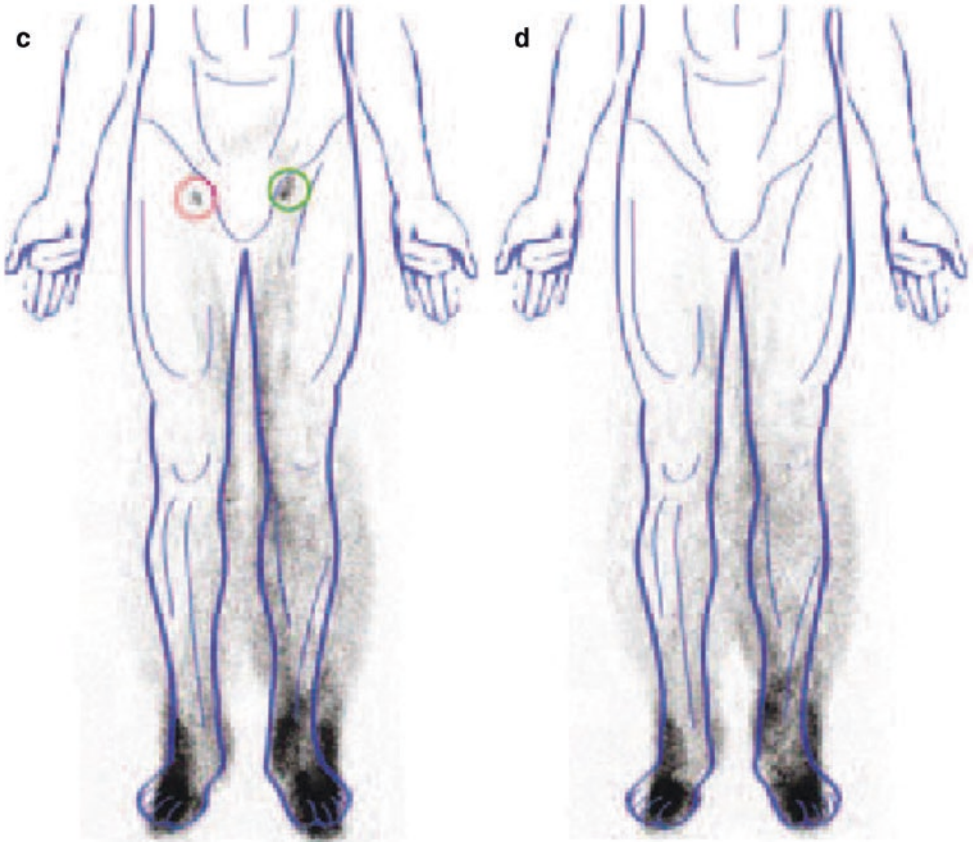

Case 5.8: Lower Limb Monocompartmental Lymphoscintigraphy in Patient Previously Submitted to Left Saphenectomy

Giuseppe Rubini and Filippo Antonica

Background Clinical Case

A 68-year-old woman previously submitted to saphenectomy of the left limb. Left limb appeared cold, size increased, and patient reported size increasing especially in the last year. Echo-color Doppler revealed decreased blood flow and tissue edema.

Anatomic location of edema: Lower limbs.

Lymphoscintigraphy

Lymphoscintigraphy was performed following injections of two 0.1 mL aliquots containing 36 MBq ^{99m}Tc-albumin nanocolloid, in the first and second intermetatarsal spaces. A dual-detector SPECT gamma camera (Millennium GE Healthcare, Milwaukee, WI) equipped with low-energy high-resolution (LEHR) collimators was used to obtain whole-body images after radiopharmaceutical injection. Whole-body planar images were acquired in anteroposterior projection, with a 256 × 1024 matrix and zoom factor 1.00 (speed: 12 cm/min) from the distal feet up to the abdomen.

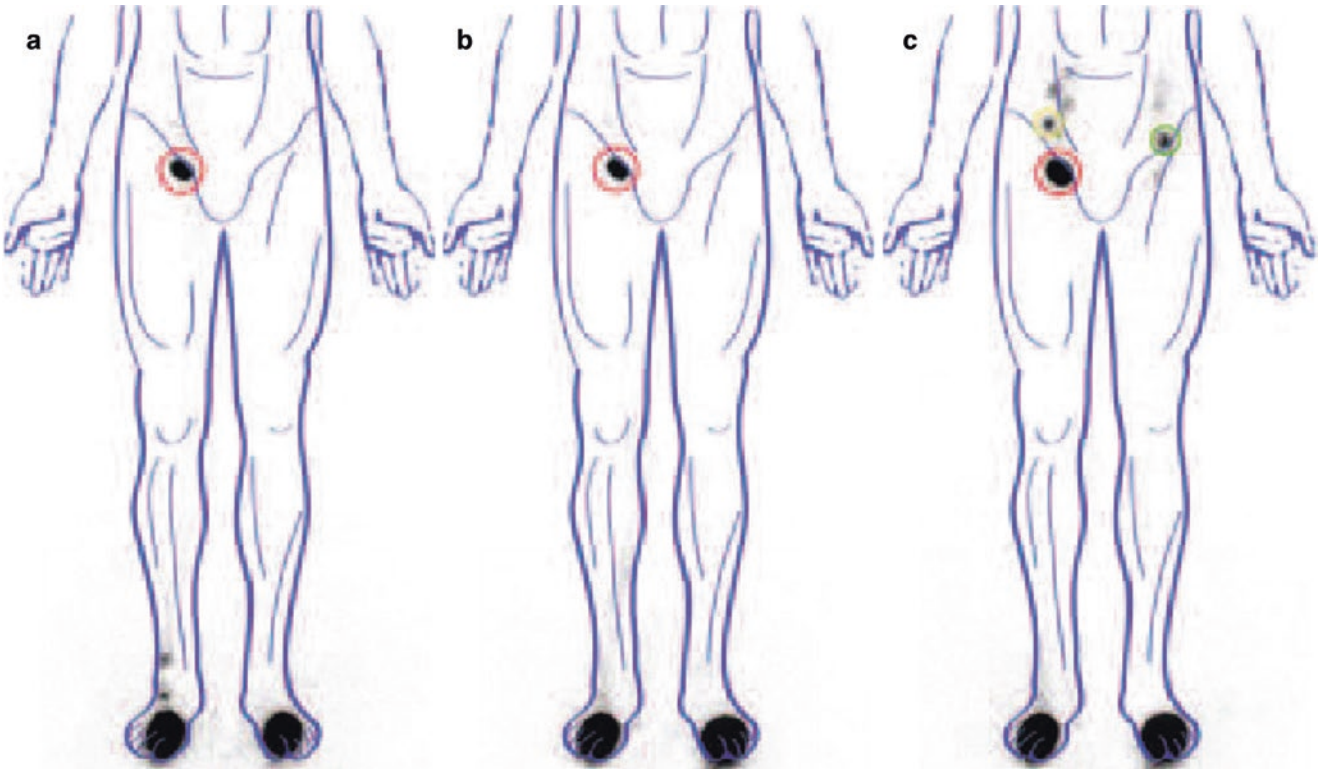

Fig. 5.24 Schematic representation of whole-body images in anterior view at 5–10, 30, and 60 min (**a**–**c**, respectively) after radiocolloid injection. Radiocolloid drainage is delayed in the left lower limb (no visualization of the groin lymph nodes in the early scans). In later acquisitions, the left groin lymph nodes appear (*green circle*). Radiocolloid drainage is normal in the right lower limb (*red* and *yellow circles*). These scintigraphic findings suggest secondary impairment of lymphatic drainage in the left lower limb

Case 5.9: Lower Limb Monocompartmental Lymphoscintigraphy in Patient with History of Lymphadenectomy of the Groin Basin for Melanoma

Giuseppe Rubini and Filippo Antonica

Background Clinical Case

Patient with a history of cutaneous melanoma of the right foot already surgically removed and submitted to lymphadenectomy of the groin basin due to groin SLN positivity for metastasis. The surgeon also removed pelvic lymph nodes to guarantee surgical radicality. Physical examination did not reveal any lymphadenopathy or lymphedema.

Anatomic location of edema: Lower limbs.

Lymphoscintigraphy

Lymphoscintigraphy was performed following injections of two 0.1 mL aliquots containing 36 MBq ^{99m}Tc-albumin nanocolloid, in the first and second intermetatarsal spaces. A dual-detector SPECT gamma camera (Millennium GE Healthcare, Milwaukee, WI) equipped with low-energy high-resolution (LEHR) collimators was used to obtain whole-body images after radiopharmaceutical injection. Whole-body planar images were acquired in anteroposterior projection, with a 256 × 1024 matrix and zoom factor 1.00 (speed: 12 cm/min) from the distal feet up to the abdomen.

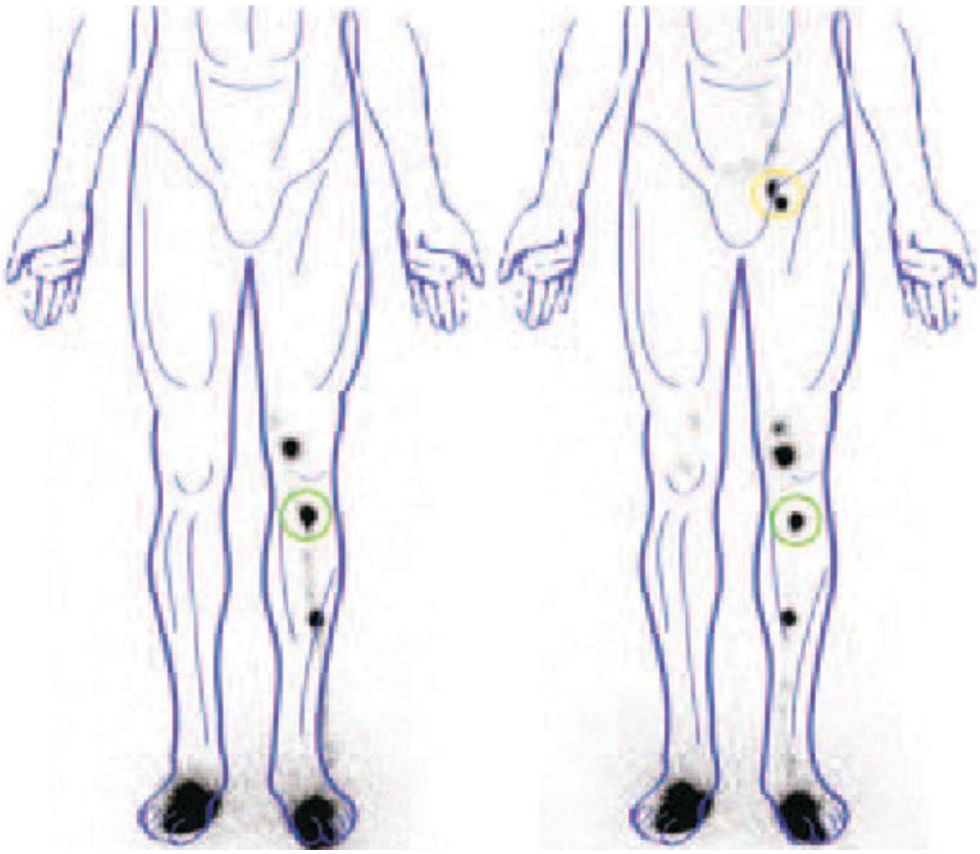

Fig. 5.25 Schematic representations of whole-body scans in anterior view, 5–10 min (*left panel*) and 30 min (*right panel*) after radiocolloid injection. Lymphatic drainage is delayed in the right lower limb (no visualization of the groin lymph nodes). Drainage is normal in the left lower limb, with normal visualization of the popliteal (*green circle*) and inguinal (*yellow circle*) lymph nodes

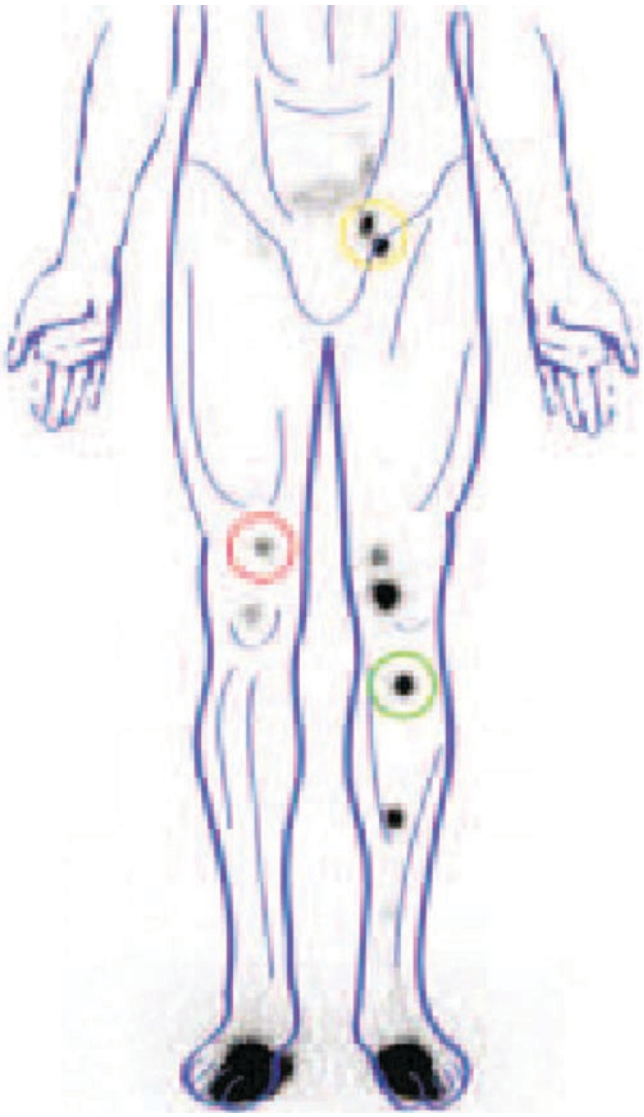

Fig. 5.26 Schematic representation of whole-body scans in anterior view 90 min after radiocolloid injection. In this delayed scan, the right popliteal lymph nodes appear (*red circle*), with faint visualization of the right groin lymph nodes. Radiocolloid drainage is normal in the left lower limb, with normal visualization of the popliteal (*green circle*) and inguinal (*yellow circle*) lymph nodes. These scintigraphic findings suggest secondary impairment of the lymphatic circulation in the right lower limb

Case 5.10: Postexercise Lower Limb Monocompartmental Lymphoscintigraphy in Patient with Bilateral Leg Edema

Luciano Feggi, Chiara Peterle, Corrado Cittanti, Valentina de Cristofaro, Stefano Panareo, Ilaria Rambaldi, Virginia Rossetti, and Ivan Santi

Background Clinical Case

A 50-year-old woman with previous hysterectomy due to uterine fibromatosis and multiple removals of lipomas of the legs underwent investigation, because of mild edema of the legs, more noticeable in the right one; ultrasound, performed before lymphoscintigraphy, showed saphenous–femoral vein junction incontinence with ectasia. Lymphadenomegaly was found in the right inguinal region.

Anatomic location of edema: Lower limbs (more evident in right one).

Lymphoscintigraphy

Lymphoscintigraphy was performed following administration of two doses of 2 mL containing 111 MBq ^{99m}Tc-albumin nanocolloid. Radiopharmaceutical injections were performed superficially and bilaterally (injection in first, second, and fourth interdigital spaces and in the outer retromalleolar space in each foot). A dual-detector SPECT gamma camera (E-cam Siemens Medical Solutions, Hoffman Estates, IL) equipped with low-energy high-resolution (LEHR) collimators was used to obtain planar images. Planar images were acquired 10 min (after radiopharmaceutical administration and walking exercise) and 4 h, respectively, after injection (256 × 256 matrix, zoom factor 1.00, acquisition time 200 s for each view) in anterior planar scans from feet to abdominal region.

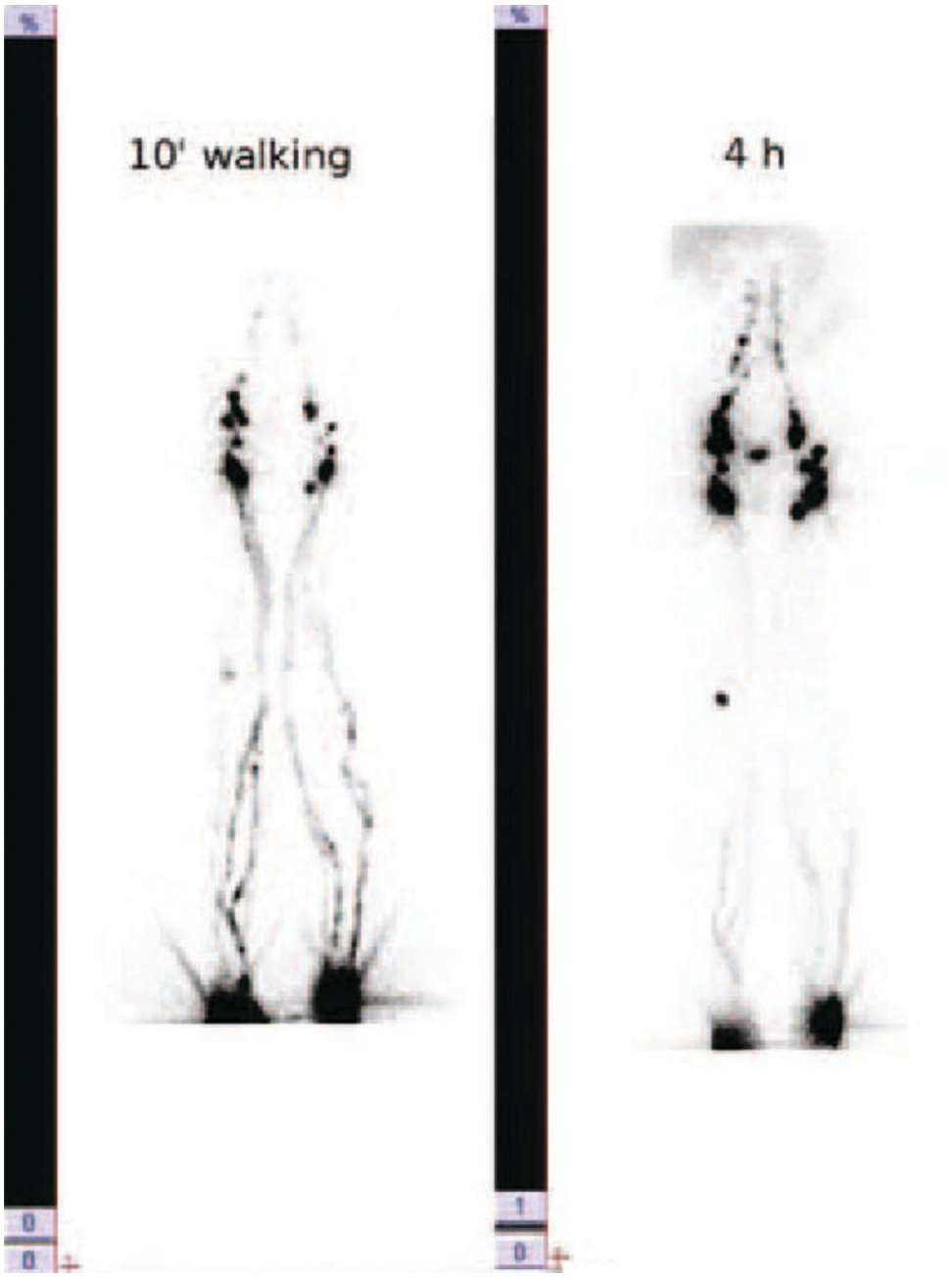

Fig. 5.27 Near-normal visualization of bilateral lymphatic trunks and inguinal lymphatic basins both in the early and in the delayed (4 h) acquisitions. A single popliteal lymph node is visualized, only in the right lower limb (mild abnormality)

Case 5.11: Lower Limb Monocompartmental Lymphoscintigraphy at Rest and Postexercise with Semiquantitative Evaluation of the Tracer Appearance Time in Patient with Lymphedema of the Left Lower Limb Post-left Groin Lymphadenectomy

Girolamo Tartaglione, Roberto Bartoletti, and Marco Pagan

Background Clinical Case

A 45-year-old woman, with lymphedema of the left lower limb and history of cutaneous melanoma of the gluteus (pN1M0) and left groin lymph nodal dissection.

Anatomic location of edema: Lower limb.

Lymphoscintigraphy

All tight clothes and elastics were removed before tracer injection. Two aliquots of 0.3 mL containing 50 MBq ^{99m}Tc-albumin-nanocolloid were injected intradermally at the first interdigital area, on the top of the feet. Gentle massage was performed after injection in the area. Two scans were acquired starting immediately after injection (the first on the legs and the second on the thighs) following these parameters: planar static scan, preset time 5 min, matrix 128 × 128, 140 Kev ± 10%, and anterior and posterior views. A dual-head gamma camera (GE-Infinia) equipped with low-energy general-purpose (LEGP) collimators was used to provide increased sensitivity. If delayed or absent lymphatic drainage was perceived, then the patient was invited to perform 2 min of continuous isotonic exercise (walking). A postexercise static scan was acquired (128 × 128, 5 min) until the regional lymph nodes were visualized. The tracer appearance time (TAT, normal value less than 10 min) and lymph drainage patterns after exercise (see timeline) were evaluated.

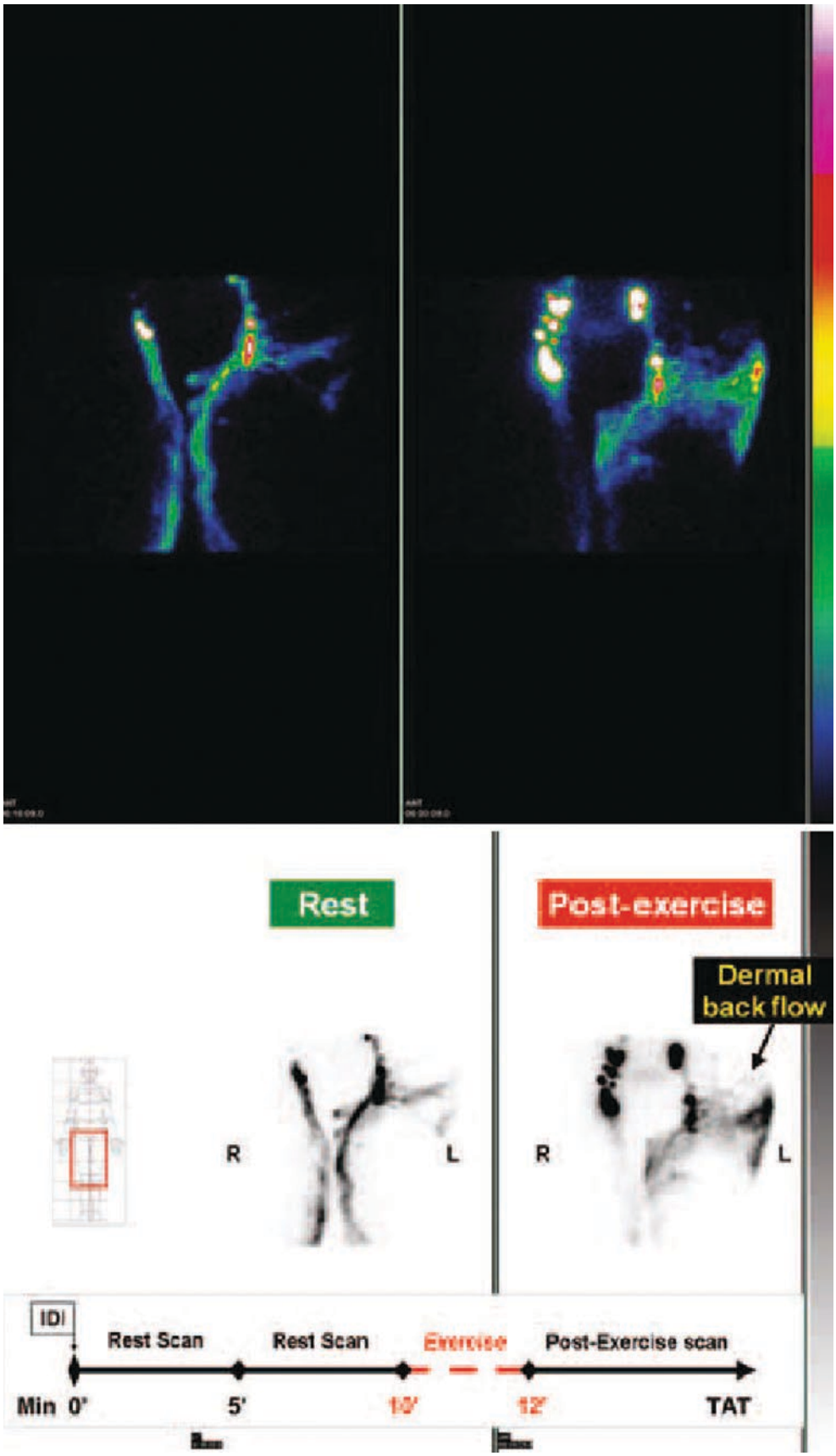

Figs. 5.28 and 5.29 The scan at rest shows near-normal visualization of the main lymphatic vessels of the lower limbs, and a normal TAT, with a time-dependent increased accumulation of the radiocolloid in the left groin region. After exercise, radioactivity accumulation increases even further in the left groin region (lymphatic leakage). In this case exercise revealed a local failure of lymphatic drainage, which was helpful to develop a combined treatment approach

Case 5.12: Lower Limb Monocompartmental Lymphoscintigraphy at Rest and Postexercise with Semiquantitative Evaluation of the Tracer Appearance Time in Patient with Right Lower Limb Primary Lymphedema, Clinical Stage 3 According to Foeldi

Girolamo Tartaglione, Roberto Bartoletti, and Marco Pagan

Background Clinical Case

A 54-year-old woman, affected by a right lower limb primary lymphedema of clinical stage 3 according to Foeldi. The tissue at this stage is hard (fibrotic) and edema is non-pitting. The swelling is almost irreversible and the limb is very large and swollen.

Anatomic location of edema: Right lower limb.

Lymphoscintigraphy

All tight clothes and elastics were removed before tracer injection. Two aliquots of 0.3 mL containing 50 MBq ^{99m}Tc-albumin-nanocolloid were injected intradermally at the first interdigital area, on the top of the feet. Gentle massage was performed after injection in the area. Two scans were acquired starting immediately after injection (the first on the legs and the second on the thighs) following these parameters: planar static scan, preset time 5 min, matrix 128 × 128, 140 Kev ± 10%, and anterior and posterior views. A dual-head gamma camera (GE-Infinia) equipped with low-energy general-purpose (LEGP) collimators was used to provide increased sensitivity. If delayed or absent lymphatic drainage was perceived, then the patient was invited to perform 2 min of continuous isotonic exercise (walking). A postexercise static scan was acquired (128 × 128, 5 min) until the regional lymph nodes were visualized. The tracer appearance time (TAT, normal value less than 10 min) and lymph drainage patterns after exercise (see timeline) were evaluated.

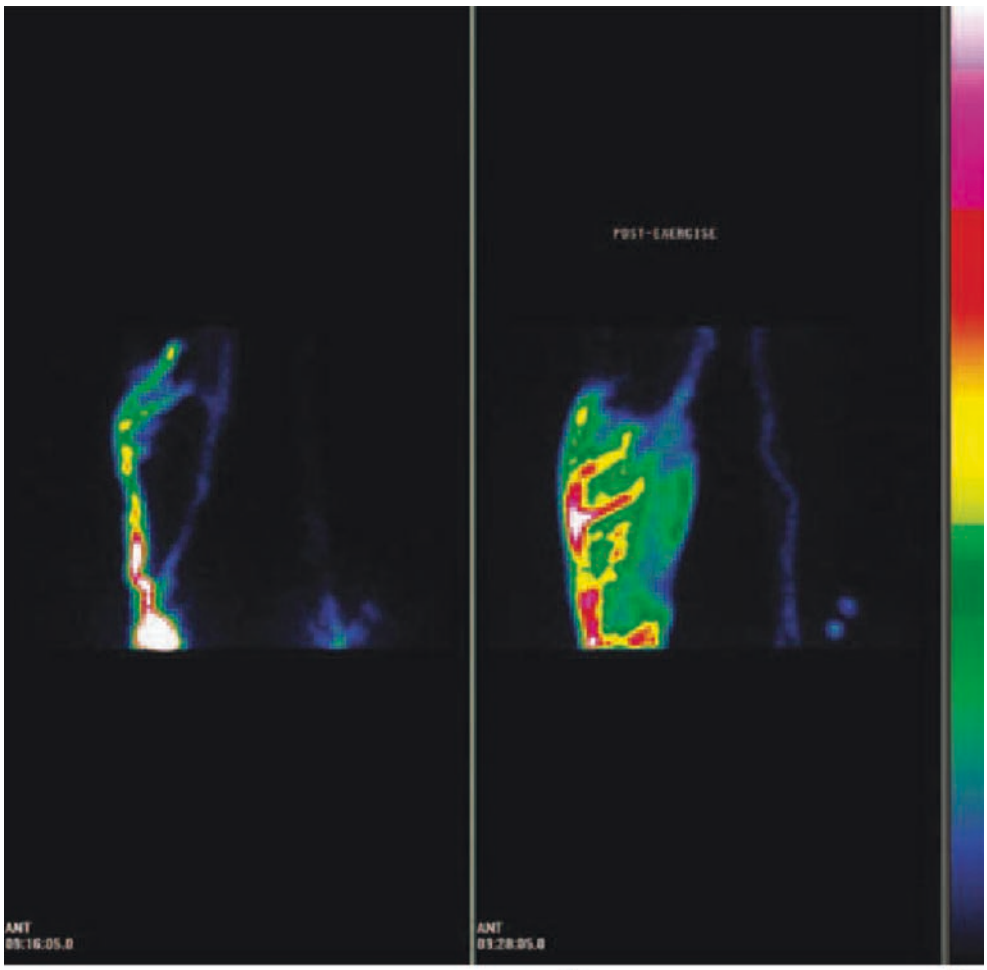

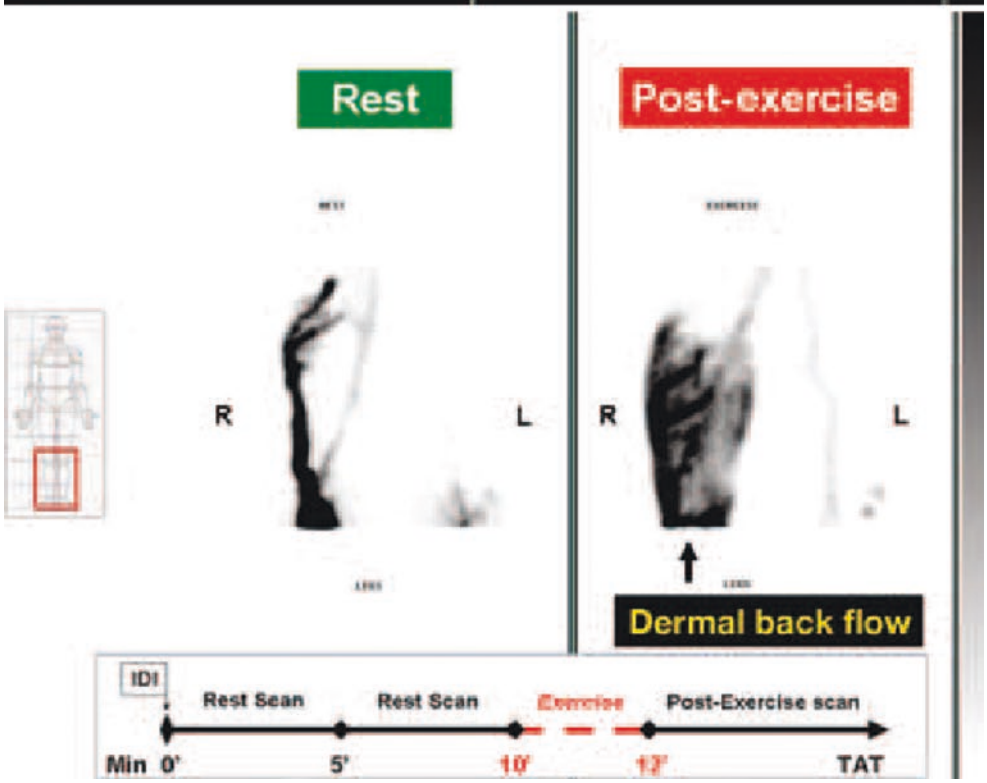

Figs. 5.30 and 5.31 The scan at rest shows severely delayed lymphatic drainage on the right side, with visualization of a rich collateral circulation along the small saphena; no detectable lymph flow on the left side. After exercise, intense dermal backflow appears on the right side, while a normal lymph drainage can be observed on the left side. Dermal backflow is usually observed in case of severe obstruction of the main lymph pathway; when the pressure gradient increases over a certain threshold, it causes incompetence of the lymphatic vessel's valves, which causes inversion of lymph flow toward the dermis. In this patient, compression bandage therapy was ineffective, whereas a standard program of combined physical therapy yielded moderate clinical improvement

Case 5.13: Lower Limb Monocompartmental Lymphoscintigraphy at Rest and Postexercise with Semiquantitative Evaluation of the Tracer Appearance Time in Patient with Post-lymph Nodal Dissection Lymphedema of the Lower Limbs

Girolamo Tartaglione, Roberto Bartoletti, and Marco Pagan

Background Clinical Case

A 46-year-old man, affected by lymphedema of the lower limbs (clinical stage 2 according to Foeldi) secondary to bilateral groin lymph nodal dissection for cutaneous melanoma (7 years previously). The patient was treated in several centers with combined physical therapy programs, including a personalized program of exercise.

Anatomic location of edema: Lower limbs.

Lymphoscintigraphy

All tight clothes and elastics were removed before tracer injection. Two aliquots of 0.3 mL containing 50 MBq ^{99m}Tc-albumin-nanocolloid were injected intradermally at the first interdigital area, on the top of the feet. Gentle massage was performed after injection in the area. Two scans were acquired starting immediately after injection (the first on the legs and the second on the thighs) following these parameters: planar static scan, preset time 5 min, matrix 128 × 128, 140 Kev ± 10%, and anterior and posterior views. A dual-head gamma camera (GE-Infinia) equipped with low-energy general-purpose (LEGP) collimators was used to provide increased sensitivity. If delayed or absent lymphatic drainage was perceived, then the patient was invited to perform 2 min of continuous isotonic exercise (walking). A postexercise static scan was acquired (128 × 128, 5 min) until the regional lymph nodes were visualized. The tracer appearance time (TAT, normal value less than 10 min) and lymph drainage patterns after exercise were evaluated.

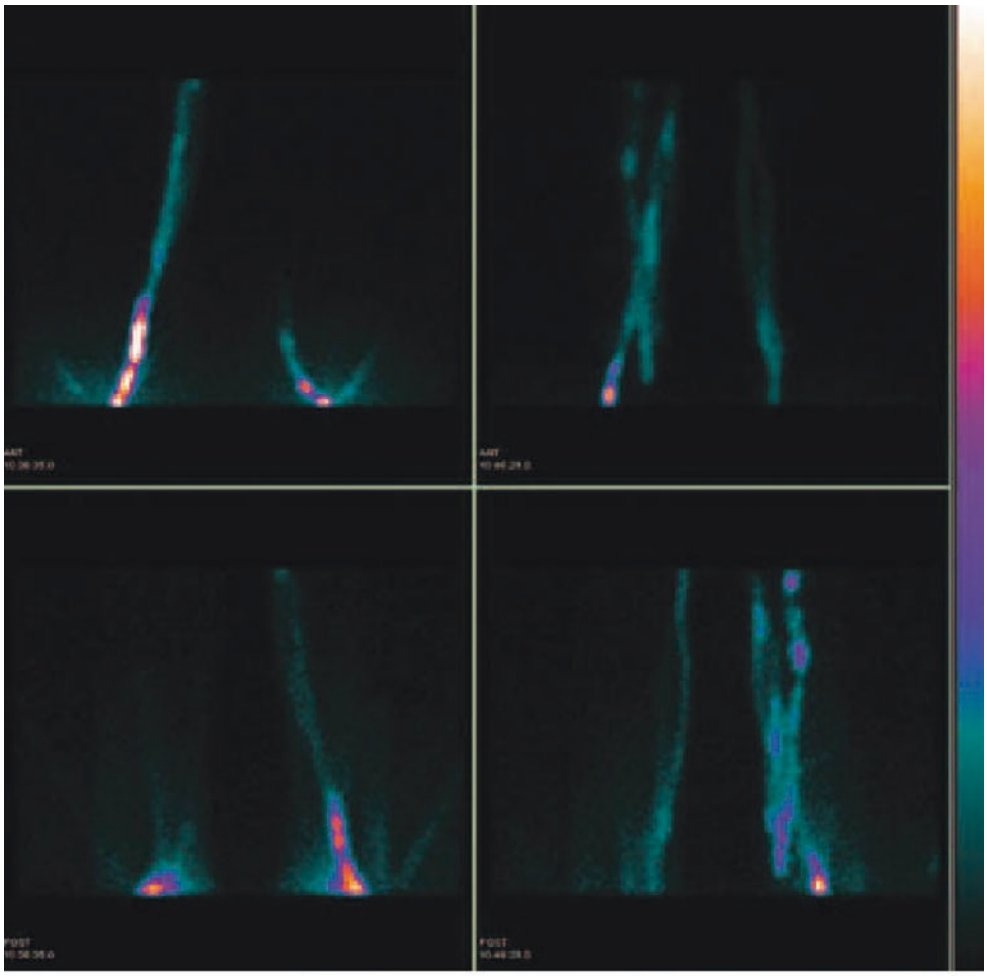

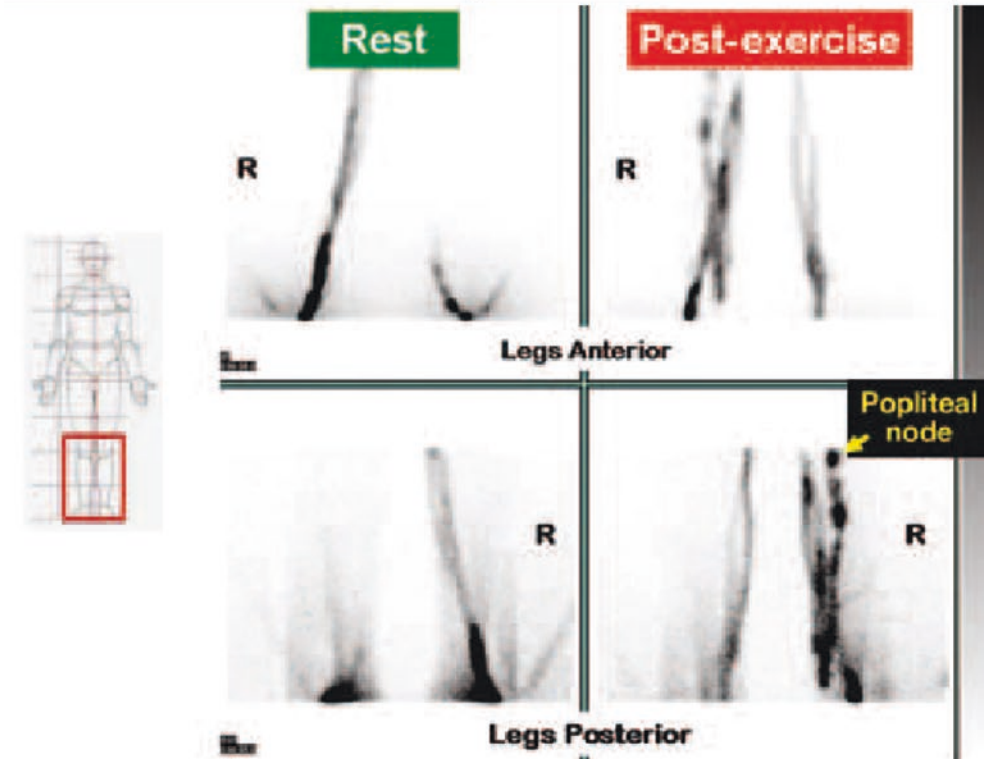

Figs. 5.32 and 5.33 The rest scan shows delayed lymph drainage in the left leg, with normal lymph drainage in the right leg. Exercise accelerated lymph drainage in the left leg. A second lymph drainage pathway was observed in the right leg, with unusual uptake of a popliteal lymph node. The scan demonstrates a shunt between the superficial and deep lymphatic system, as a compensatory mechanism in lymphedema of the right lower limb

Case 5.14: Postexercise Lower Limb Monocompartmental Lymphoscintigraphy in Patient with Acute Edema of the Left Lower Limb and Painful Left Inguinal Lymphadenomegaly

Luciano Feggi, Chiara Peterle, Corrado Cittanti, Valentina de Cristofaro, Stefano Panareo, Ilaria Rambaldi, Virginia Rossetti, Ivan Santi, and Paolo Carcoforo

Background Clinical Case

A 77-year-old woman with pain and swelling of the left lower limb; ultrasound detected left inguinal lymphadenomegaly; after surgical removal, histological diagnosis was metastasis of neuroendocrine carcinoma (poorly differentiated), consistent with Merkel cell carcinoma metastasis (T2N1Mx). Her clinical presentation included edema of the left lower limb and pain; there was a left inguinal scar after surgical removal.

Anatomic location of edema: Left lower limb.

Lymphoscintigraphy

Lymphoscintigraphy was performed following administration of two aliquots of 2 mL containing 111 MBq ^{99m}Tc-albumin nanocolloid. Radiopharmaceutical injections were performed superficially and bilaterally (injection in first, second, and fourth interdigital spaces and in the outer retromalleolar space in each foot). A dual-detector SPECT gamma camera (E-cam Siemens Medical Solutions, Hoffman Estates, IL) equipped with low-energy high-resolution (LEHR) collimators was used to obtain planar images. Planar images were acquired 5 min and 4 h, respectively, after injection (256 × 256 matrix, zoom factor 1.00, acquisition time 200 s for each view) in anterior planar views of the feet and legs, thighs, and inguinal regions.

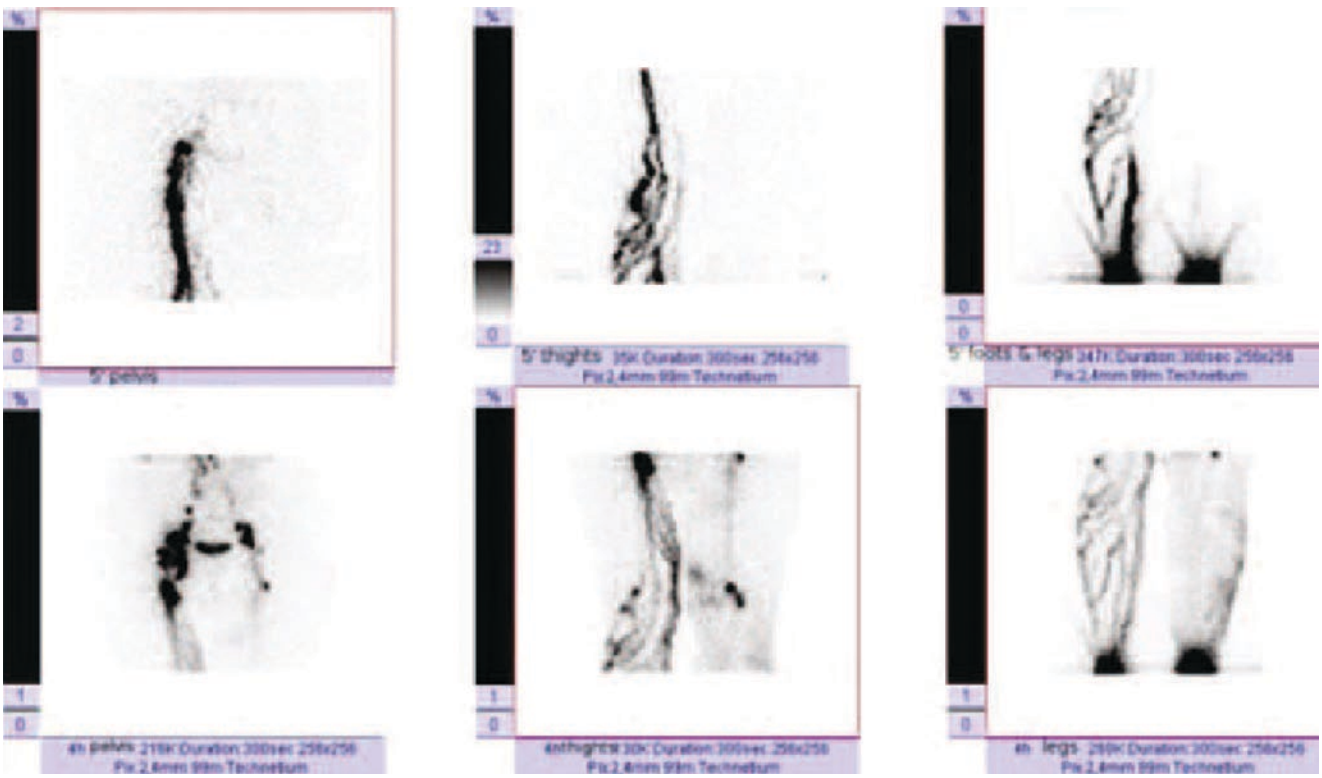

Fig. 5.34 Delayed lymphatic drainage of the left lower limb, with abnormal lymphatic function both in the early acquisition (only the right main lymphatic channel being visualized) and in the 4-h image (mild "dermal flow" in left leg). In the inguinal regions, asymmetrical radiocolloid uptake is observed in the lymph nodes (fewer nodes in left inguinal region). This pattern suggested involvement of the left inguinal lymph nodes causing abnormal drainage in the left lower limb. The patient therefore underwent further examinations, including a [18F] FDG PET/CT scan that visualized a primary tumor in the skin covering the left knee

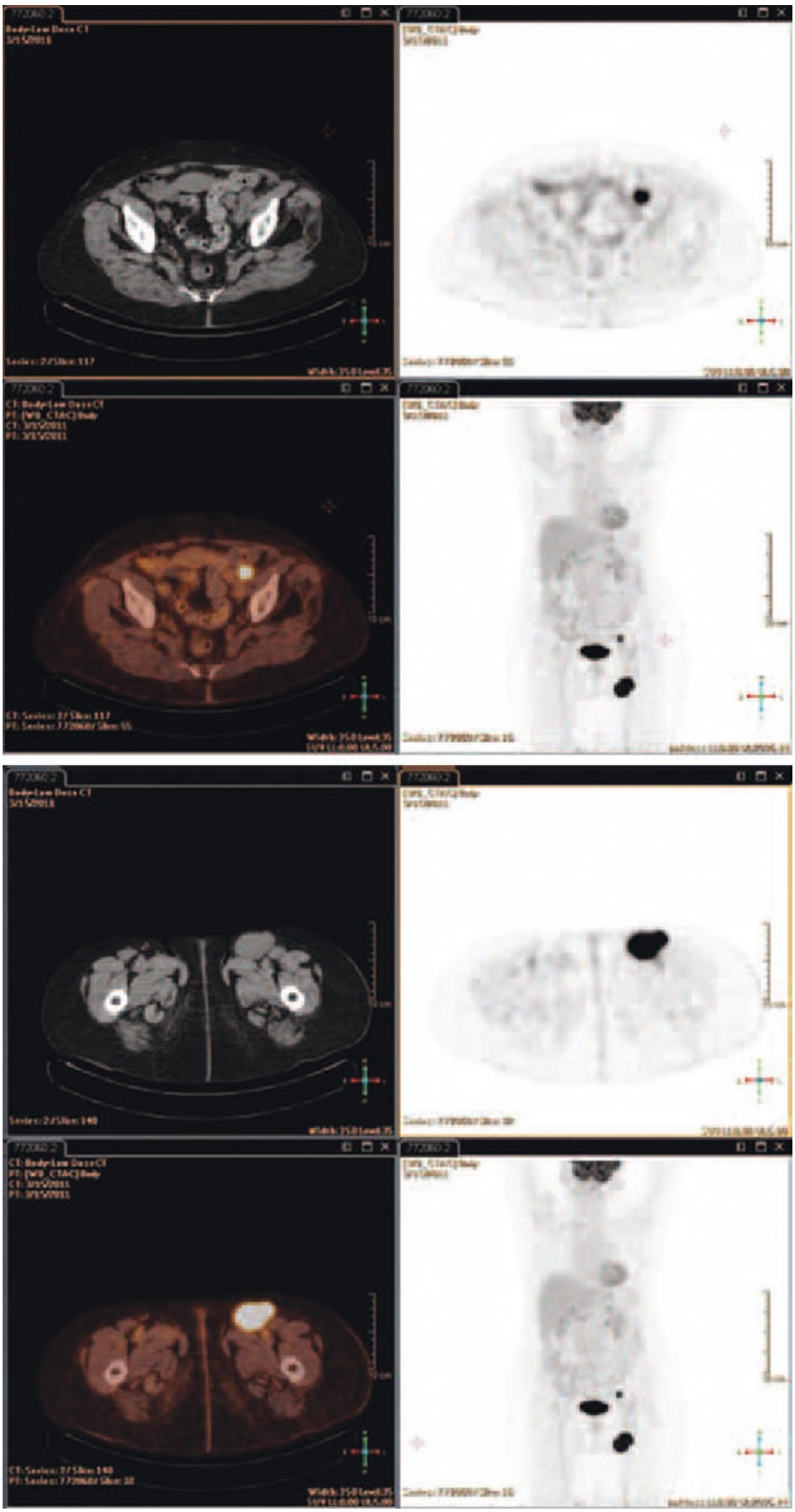

Figs. 5.35 and 5.36 [18F] FDG PET/CT scan visualizing metastatic nodes in the left inguinal basin causing the abnormal lymphatic drainage in the left extremity

Case 5.15: Lower Limb Monocompartmental Lymphoscintigraphy at Rest and Postexercise with Semiquantitative Evaluation of the Tracer Appearance Time in Patient with Secondary Lymphedema of the Right Lower Limb

Girolamo Tartaglione, Roberto Bartoletti, and Marco Pagan

Background Clinical Case

A 71-year-old woman was submitted to surgical removal of primary melanoma of the right leg and sentinel lymph node biopsy (SLNB) of the popliteal lymph node (pN0). About 3 months after surgery she developed a lymphedema of right lower limb.

Anatomic location of edema: Right lower limb.

Lymphoscintigraphy

All tight clothes and elastics were removed before tracer injection. Aliquots of 0.3 mL containing 50 MBq ^{99m}Tc-albumin-nanocolloid were injected intradermally at the first interdigital area, on the top of the feet. Gentle massage was performed after injection in the area. Two scans were acquired starting immediately after injection (the first on the legs and the second on the thighs) following these parameters: planar static scan, preset time 5 min, matrix 128 × 128, 140 Kev ± 10%, and anterior and posterior views. A dual-head gamma camera (GE-Infinia) equipped with low-energy general-purpose (LEGP) collimators was used to provide increased sensitivity. If delayed or absent lymphatic drainage was perceived, then the patient was invited to perform 2 min of continuous isotonic exercise (walking). A postexercise static scan was acquired (128 × 128, 5 min) until the regional lymph nodes were visualized. The tracer appearance time (TAT, normal value less than 10 min) and lymph drainage patterns after exercise were evaluated.

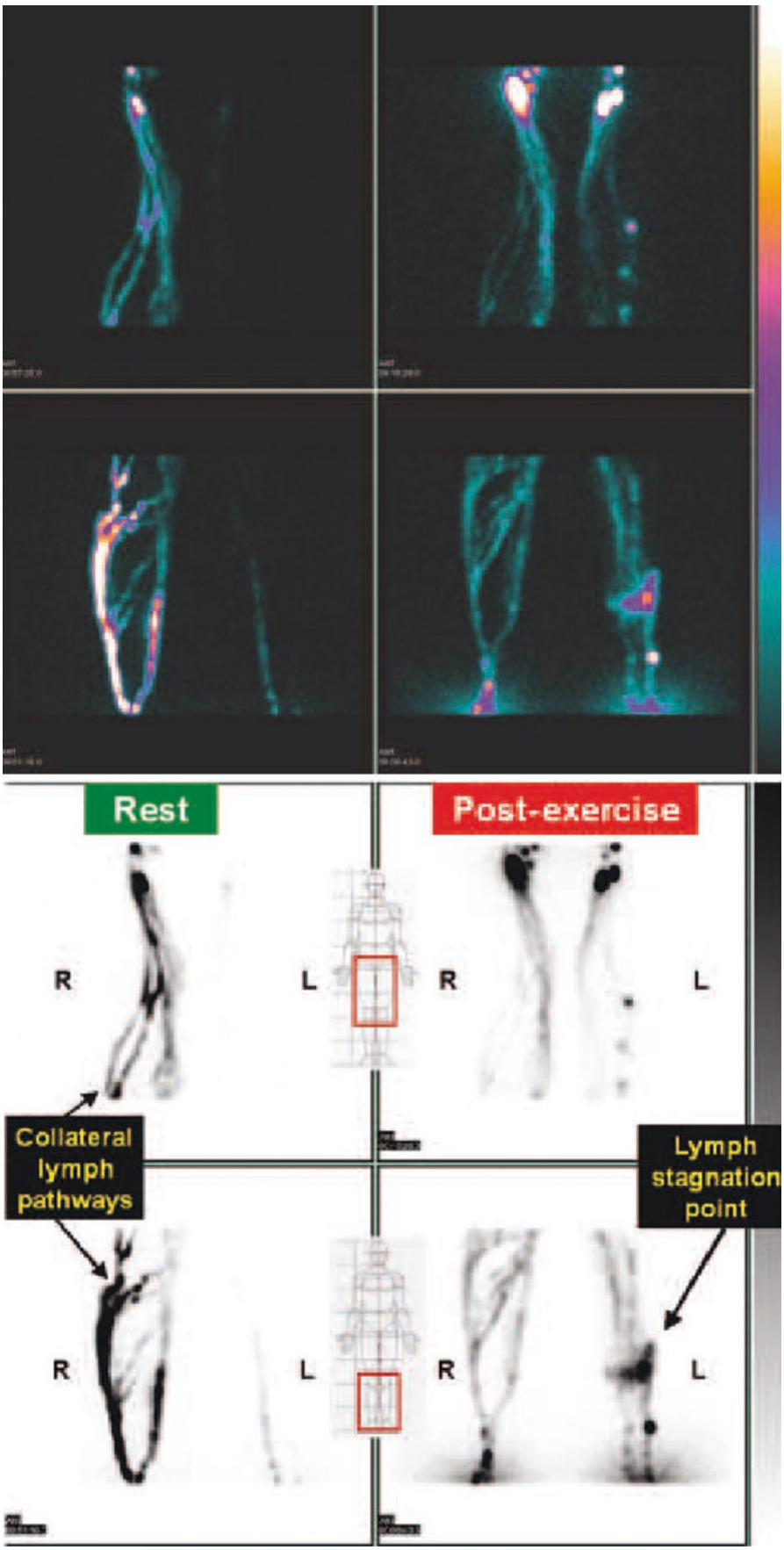

Figs. 5.37 and 5.38 The scans at rest visualize three superficial collateral lymph channels of the right limb with normal visualization of lymph nodes in the right groin (TAT <10 min), and delayed lymph drainage of the left leg. Isotonic exercise accelerated lymph drainage toward the left groin's lymph nodes (TAT = 16 min), with a collateral lymph pathway and an area of radiocolloid collection in the middle third of the left leg. This test revealed a preexisting lymphatic disease of the lower limbs. A personalized program of combined physical therapy was based on the findings of lymphoscintigraphy

Case 5.16: Lower Limb Monocompartmental Lymphoscintigraphy in Patient with Secondary Bilateral Non-pitting Edema of the Lower Extremities, More Evident on the Left, and Left Ureteral Obstruction Due to Lymphocele

Luciano Feggi, Chiara Peterle, Corrado Cittanti, Valentina de Cristofaro, Stefano Panareo, Ilaria Rambaldi, Virginia Rossetti, Ivan Santi, and Paolo Carcoforo

Background Clinical Case

A 47-year-old woman with melanoma of the left leg and metastasis of the inguinal homolateral lymph nodes underwent surgery (removal of melanoma and left inguinal and iliac lymphadenectomy). After 7 years, during follow-up, CT detected a large pelvic mass, which remained undiagnosed (lymphocele? ovarian cyst?). Two years later, the patient suffered from left ureteral obstruction by compression of a pelvic mass on the third tract of the ureter. Patient reported bilateral swelling in the lower limbs, more evident on the left. Therefore her clinical presentation includes bilateral non-pitting edema of the lower extremities, more evident on the left, and left ureteral obstruction, which needs nephrostomy.

Anatomic location of edema: Lower limbs (more evident in left one).

Lymphoscintigraphy

Lymphoscintigraphy was performed following administration of two aliquots of 2 mL containing 111 MBq ^{99m}Tc-albumin nanocolloid. Radiopharmaceutical injections were performed superficially and bilaterally (injection in first, second, and fourth interdigital spaces and in the outer retromalleolar space in each foot). A dual-detector SPECT gamma camera (E-cam Siemens Medical Solutions, Hoffman Estates, IL) equipped with low-energy high-resolution (LEHR) collimators was used to obtain planar images. Planar images were acquired 5 min, 1 h, 4 h, and 24 h, respectively, after injection in an anterior view (256 × 256 matrix, zoom factor 1.00, acquisition time 200 s for each view). SPECT/CT was acquired 24 h after radiopharmaceutical administration (60 s for each frame, CT slice thickness: 1 mm, tube current of 30 mA, tube voltage of 13 kV).

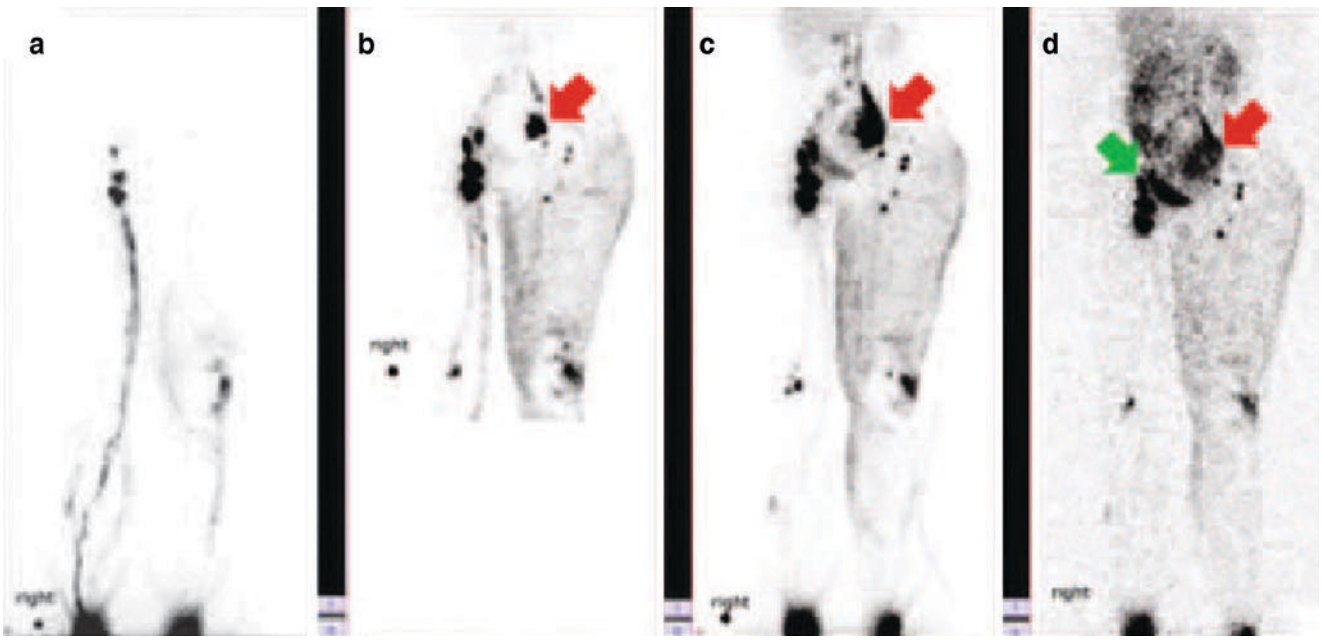

Fig. 5.39 "Whole-body" images extending from the feet to the lower abdomen. From left to right: (**a**) 5 min after radiocolloid injection, normal drainage is noted in the right limb (visualization of a main lymphatic channel and inguinal lymph nodes), whereas in the left limb lymphatic drainage is delayed (the radiocolloid almost stops at the knee). (**b**) 1 h after injection, acquisition from knees to abdomen: normal drainage in right limb with "dermal flow/backflow" in the left thigh, without visualization of the inferior inguinal lymph nodes (prior lymphadenectomy). Bilateral iliac nodes and an area of tracer uptake only on the left (*red arrow*) are visualized. (**c**) Planar scan (feet to abdomen) at 4 h: normal lymphatic drainage on the right limb; popliteal lymph nodes are visualized bilaterally (mostly on the left side), with "dermal flow/backflow" in the thigh; faint radiocolloid uptake in the left inguinal region; in this scan, the pelvic area of radiocolloid accumulation on the left (*red arrow*) appears more evident and larger; there is slight visualization of the bladder and the reticuloendothelial system. (**d**) 24-h scan: the radiocolloid has cleared almost completely from the right lower limb; radioactivity accumulation in the left pelvic area (*red arrow*) has expanded to a larger area. Radioactivity accumulation in the bladder is more evident (*green arrow*), whereas the other sites of uptake remain almost identical. SPECT/CT was performed in order to better characterize this pattern of distribution of the radiocolloid

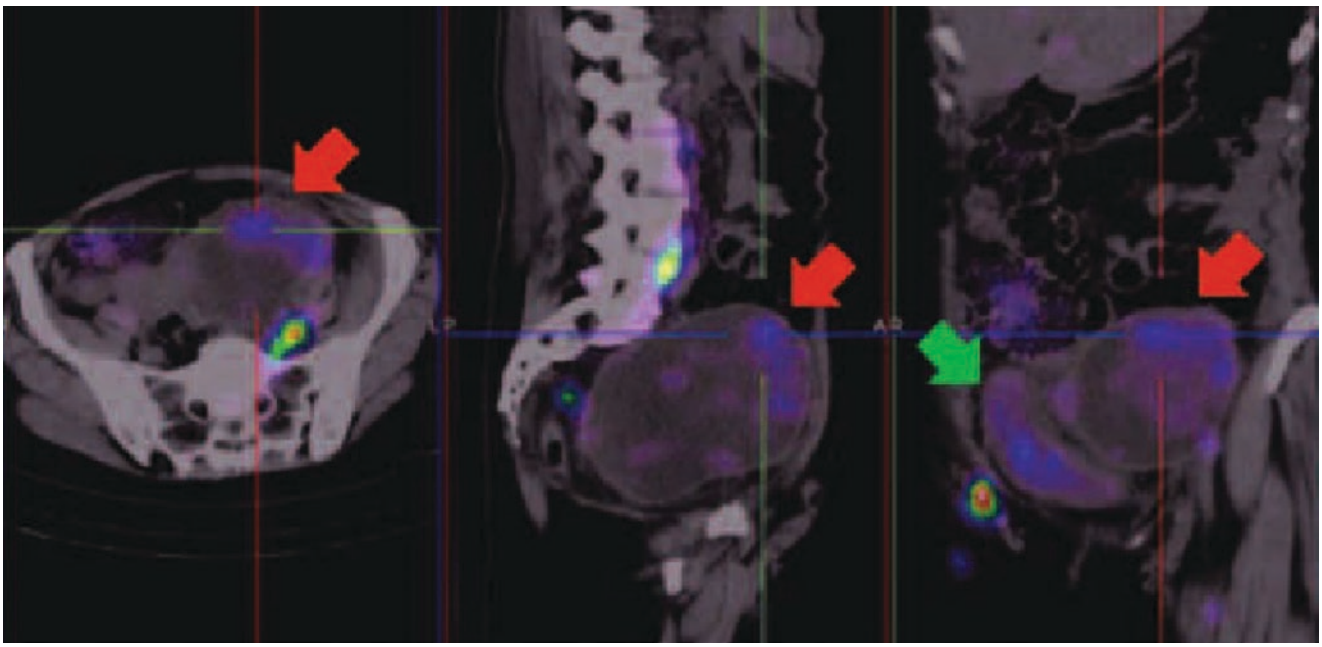

Fig. 5.40 Multiplanar reconstruction (MPR) fusion SPECT/CT (24 h after injection): a large pelvic mass is seen on the left (*red arrow*), near to the bladder (*green arrow*), with retention of a very low amount of radioactivity

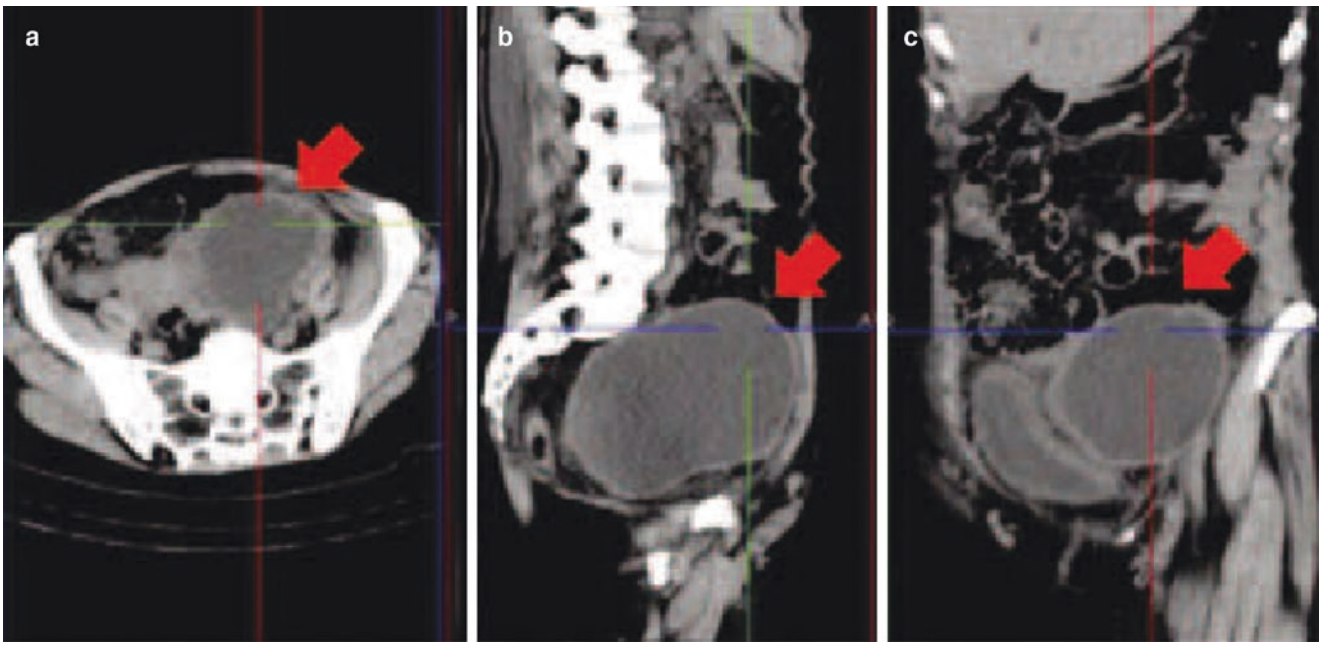

Fig. 5.41 MPR SPECT/CT acquisition (CT only). In the CT component of the acquisition, the content of the pelvic mass (*red arrow*) has radiodensity Hounsfield Unit values typical of a fluid (**a**–**c**). In a diagnostic CT the pelvic mass does not show contrast enhancement: **d** contrast-enhanced transaxial section; **e** corresponding noncontrast CT section

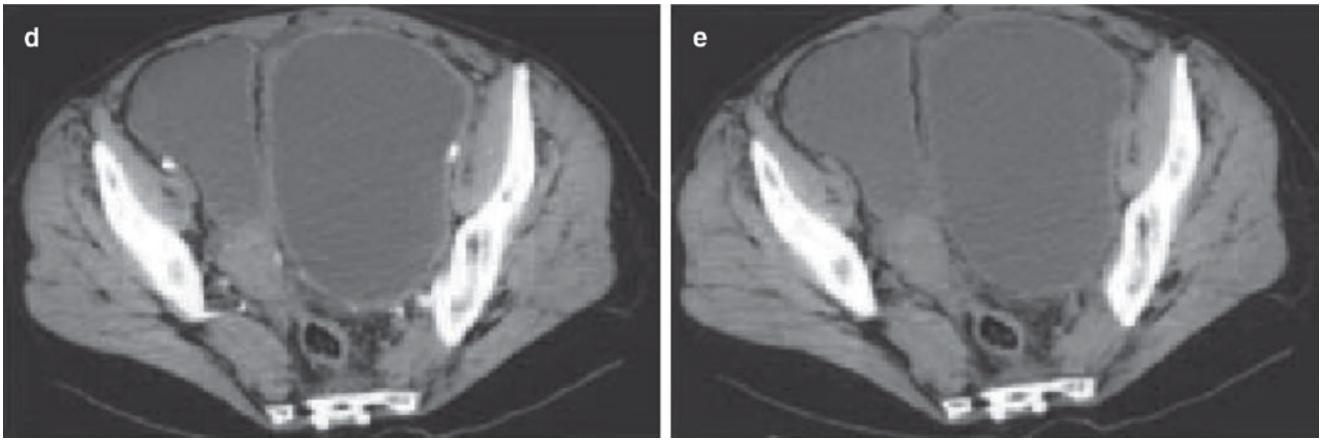

Fig. 5.41 (continued)

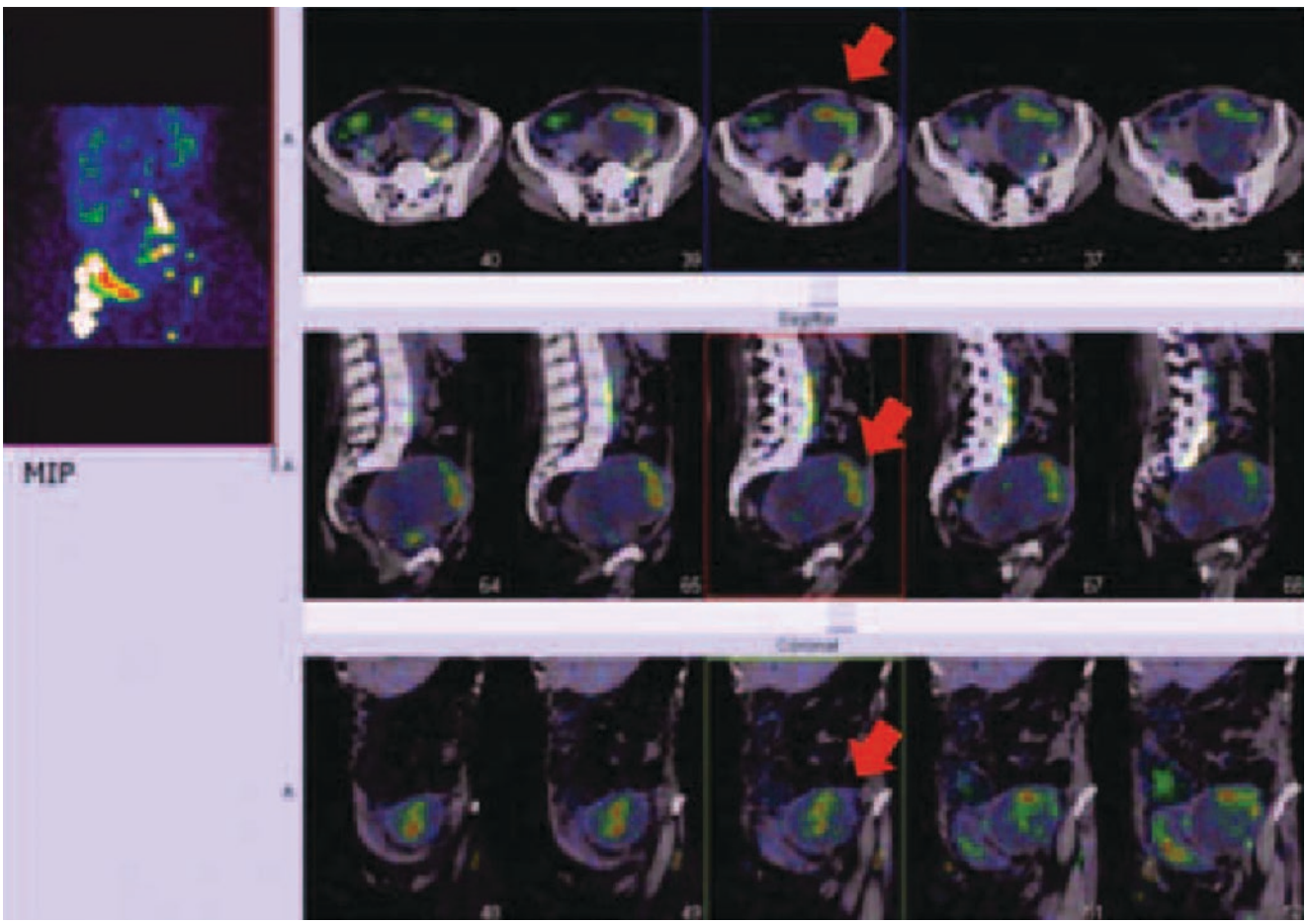

Fig. 5.42 MPR SPECT/CT fusion images. Lymphoscintigraphy confirmed the suspicion that the pelvic mass was a lymphocele. Therefore, the patient underwent surgery, which restored a normal left nephro-ureteral function

Case 5.17: Lower Limb Bicompartmental Lymphoscintigraphy in Patient with Posttraumatic Edema of the Left Leg Associated with Disability Grade 3 According to Ricci Scale, at Baseline and After 5 Years of Multiple Surgeries and Cycles of Therapy

Paola Anna Erba and Luisa Locantore

Background Clinical Case

A 36-year-old man with posttraumatic edema of the left leg. After crush injury, the patient had multiple surgical procedures for the presence of tissue necrosis and cheloids, with cutaneous graft. Before the accident, the patient had had a left leg saphenectomy performed. There is stage V lymphedema of the lower left limb with cutaneous retraction of the proximal and medial portion of the leg, hyperkeratosis, lymphatic vesicles, eczema, and ulcerations. A disability grade 3 according to Ricci scale was present.

Anatomic location of edema: Lower left limb.

Lymphoscintigraphy

Lower Limbs

For the deep lymphatic circulation (DLC): two aliquots of ^{99m}Tc-nanocolloid, 7 MBq each of injection in 0.1 mL in the first and second intermetatarsal spaces, identified by palpating the soles of both feet immediately proximal to the distal heads of the metatarsal bones on each side, inserting the needle by about 12–13 mm to reach the intermetatarsal muscles below the deep fascia plantaris.

For the superficial lymphatic circulation (SLC): three aliquots of about 10 MBq in 0.1 mL on the dorsum of each foot, inserting the needle subdermally in sites corresponding approximately to the prior palmar injections, about 1–2 cm proximally to the interdigital web. Spot and whole-body images were obtained from the distal feet up to the abdomen.

Spot images: 180 s/view, matrix 128 × 128, zoom 1.33.

Whole-body images: matrix 256 × 1024, zoom 1, speed: 12 cm/min

Fig. 5.43 The patient's legs at baseline scan

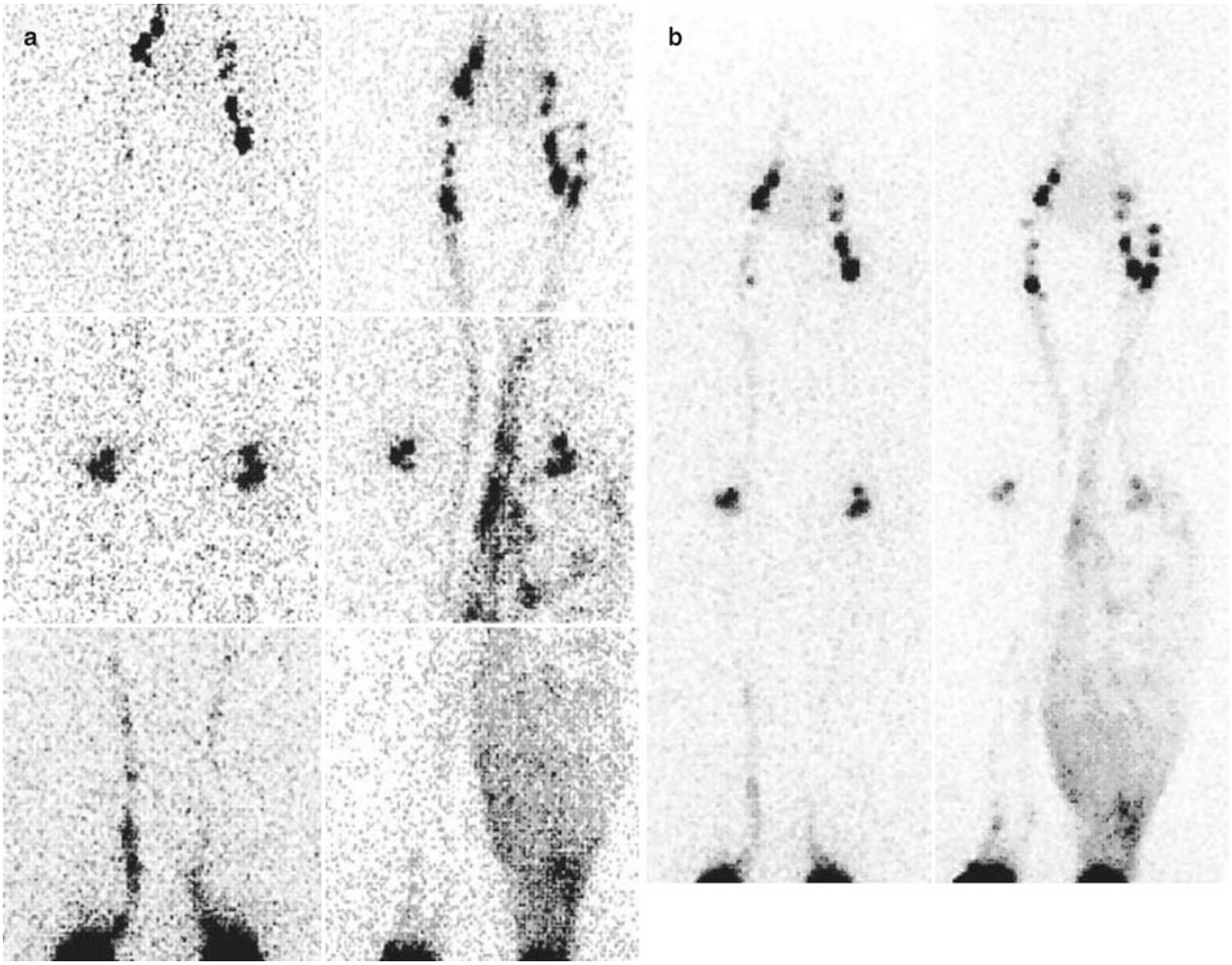

Fig. 5.44 Baseline lymphoscintigraphy. The spot images (**a**, *right*) and the whole-body image (**b**, *right*) show a normal deep lymphatic circulation with a relatively delayed right distal flow; normal popliteal and inguinal lymph nodes are detected with only faint visualization of the inferior right inguinal lymph nodes. After radiocolloid injection for assessing the superficial lymphatic circulation, a normal right lymph flow was depicted. Conversely, "dermal flow" and "dermal backflow" up to mid-thigh are present at the left limb, with preservation of the main lymphatic vessel. New lymph nodes appear in the inguinal region. No radiocolloid progression through the lumbo-aortic lymph nodes is detected and liver uptake of the radiocolloid is not observed

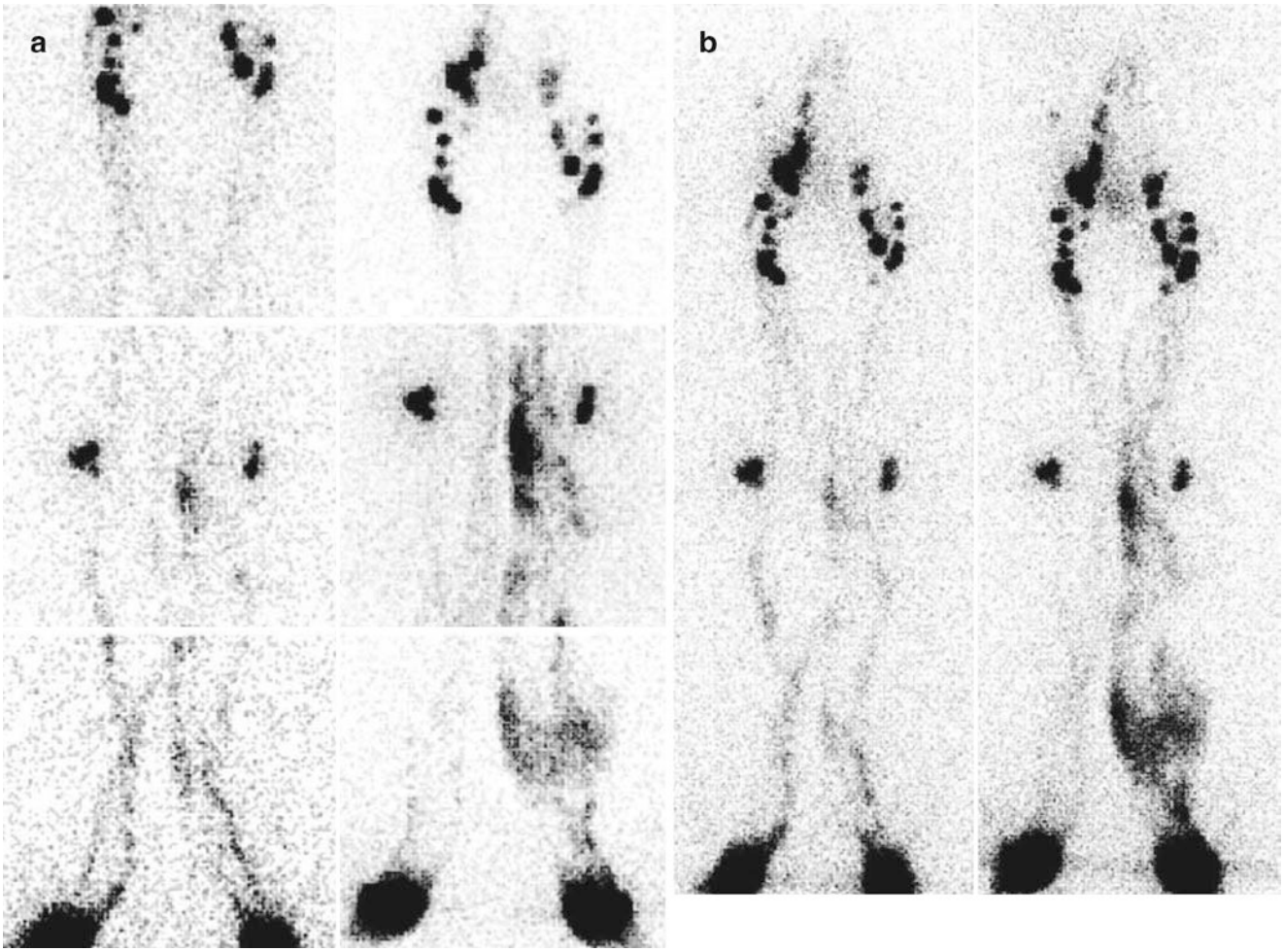

Fig. 5.45 Follow-up lymphoscintigraphy performed after 5 years of subsequent surgical procedures and multiple cycles of therapy. Spot images (anterior view, **a** *left column* DLC, *right column* DLC and SLC) and whole-body images (**b**, *left column* DLC, *right column* DLC and SLC) demonstrated a significant reduction of the left limb "dermal flow" and "dermal backflow" with enhanced lymphatic flow through both the deep and the superficial lymphatic circulation. However, collateral lymphatic channels are still visualized after injection for evaluation of the SLC, with enhanced uptake at the site of popliteal lymph nodes; furthermore, increased radiocolloid accumulation along the soft tissue of the lower part of the leg is still present. The pattern of lymphatic drainage for the right leg remains normal. Based on these findings, a new, less aggressive treatment plan was designed, to maintain these favorable results

Case 5.18: Upper and Lower Limb Bicompartmental Lymphoscintigraphy in Patient with Bilateral Feet and Ankle Edema, More Prevalent on Left Side

Paola Anna Erba and Luisa Locantore

Background Clinical Case

A 62-year-old woman with bilateral edema mainly at the distal part of the leg and the feet, worsening in the last 10 months. Doppler ultrasound negative. Ultrasound of the soft tissue showing an increased thickening of the derma, which is hypoechogenic, representing an interstitial edema.

Anatomic location of edema: Bilateral feet and ankles, major at the left side.

Lymphoscintigraphy

Upper Limbs

For the deep lymphatic circulation (DLC): two aliquots of 99mTc-nanocolloid, 7 MBq each of injection in 0.1 mL in the first and second intermetacarpal spaces, identified by palpating the palms of both hands immediately proximal to the distal heads of the metacarpal bones on each side, inserting the needle by about 12–13 mm to reach the intermetacarpal muscles below the deep fascia. *For the superficial lymphatic circulation (SLC)*: three aliquots of about 10 MBq in 0.1 mL on the dorsum of each hand, inserting the needle subdermally in sites corresponding approximately to the prior palmar injections, about 1–2 cm proximally to the interdigital web. Spot and whole-body images of both arms, thorax, and upper abdomen.

Lower Limbs

For the DLC: two aliquots of 99mTc-nanocolloid, 7 MBq each of injection in 0.1 mL in the first and second intermetatarsal spaces, identified by palpating the soles of both feet immediately proximal to the distal heads of the metatarsal bones on each side, inserting the needle by about 12–13 mm to reach the intermetatarsal muscles below the deep fascia plantaris.

For the SLC: three aliquots of about 10 MBq in 0.1 mL on the dorsum of each foot, inserting the needle subdermally in sites corresponding approximately to the prior palmar injections, about 1–2 cm proximally to the interdigital web. Spot and whole-body images were obtained from the distal feet up to the abdomen.

Spot images: 180 s/view, matrix 128 × 128, zoom 1.33

Whole-body images: matrix 256 × 1024, zoom 1, speed: 12 cm/min

This is a typical example of lower limb lymphedema due to an impairment of the DLC with conserved function of the SLC; however, signs of overload of the SLC are also present at the left lower limb. Arm circulation is normal.

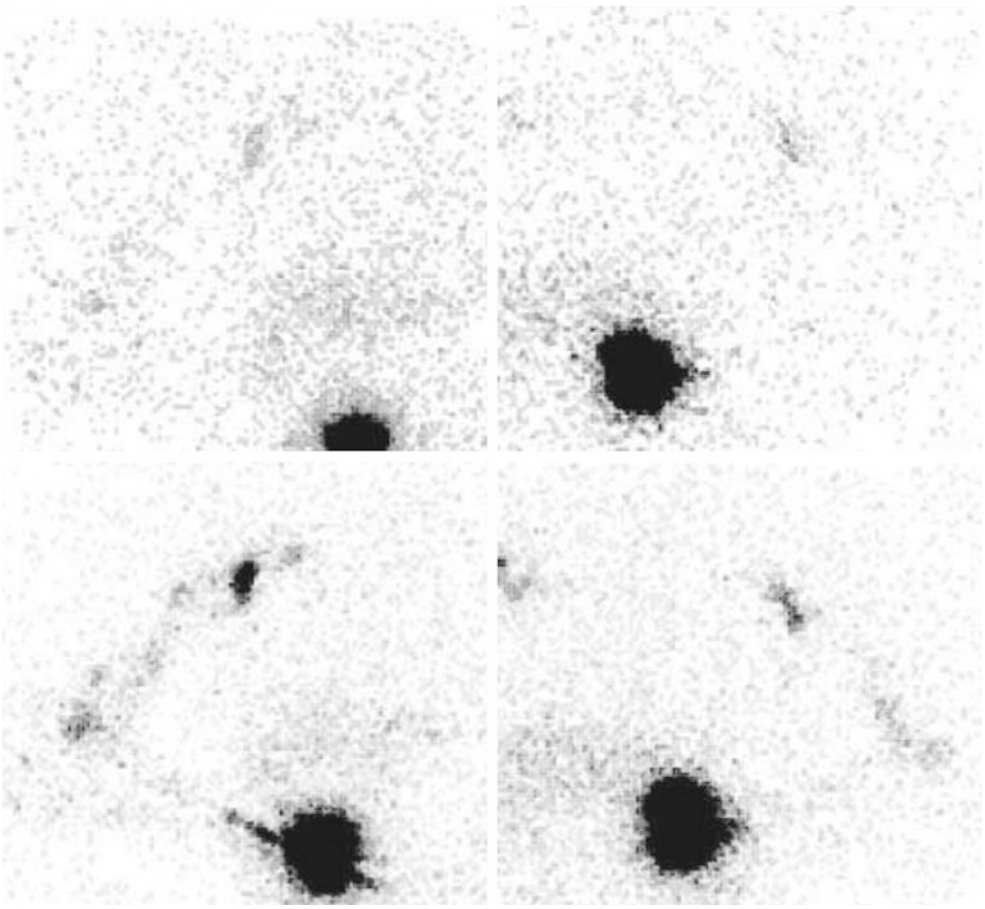

Fig. 5.46 Lymphoscintigraphy of upper limbs, spot images (*upper panel*: DLC; *lower panel*: SLC). A normal deep and superficial lymphatic circulation of the left upper limb is present with mild delay of the superficial circulation. Faint uptake is present at epitrochlear lymph nodes, while axillary lymph nodes are bilaterally visualized, despite being low in number

Fig. 5.47 Spot images of lymphoscintigraphy of the lower limbs of the DLC from the distal feet to the inguinal region of the lower limbs. No radiocolloid migration from the injection sites

Fig. 5.48 Spot images of lymphoscintigraphy of the lower limbs of the DLC and SLC from the distal feet to the inguinal region. Images show a normal SLC at the right lower limb, while at the left limb collateral channels are visualized, with sites of uptake representing lymphatic collection along the external margin thigh. No popliteal lymph nodes can be detected, while only few lymph nodes are detected at the inguinal region

Case 5.19: Upper and Lower Limb Bicompartmental Lymphoscintigraphy in Patient with Right Pelvic Paravesical and Inguinal Swelling

Paola Anna Erba and Luisa Locantore

Background Clinical Case

A 33-year-old man with right pelvic (alongside the bladder) and right inguinal swelling. CT finding of multiple cystic lesions suspected for cystic lymphangiomatosis, localized in the retroperitoneal space, at the splenic lodge, in the bone (ribs, vertebral bodies, and pelvic bones of maximum 23 mm) and in the pelvis (about 10 cm). Negative [18F] FDGPET/CT findings.

Anatomic location of edema: Right inguinal.

Lymphoscintigraphy

Upper Limbs

For the deep lymphatic circulation (DLC): two aliquots of 99mTc-nanocolloid, 7 MBq each of injection in 0.1 mL in the first and second intermetacarpal spaces, identified by palpating the palms of both hands immediately proximal to the distal heads of the metacarpal bones on each side, inserting the needle by about 12–13 mm to reach the intermetacarpal muscles below the deep fascia.

For the superficial lymphatic circulation (SLC): three aliquots of about 10 MBq in 0.1 mL on the dorsum of each hand, inserting the needle subdermally in sites corresponding approximately to the prior palmar injections, about 1–2 cm proximally to the interdigital web. Spot and whole-body images of both arms, thorax, and upper abdomen.

Lower Limbs

For the DLC: two aliquots of 99mTc-nanocolloid, 7 MBq each of injection in 0.1 mL in the first and second intermetatarsal spaces, identified by palpating the soles of both feet immediately proximal to the distal heads of the metatarsal bones on each side, inserting the needle by about 12–13 mm to reach the intermetatarsal muscles below the deep fascia plantaris.

For the SLC: three aliquots of about 10 MBq in 0.1 mL on the dorsum of each foot, inserting the needle subdermally in sites corresponding approximately to the prior palmar injections, about 1–2 cm proximally to the interdigital web. Spot and whole-body images were obtained from the distal feet up to the abdomen.

Spot images: 180 s/view, matrix 128 × 128, zoom 1.33

Whole-body images: matrix 256 × 1024, zoom 1, speed: 12 cm/min

Normal bilateral lymph flow was depicted, with only mild delay for the right SLC in the medial and distal part of the leg. Interestingly, two sites of radiopharmaceutical accumulation are evident. The first is at the pelvis localized near the bladder, at the right side, and which is receiving the lymph from the deep lymphatic system. The second is in the upper abdominal area, at the level of the upper right kidney portion which is supplied by the SLC. Normal lymph node images were seen for the popliteal lymph nodes bilaterally and for the left inguinal node. Progression through the lumbo-aortic lymph nodes is present, as well as faint liver uptake of the radiocolloids.

The exam demonstrated the lymphatic nature of both the pelvic and the abdominal collections, therefore confirming the clinical diagnosis of cystic lymphangiomatosis.

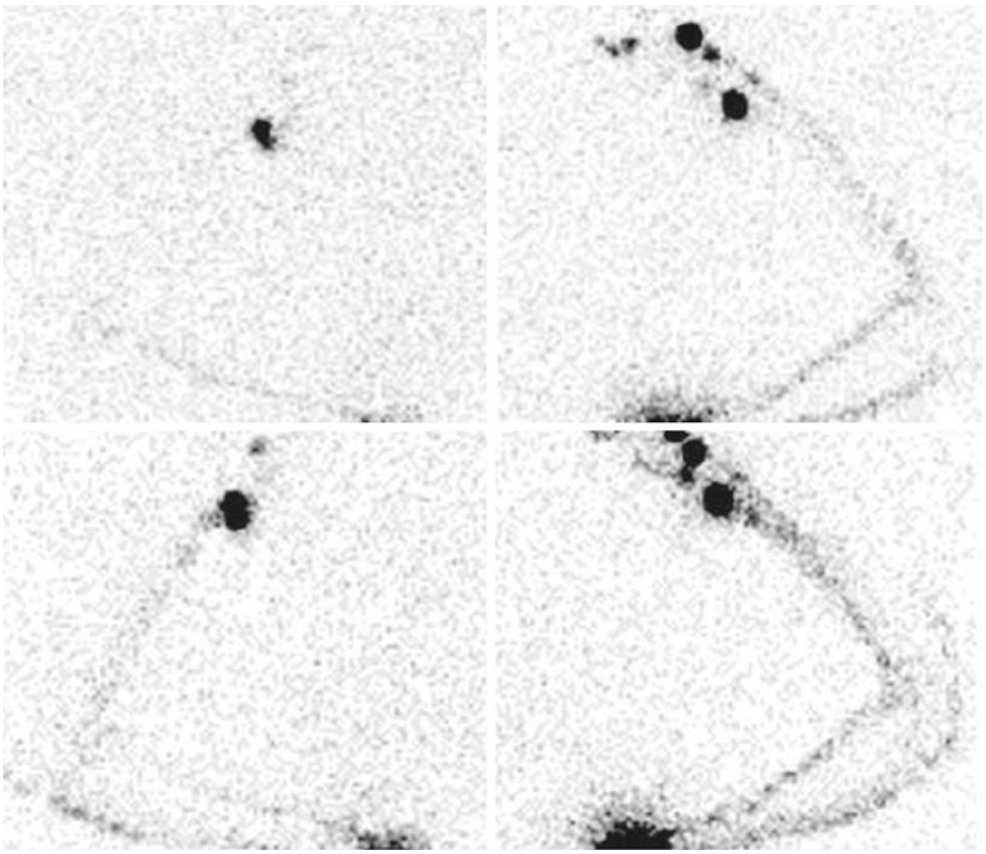

Fig. 5.49 Lymphoscintigraphy of the upper limbs, spot images. *Upper panels*: DLC. *Lower panels*: DLC and SLC

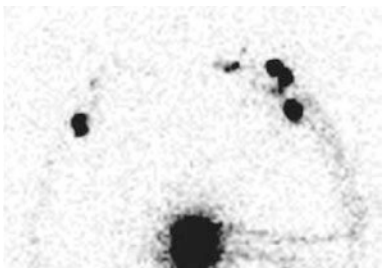

Fig. 5.50 Anterior view of the thoracic and upper abdominal regions, showing a normal deep and superficial lymphatic circulation of the right upper limb; for the left upper limb simultaneous visualization of DLC and SCL was observed immediately after the first injection (for DLC). No epitrochlear lymph nodes were detected and also the right axillary lymph nodes were faintly visualized (mainly first-level nodes). The left axillary nodes were normal. At the end of this phase of the scan radiocolloids had not yet localized in the liver

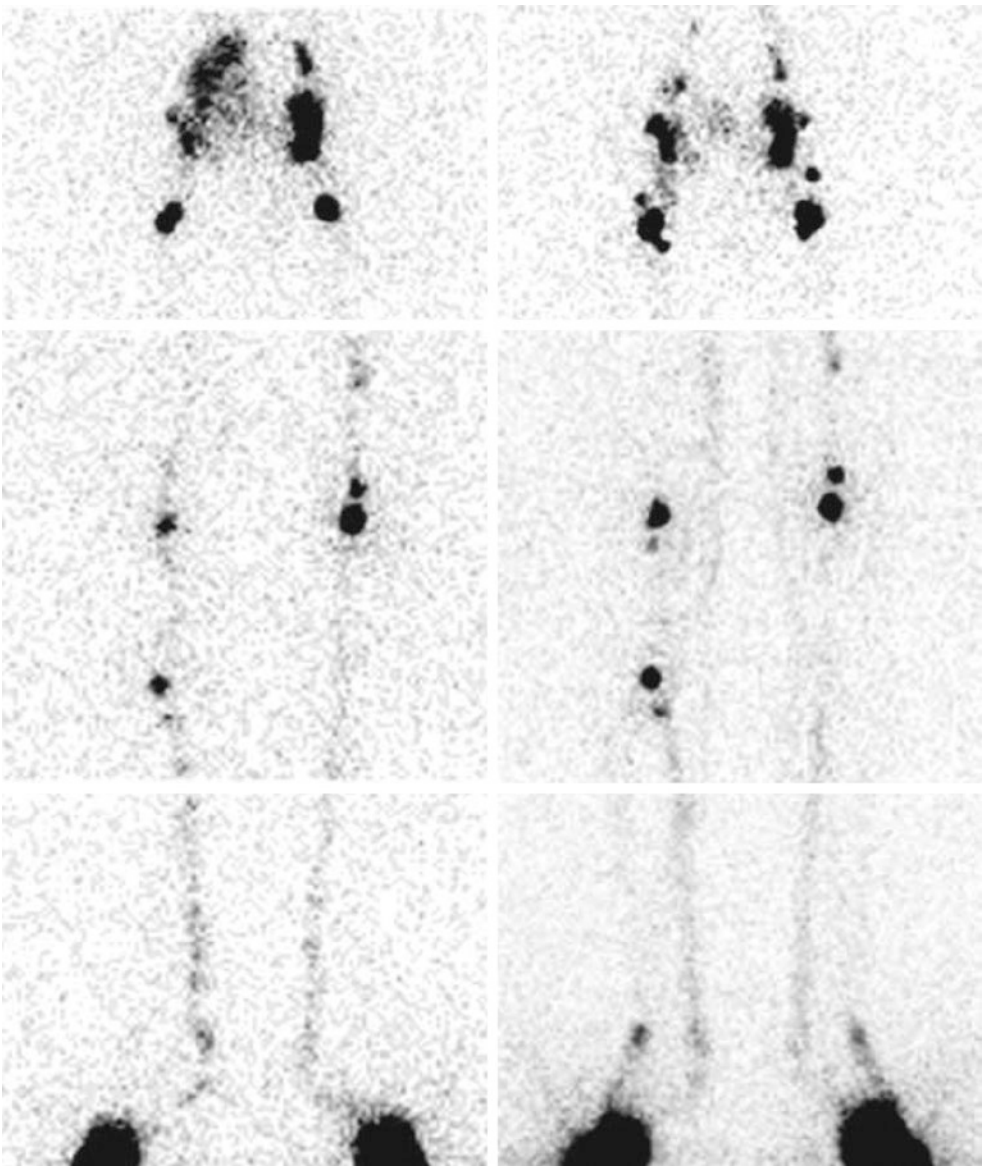

Fig. 5.51 Spot images of lower limbs during lymphoscintigraphy from the distal feet to the inguinal region. *Left column*: DLC. *Right column*: SLC

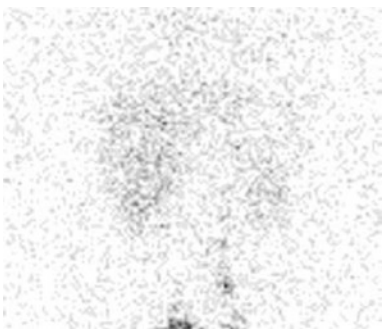

Fig. 5.52 Spot images of the abdomen, anterior view

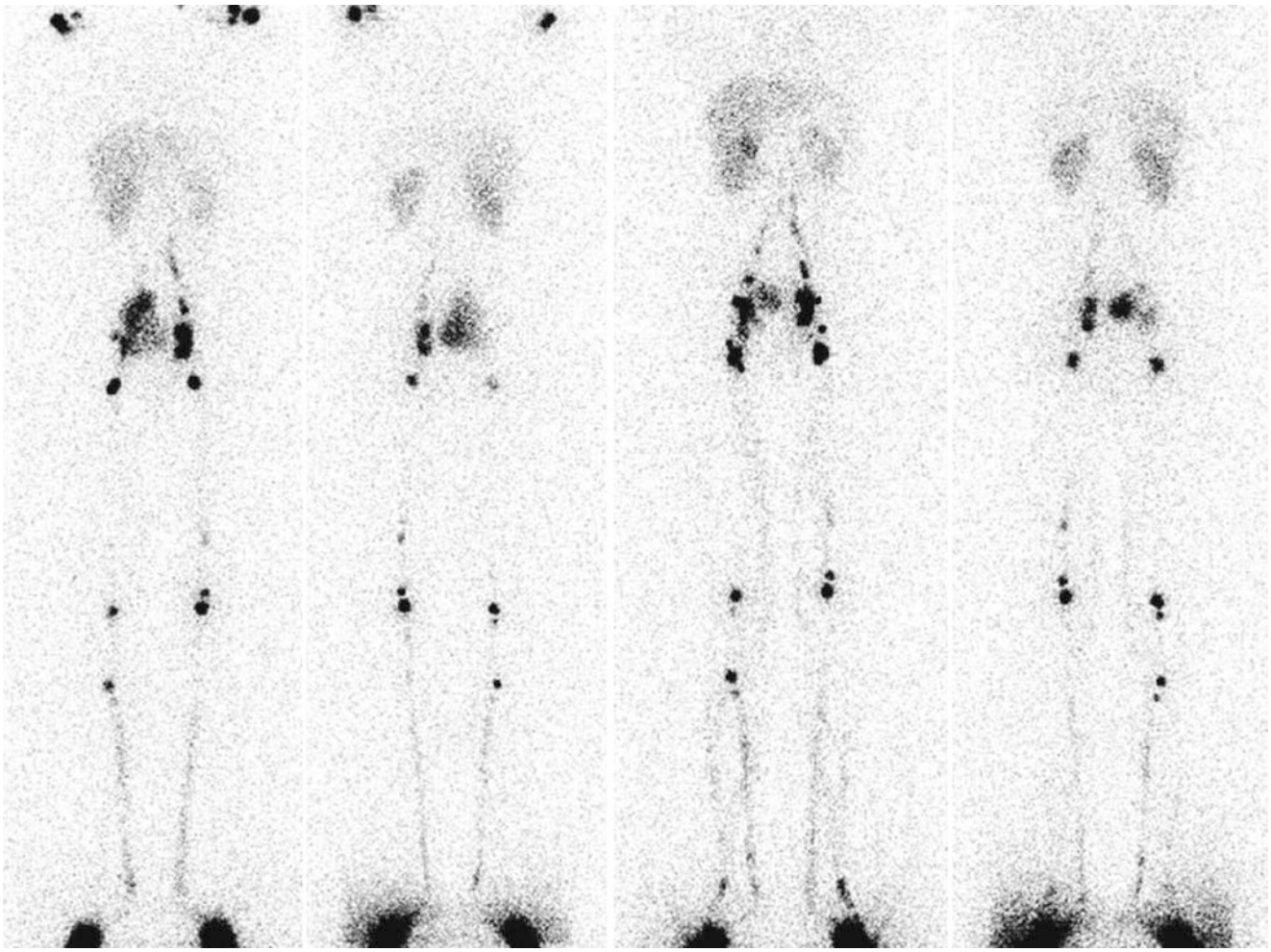

Fig. 5.53 Whole-body images (*left column*, anterior view; *right column*, posterior view) after radiocolloid injection for the assessment of DLC

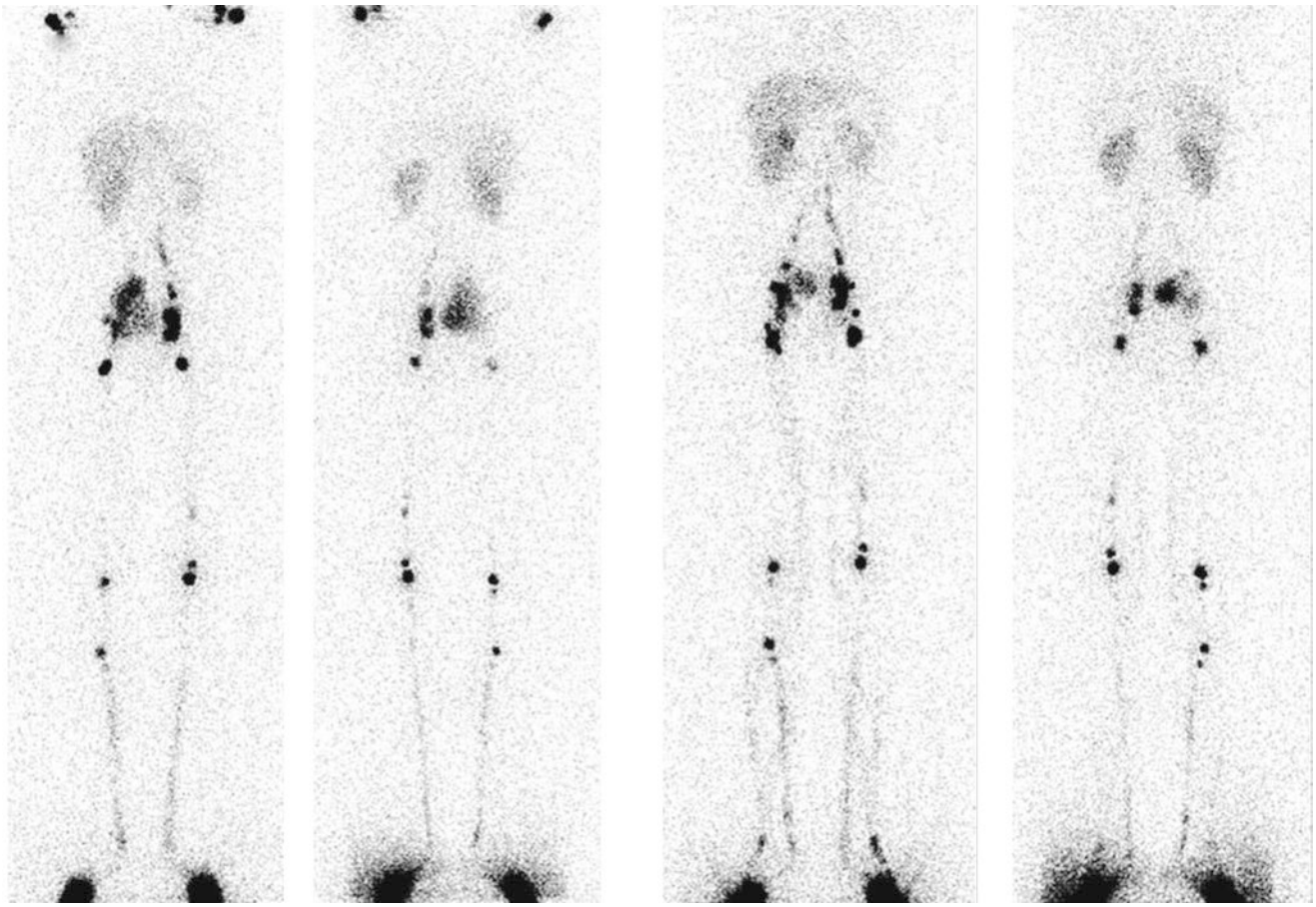

Fig. 5.54 With both DLC and SLC

Case 5.20: Lower Limb Bicompartmental Lymphoscintigraphy in Patient with Edema of the Scrotum

Paola Anna Erba and Luisa Locantore

Background Clinical Case

A 72-year-old man with edema of the scrotum but no edema of upper or lower extremities. Previous surgery for left inguinal hernia.

Anatomic location of edema: Scrotum.

Lymphoscintigraphy

For the deep lymphatic circulation (DLC): two aliquots of 99mTc-nanocolloid, 7 MBq each of injection in 0.1 mL into the first and second intermetatarsal spaces, identified by palpating the soles of both feet immediately proximal to the distal heads of the metatarsal bones on each side, inserting the needle by about 12–13 mm to reach the intermetatarsal muscles below the deep fascia plantaris.

For the superficial lymphatic circulation (SLC): three aliquots of about 10 MBq in 0.1 mL on the dorsum of each foot, inserting the needle subdermally in sites corresponding approximately to the prior palmar injections, about 1–2 cm proximally to the interdigital web. Spot and whole-body images were obtained from the distal feet up to the abdomen.

Spot images: 180 s/view, matrix 128 × 128, zoom 1.33

Whole-body images: matrix 256 × 1024, zoom 1, speed: 12 cm/min

After injections for assessment of the SLC, a normal right lymph flow was depicted, with only mild delay in the medial and distal part of the leg. Conversely, at the left limb, multiple collateral vessels are evident with lymph collection at the proximal left leg; preservation of the main lymphatic vessel is present. New images of the lymph nodes appear at the inguinal region. The lymph collection at the left scrotum persists, without increasing significantly the uptake of the radiocolloid. Progression through the lumbo-aortic lymph nodes is present, as well as faint liver uptake of the radiocolloids.

The exam demonstrated the lymphatic origin of the edema of the scrotum, which is alimented by both the deep and the superficial lymphatic circulation and is evident after injection at the intermetatarsal space. Therefore, the same technique of injection was used for the subsequent injection of the blue dye during surgery performed to detect the site of lymphatic leakage. After the injection, which was performed after the preparation of the main operative field, a passive movement of the patient's leg was performed to allow the blue dye to reach the site of leak. As soon as the operative field became blue, indicating blue dye extravasation, the surgeon searched for the site of leakage, and then performed the suture.

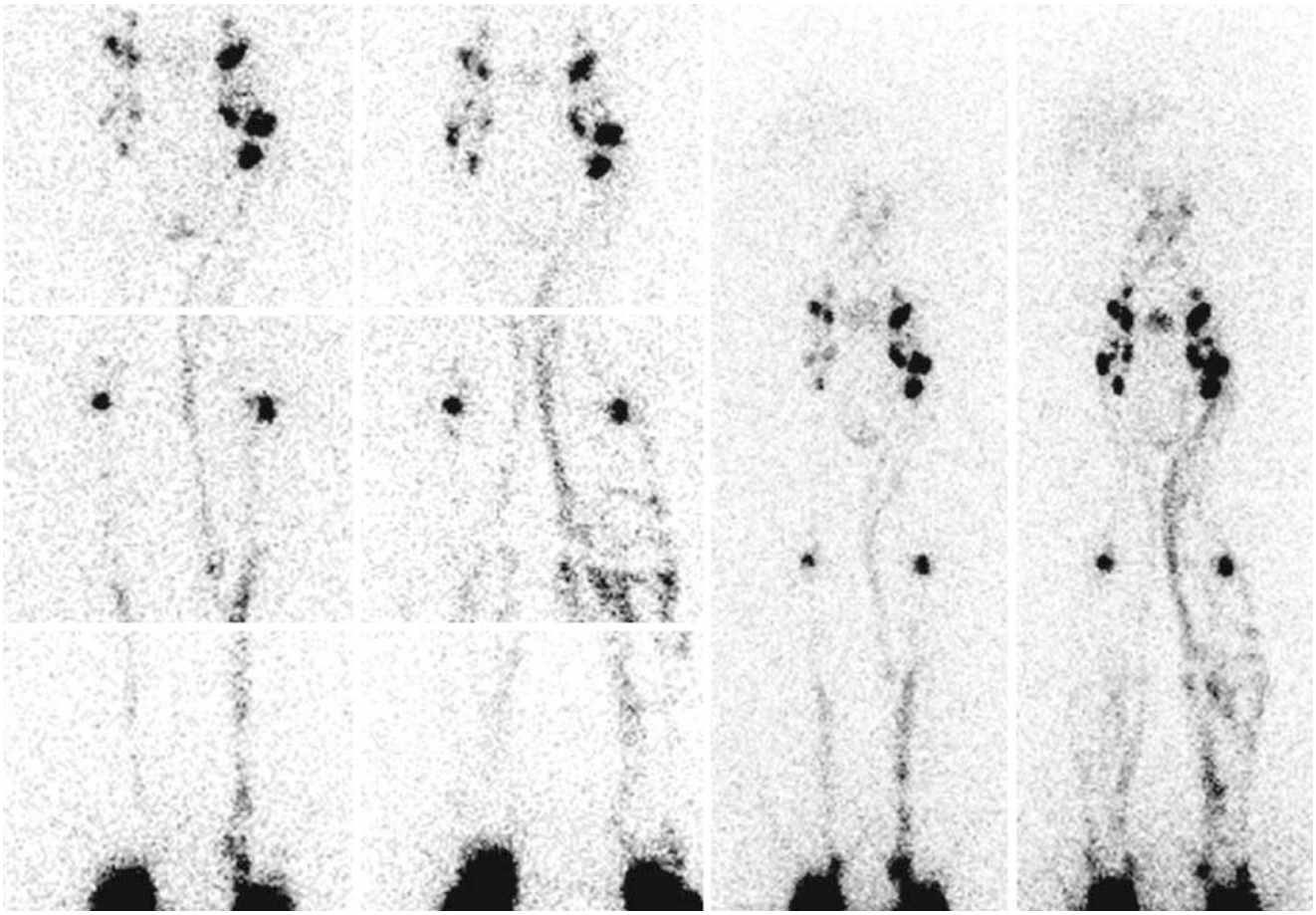

Figs. 5.55 and 5.56 Lymphoscintigraphy, spot images (Fig. 5.55), and whole-body images (Fig. 5.56) of the lower limbs (*left column*, DLC; *right column* DLC and SLC). Normal deep lymphatic circulation of the right lower limbs with a relatively slow right distal flow; normal popliteal and inguinal nodes are detected, with only faint visualization of the inferior right inguinal lymph nodes. At the left lower limb, concomitant DLC and SLC are visible, both delayed as compared to the right DLC and SLC. In addition, radiocolloid accumulation is also clearly depicted, localized medially at the left proximal thigh, which is consistent with the edema of the scrotum. Normal popliteal and inguinal nodes are detected also on the left side

Case 5.21: Lower Limb Monocompartmental Lymphoscintigraphy in Patient with Postsurgical Chylopericardium (Ductus Arteriosus), Treated with Thoracentesis

Paola Anna Erba and Luisa Locantore

Background Clinical Case

Girl, aged 1 year, with postsurgical chylopericardium (ductus arteriosus), treated with thoracentesis.

Anatomic location of edema: Pericardium.

Lymphoscintigraphy

Lower Limbs

For the superficial lymphatic circulation (SLC): three aliquots of about 10 MBq in 0.1 mL on the dorsum of each foot, inserting the needle subdermally, about 1–2 cm proximally to the interdigital web. Spot and whole-body images were obtained from the distal feet up to the abdomen.

Spot images: 180 s/view, matrix 128 × 128, zoom 1.33

Whole-body images: matrix 256 × 1024, zoom 1, speed: 12 cm/min

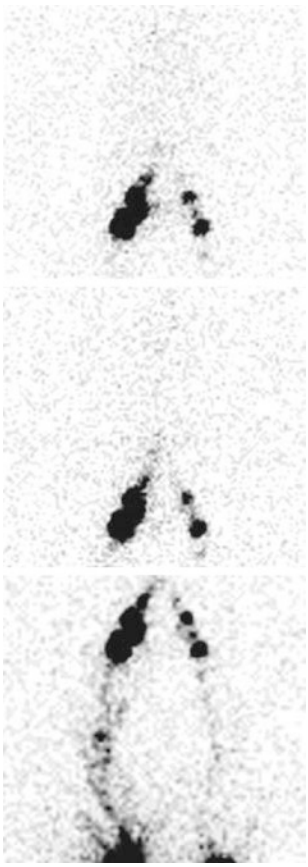

Fig. 5.57 Early spot lymphoscintigraphic acquisitions (SLC) of the lower limbs from the distal feet to the liver, acquired immediately after subdermal radiocolloid administration. A normal lymphatic drainage pattern is present at the left side. At the right side, there are indirect signs of overloaded drainage with delayed radiocolloid migration along dilated lymphatic vessels and delayed appearance of dermal backflow at the leg. Popliteal and inguinal lymph nodes are detected (mainly at right side). At this time, no radiocolloid accumulation is detectable in the thorax

Fig. 5.58 Delayed spot lymphoscintigraphic acquisitions (SLC) of the lower limbs from the distal feet to the liver acquired 2 h after radiocolloid injection. A clear pattern of dermal backflow at the leg is observed, with persisting uptake in lymph nodes. Physiological visualization of the liver. In these images, faint radiocolloid accumulation can be detected in the thorax, localized in the mediastinal space and cardiac region, demonstrating the persistence of chylopericardium. A sample of pleuropericardial fluid was withdrawn from a mediastinal catheter; gamma counting of this sample confirmed radiocolloid localization, further confirming the lymphatic origin of the effusion

References

1. Mortimer PS. Managing lymphedema. Clin Dermatol. 1995;13:499–505.
2. Ely JW, Osheroff JA, Chambliss ML, et al. Approach to leg edema of unclear etiology. J Am Board Fam Med. 2006;19:148–60.
3. Tiwari A, Cheng KS, Button M, et al. Differential diagnosis, investigation, and current treatment of lower limb lymphedema. Arch Surg. 2003;138:152–61.
4. Nakazono T, Kudo S, Matsuo Y, et al. Angiosarcoma associated with chronic lymphedema (Stewart-Treves syndrome) of the leg: MR imaging. Skelet Radiol. 2000;29:413–6.
5. Executive Committee. The diagnosis and treatment of peripheral lymphedema: 2016 consensus document of the International Society of Lymphology. Lymphology. 2016;49:170–84.
6. Gasbarro V, Michelini S, Antignani PL, et al. The CEAP-L classification for lymphedemas of the limbs: the Italian experience. Int Angiol. 2009;28:315–24.
7. Mortimer PS. Swollen lower limb-2: lymphoedema. BMJ. 2000;320:1527–9.
8. Stemmer R. A clinical symptom for the early and differential diagnosis of lymphedema. Vasa. 1976;5:261–2.
9. Fries R. Differential diagnosis of leg edema. MMW Fortschr Med. 2004;146:39–41.
10. Brorson H, Ohlin K, Olsson G, et al. Adipose tissue dominates chronic arm lymphedema following breast cancer: an analysis using volume rendered CT images. Lymphat Res Biol. 2006;4:199–210.
11. Ghanta S, Cuzzone DA, Torrisi JS, et al. Regulation of inflammation and fibrosis by macrophages in lymphedema. Am J Physiol Heart Circ Physiol. 2015;308:H1065–77.
12. Ly CL, Kataru RP, Mehrara BJ. Inflammatory manifestations of lymphedema. Int J Mol Sci. 2017;18.
13. Savetsky IL, Torrisi JS, Cuzzone DA, et al. Obesity increases inflammation and impairs lymphatic function in a mouse model of lymphedema. Am J Physiol Heart Circ Physiol. 2014;307:H165–72.
14. Weitman ES, Aschen SZ, Farias-Eisner G, et al. Obesity impairs lymphatic fluid transport and dendritic cell migration to lymph nodes. PLoS One. 2013;8:e70703.
15. Greene AK, Grant FD, Slavin SA. Lower-extremity lymphedema and elevated body-mass index. N Engl J Med. 2012;366:2136–7.
16. Goss JA, Greene AK. Sensitivity and specificity of the Stemmer sign for lymphedema: a clinical lymphoscintigraphic study. Plast Reconstr Surg Glob Open. 2019;7:e2295. https://doi.org/10.1097/GOX.0000000000002295.
17. Kaulesar Sukul DM, den Hoed PT, Johannes EJ, et al. Direct and indirect methods for the quantification of leg volume: comparison between water displacement volumetry, the disk model method and the frustum sign model method, using the correlation coefficient and the limits of agreement. J Biomed Eng. 1993;15:477–80.
18. Mikes DM, Cha BA, Dym CL, et al. Bioelectrical impedance analysis revisited. Lymphology. 1999;32:157–65.
19. Cornish BH, Bunce IH, Ward LC, et al. Bioelectrical impedance for monitoring the efficacy of lymphoedema treatment programmes. Breast Cancer Res Treat. 1996;38:169–76.
20. Cornish BH, Chapman M, Thomas BJ, et al. Early diagnosis of lymphedema in postsurgery breast cancer patients. Ann N Y Acad Sci. 2000;904:571–5.
21. Cha K, Chertow GM, Gonzalez J, et al. Multifrequency bioelectrical impedance estimates the distribution of body water. J Appl Physiol (1985). 1995;79:1316–9.
22. Cavezzi A, Schingale F, Elio C. Limb volume measurement: from the past methods to optoelectronic technologies, bioimpedance analysis and laser based devices. Int Angiol. 2010;29:392–4.
23. Mayrovitz HN, Sims N, Macdonald J. Assessment of limb volume by manual and automated methods in patients with limb edema or lymphedema. Adv Skin Wound Care. 2000;13:272–6.
24. Mellor RH, Bush NL, Stanton AW, et al. Dual-frequency ultrasound examination of skin and subcutis thickness in breast cancer-related lymphedema. Breast J. 2004;10:496–503.
25. Gniadecka M. Localization of dermal edema in lipodermatosclerosis, lymphedema, and cardiac insufficiency. High-frequency ultrasound examination of intradermal echogenicity. J Am Acad Dermatol. 1996;35:37–41.
26. Hu D, Phan TT, Cherry GW, et al. Dermal oedema assessed by high frequency ultrasound in venous leg ulcers. Br J Dermatol. 1998;138:815–20.
27. Naouri M, Samimi M, Atlan M, et al. High-resolution cutaneous ultrasonography to differentiate lipoedema from lymphoedema. Br J Dermatol. 2010;163:296–301.
28. Cambria RA, Gloviczki P, Naessens JM, et al. Noninvasive evaluation of the lymphatic system with lymphoscintigraphy: a prospective, semiquantitative analysis in 386 extremities. J Vasc Surg. 1993;18:773–82.
29. Hreshchyshn MM, Sheehan FR. Lymphangiography in advanced gynecologic cancer. Obstet Gynecol. 1964;24:525–9.
30. Guermazi A, Brice P, Hennequin C, et al. Lymphography: an old technique retains its usefulness. Radiographics. 2003;23:1541–58; discussion 59–60.
31. Jackson RJ. Complications of lymphography. Br Med J. 1966;1:1203–5.
32. Weil GJ, Ramzy RM. Diagnostic tools for filariasis elimination programs. Trends Parasitol. 2007;23:78–82.
33. Rockson SG, Miller LT, Senie R, et al. American Cancer Society Lymphedema Workshop. Workgroup III: diagnosis and management of lymphedema. Cancer. 1998;83:2882–5.
34. Vignes S, Trévidic P. Role of surgery in the treatment of lymphedema. Rev Med Interne. 2002;23 Suppl 3:426s–30s.
35. Andréjak M, Gersberg M, Sgro C, et al. French pharmacovigilance survey evaluating the hepatic toxicity of coumarin. Pharmacoepidemiol Drug Saf. 1998;7:S45–50.
36. Campisi C. Lymphoedema: modern diagnostic and therapeutic aspects. Int Angiol. 1999;18:14–24.
37. Hwang JH, Choi JY, Lee JY, et al. Lymphoscintigraphy predicts response to complex physical therapy in patients with early stage extremity lymphedema. Lymphology. 2007;40:172–6.
38. Lee BB, Laredo J, Neville R. Current status of lymphatic reconstructive surgery for chronic lymphedema: it is still an uphill battle! Int J Angiol. 2011;20:73–80.
39. Lee BB, Laredo J, Neville R. Reconstructive surgery for chronic lymphedema: a viable option, but. Vascular. 2011;19:195–205.
40. Pecking AP, Albérini JL, Wartski M, et al. Relationship between lymphoscintigraphy and clinical findings in lower limb lymphedema (LO): toward a comprehensive staging. Lymphology. 2008;41:1–10.
41. Watt H, Singh-Grewal D, Wargon O, et al. Paediatric lymphoedema: a retrospective chart review of 86 cases. J Paediatr Child Health. 2017;53:38–42.
42. Ter SE, Alavi A, Kim CK, et al. Lymphoscintigraphy. A reliable test for the diagnosis of lymphedema. Clin Nucl Med. 1993;18:646–54.
43. Williams WH, Witte CL, Witte MH, et al. Radionuclide lymphangioscintigraphy in the evaluation of peripheral lymphedema. Clin Nucl Med. 2000;25:451–64.
44. Weissleder H, Weissleder R. Lymphedema: evaluation of qualitative and quantitative lymphoscintigraphy in 238 patients. Radiology. 1988;167:729–35.
45. Kandeel AA, Ahmed Younes J, Mohamed ZA. Significance of popliteal lymph nodes visualization during radionuclide lymphoscintigraphy for lower limb lymphedema. Indian J Nucl Med. 2013;28:134–7.

46. Karaçavuş S, Yılmaz YK, Ekim H. Clinical significance of lymphoscintigraphy findings in the evaluation of lower extremity lymphedema. Mol Imaging Radionucl Ther. 2015;24:80–4.
47. Maclellan RA, Zurakowski D, Voss S, et al. Correlation between lymphedema disease severity and lymphoscintigraphic findings: a clinical-radiologic study. J Am Coll Surg. 2017;225:366–70.
48. Hassanein AH, Maclellan RA, Grant FD, et al. Diagnostic accuracy of Lymphoscintigraphy for lymphedema and analysis of false-negative tests. Plast Reconstr Surg Glob Open. 2017;5:e1396.
49. Forner-Cordero I, Oliván-Sasot P, Ruiz-Llorca C, et al. Lymphoscintigraphic findings in patients with lipedema. Rev Esp Med Nucl Imagen Mol. 2018;37:341–8.
50. Gould DJ, El-Sabawi B, Goel P, et al. Uncovering lymphatic transport abnormalities in patients with primary lipedema. J Reconstr Microsurg. 2020;36:136–41.
51. Frühling JG, Bourgeois P. Axillary lymphoscintigraphy: current status in the treatment of breast cancer. Crit Rev Oncol Hematol. 1983;1:1–20.
52. Das IJ, Cheville AL, Scheuermann J, et al. Use of lymphoscintigraphy in radiation treatment of primary breast cancer in the context of lymphedema risk reduction. Radiother Oncol. 2011;100:293–8.
53. Yoo JN, Cheong YS, Min YS, et al. Validity of quantitative lymphoscintigraphy as a lymphedema assessment tool for patients with breast cancer. Ann Rehabil Med. 2015;39:931–40.
54. Szuba A, Chacaj A, Koba-Wszedybyl M, et al. Upper extremity lymphedema after axillary lymph node dissection: prospective lymphoscintigraphic evaluation. Lymphology. 2016;49:44–56.
55. de Oliveira MM, Sarian LO, Gurgel MS, et al. Lymphatic function in the early postoperative period of breast cancer has no short-term clinical impact. Lymphat Res Biol. 2016;14:220–5.
56. Cintolesi V, Stanton AW, Bains SK, et al. Constitutively enhanced lymphatic pumping in the upper limbs of women who later develop breast cancer-related lymphedema. Lymphat Res Biol. 2016;14:50–61.
57. Kim P, Lee JK, Lim OK, et al. Quantitative lymphoscintigraphy to predict the possibility of lymphedema development after breast cancer surgery: retrospective clinical study. Ann Rehabil Med. 2017;41:1065–75.
58. Yoo J, Choi JY, Hwang JH, et al. Prognostic value of lymphoscintigraphy in patients with gynecological cancer-related lymphedema. J Surg Oncol. 2014;109:760–3.
59. Boccardo F, De Cian F, Campisi CC, et al. Surgical prevention and treatment of lymphedema after lymph node dissection in patients with cutaneous melanoma. Lymphology. 2013;46:20–6.
60. Feldman S, Bansil H, Ascherman J, et al. Single institution experience with lymphatic microsurgical preventive healing approach (LYMPHA) for the primary prevention of lymphedema. Ann Surg Oncol. 2015;22:3296–301.
61. Boccardo F, Casabona F, De Cian F, et al. Lymphatic microsurgical preventing healing approach (LYMPHA) for primary surgical prevention of breast cancer-related lymphedema: over 4 years follow-up. Microsurgery. 2014;34:421–4.
62. Roman MM, Barbieux R, Nogaret JM, et al. Use of lymphoscintigraphy to differentiate primary versus secondary lower extremity lymphedema after surgical lymphadenectomy: a retrospective analysis. World J Surg Oncol. 2018;16:75. https://doi.org/10.1186/s12957-018-1379-5.
63. Notohamiprodjo M, Weiss M, Baumeister RG, et al. MR lymphangiography at 3.0 T: correlation with lymphoscintigraphy. Radiology. 2012;264:78–87.
64. Proby CM, Gane JN, Joseph AE, et al. Investigation of the swollen limb with isotope lymphography. Br J Dermatol. 1990;123:29–37.
65. Hwang JH, Kwon JY, Lee KW, et al. Changes in lymphatic function after complex physical therapy for lymphedema. Lymphology. 1999;32:15–21.
66. Kim DI, Huh S, Hwang JH, et al. Venous dynamics in leg lymphedema. Lymphology. 1999;32:11–4.
67. Kafejian-Haddad AP, Perez JM, Castiglioni ML, et al. Lymphoscintigraphic evaluation of manual lymphatic drainage for lower extremity lymphedema. Lymphology. 2006;39:41–8.
68. Chang L, Cheng MF, Chang HH, et al. The role of lymphoscintigraphy in diagnosis and monitor the response of physiotherapeutic technique in congenital lymphedema. Clin Nucl Med. 2011;36:e11–2.
69. Partsch H, Stöberl C, Wruhs M, et al. Indirect lymphography with iotrolan. Fortschr Geb Rontgenstrahlen Nuklearmed Erganzungsbd. 1989;128:178–81.
70. Baulieu F, Baulieu JL, Vaillant L, et al. Factorial analysis in radionuclide lymphography: assessment of the effects of sequential pneumatic compression. Lymphology. 1989;22:178–85.
71. Olszewski WL, Cwikla J, Zaleska M, et al. Pathways of lymph and tissue fluid flow during intermittent pneumatic massage of lower limbs with obstructive lymphedema. Lymphology. 2011;44:54–64.
72. Liu NF, Olszewski W. The influence of local hyperthermia on lymphedema and lymphedematous skin of the human leg. Lymphology. 1993;26:28–37.
73. Pecking AP, Février B, Wargon C, et al. Efficacy of Daflon 500 mg in the treatment of lymphedema (secondary to conventional therapy of breast cancer). Angiology. 1997;48:93–8.
74. Moore TA, Reynolds JC, Kenney RT, et al. Diethylcarbamazine-induced reversal of early lymphatic dysfunction in a patient with bancroftian filariasis: assessment with use of lymphoscintigraphy. Clin Infect Dis. 1996;23:1007–11.
75. Szuba A, Cooke JP, Yousuf S, et al. Decongestive lymphatic therapy for patients with cancer-related or primary lymphedema. Am J Med. 2000;109:296–300.
76. Ho LC, Lai MF, Yeates M, et al. Microlymphatic bypass in obstructive lymphoedema. Br J Plast Surg. 1988;41:475–84.
77. Campisi C, Davini D, Bellini C, et al. Lymphatic microsurgery for the treatment of lymphedema. Microsurgery. 2006;26:65–9.
78. Gloviczki P, Fisher J, Hollier LH, et al. Microsurgical lymphovenous anastomosis for treatment of lymphedema: a critical review. J Vasc Surg. 1988;7:647–52.
79. François A, Richaud C, Bouchet JY, et al. Does medical treatment of lymphedema act by increasing lymph flow? Vasa. 1989;18:281–6.
80. Ciudad P, Manrique OJ, Adabi K, et al. Combined double vascularized lymph node transfers and modified radical reduction with preservation of perforators for advanced stages of lymphedema. J Surg Oncol. 2019;119:439–48.
81. Gironet N, Baulieu F, Giraudeau B, et al. Lymphedema of the limb: predictors of efficacy of combined physical therapy. Ann Dermatol Venereol. 2004;131:775–9.
82. Slavin SA, Upton J, Kaplan WD, et al. An investigation of lymphatic function following free-tissue transfer. Plast Reconstr Surg. 1997;99:730–41; discussion 42–3.
83. Seo KS, Suh M, Hong S, et al. The new possibility of lymphoscintigraphy to guide a clinical treatment for lymphedema in patient with breast cancer. Clin Nucl Med. 2019;44:179–85.
84. Weiss M, Baumeister RG, Hahn K. Planning and monitoring of autologous lymph vessel transplantation by means of nuclear medicine lymphoscintigraphy. Handchir Mikrochir Plast Chir. 2003;35:210–5.
85. Mikami T, Hosono M, Yabuki Y, et al. Classification of lymphoscintigraphy and relevance to surgical indication for lymphaticovenous anastomosis in upper limb lymphedema. Lymphology. 2011;44:155–67.
86. Burnand KM, Glass DM, Mortimer PS, et al. Lymphatic dysfunction in the apparently clinically normal contralateral limbs of patients with unilateral lower limb swelling. Clin Nucl Med. 2012;37:9–13.

87. Bourgeois P, Frühling J, Henry J. Postoperative axillary lymphoscintigraphy in the management of breast cancer. Int J Radiat Oncol Biol Phys. 1983;9:29–32.
88. Hara H, Mihara M. Postoperative changes in lymphoscintigraphic findings after lymphaticovenous anastomosis. Ann Plast Surg. 2019;83:548–52.
89. Weiss M, Baumeister RG, Frick A, et al. Lymphedema of the upper limb: evaluation of the functional outcome by dynamic imaging of lymph kinetics after autologous lymph vessel transplantation. Clin Nucl Med. 2015;40:e117–23.
90. Baumeister RG, Mayo W, Notohamiprodjo M, et al. Microsurgical lymphatic vessel transplantation. J Reconstr Microsurg. 2016;32:34–41.
91. Ciudad P, Agko M, Perez Coca JJ, et al. Comparison of long-term clinical outcomes among different vascularized lymph node transfers: 6-year experience of a single center's approach to the treatment of lymphedema. J Surg Oncol. 2017;116:671–82.
92. Zhang W, Wu P, Li F, et al. Potential applications of using ^{68}Ga-Evans blue PET/CT in the evaluation of lymphatic disorder: preliminary observations. Clin Nucl Med. 2016;41:302–8.
93. Aström KG, Abdsaleh S, Brenning GC, et al. MR imaging of primary, secondary, and mixed forms of lymphedema. Acta Radiol. 2001;42:409–16.
94. Hadjis NS, Carr DH, Banks L, et al. The role of CT in the diagnosis of primary lymphedema of the lower limb. AJR Am J Roentgenol. 1985;144:361–4.
95. Monnin-Delhom ED, Gallix BP, Achard C, et al. High resolution unenhanced computed tomography in patients with swollen legs. Lymphology. 2002;35:121–8.
96. Lohrmann C, Földi E, Bartholomä JP, et al. MR imaging of the lymphatic system: distribution and contrast enhancement of gadodiamide after intradermal injection. Lymphology. 2006;39:156–63.
97. Suga K, Yuan Y, Okada M, et al. Breast sentinel lymph node mapping at CT lymphography with iopamidol: preliminary experience. Radiology. 2004;230:543–52.
98. Yamada K, Shinaoka A, Kimata Y. Three-dimensional imaging of lymphatic system in lymphedema legs using interstitial computed tomography-lymphography. Acta Med Okayama. 2017;71:171–7.
99. Lohrmann C, Foeldi E, Speck O, et al. High-resolution MR lymphangiography in patients with primary and secondary lymphedema. AJR Am J Roentgenol. 2006;187:556–61.
100. Lohrmann C, Kautz O, Speck O, et al. Chronic lymphedema: detected with high-resolution magnetic resonance lymphangiography. J Comput Assist Tomogr. 2006;30:688.
101. Lohrmann C, Foeldi E, Langer M. MR imaging of the lymphatic system in patients with lipedema and lipo-lymphedema. Microvasc Res. 2009;77:335–9.
102. Liu NF, Lu Q, Jiang ZH, et al. Anatomic and functional evaluation of the lymphatics and lymph nodes in diagnosis of lymphatic circulation disorders with contrast magnetic resonance lymphangiography. J Vasc Surg. 2009;49:980–7.
103. Bull RH, Gane JN, Evans JE, et al. Abnormal lymph drainage in patients with chronic venous leg ulcers. J Am Acad Dermatol. 1993;28:585–90.
104. Bae JS, Yoo RE, Choi SH, et al. Evaluation of lymphedema in upper extremities by MR lymphangiography: comparison with lymphoscintigraphy. Magn Reson Imaging. 2018;49:63–70.
105. White RD, Weir-McCall JR, Budak MJ, et al. Contrast-enhanced magnetic resonance lymphography in the assessment of lower limb lymphoedema. Clin Radiol. 2014;69:e435–44.
106. Kiang SC, Ahmed KA, Barnes S, et al. Direct contrast-enhanced magnetic resonance lymphangiography in the diagnosis of persistent occult chylous effusion leak after thoracic duct embolization. J Vasc Surg Venous Lymphat Disord. 2019;7:251–7.
107. Long X, Zhang J, Zhang D, et al. Microsurgery guided by sequential preoperative lymphography using ^{68}Ga-NEB PET and MRI in patients with lower-limb lymphedema. Eur J Nucl Med Mol Imaging. 2017;44:1501–10.
108. Hou G, Hou B, Jiang Y, et al. ^{68}Ga-NOTA-Evans Blue TOF PET/MR lymphoscintigraphy evaluation of the severity of lower limb lymphedema. Clin Nucl Med. 2019;44:439–45.
109. Giacalone G, Yamamoto T, Belva F, et al. The application of virtual reality for preoperative planning of lymphovenous anastomosis in a patient with a complex lymphatic malformation. J Clin Med. 2019;8.